TRANS-SPINAL ELECTRICAL STIMULATION-INDUCED SENSORIMOTOR REHABILITATION AND EEG-BASED MACHINE LEARNING EVALUATION FOR UPPER EXTREMITY AFTER STROKE

ZHANG JIANING

PhD

The Hong Kong Polytechnic University

2024

The Hong Kong Polytechnic University

Department of Biomedical Engineering

Trans-spinal Electrical Stimulation-induced Sensorimotor Rehabilitation and EEG-based Machine Learning Evaluation for Upper Extremity after Stroke

Zhang Jianing

A thesis submitted in partial fulfilment of the requirements for the degree of Doctor of Philosophy

December 2023

CERTIFICATE OF ORIGINALITY

I hereby declare that this thesis is my own work and that, to the best of my knowledge and belief, it reproduces no material previously published or written, nor material that has been accepted for the award of any other degree or diploma, except where due acknowledgement has been made in the text.

_____(Signed)

Zhang Jianing (Name of student)

ABSTRACT

Upper extremity (UE) sensorimotor impairments are a significant cause of post-stroke long-term disability. Sensory deficits can impact motor outcomes and hinder participation in daily activities. However, sensory impairments are often ignored in traditional practices because of the lack of reliable measures. Manual measurements depend on subjective experiences, which are hard to maintain consistently across a larger stroke population. To address this issue, electroencephalography (EEG) has been used to identify transient sensory neural responses and provide objective data for sensory impairments. However, its interpretation still relies heavily on human professionals, a process that can be both time-consuming and labor-intensive given the large amount of data generated. Machine-learning (ML) techniques, specifically support vector machine (SVM) models with kernel functions, can help reduce the burden of analyzing neuroimaging data. These models can automatically analyze massive amounts of data and make predictions. However, the automatic evaluation of EEG data in post-stroke sensory impairments using SVM techniques is yet to be fully investigated.

In addition to the sensorimotor evaluation, conventional physical training is the usual therapy for motor recovery after stroke, along with sensorimotor evaluation. These therapies require intensive and repeated exercises to improve sensorimotor function. However, they do not produce significant long-term results. This may be due to the inadequate central nervous system (CNS) stimulation for neuronal changes.

Noninvasive stimulation of the spinal cord, such as trans-spinal electrical stimulation (tsES), aims to increase the excitability of the spinal circuits and the responsiveness of the remaining neural pathways. Some studies have shown that spinal cord electrical stimulation can enhance upper limb motor control and decrease muscle spasticity after stroke. However, more research is needed to assess the immediate effect of tsES on the cortical signals that control the peripheral muscles during voluntary movements of the UE after stroke. Also, the rehabilitation effects of tsES on the interactions of cortical, spinal, and muscle activities after stroke are poorly understood.

Therefore, the main objectives of this study were: (i) to establish an EEG-based SVM classification model to evaluate poststroke impairments in fine tactile sensation automatically; (ii) to evaluate the immediate effects of tsES on the cortical and muscular signals during voluntary UE contractions; (iii) to investigate the rehabilitation effects of tsES and voluntary physical training on the interactions of cortical, spinal, and muscular signals during upper limb movements in the long-term. The study was conducted as follows:

The first section developed an ML model incorporating SVM to assess post-stroke impairments related to fine tactile sensation. The experiment involved stroke and unimpaired participants. Stimulations were administered using cotton, nylon, and wool fabrics, targeting different UE of stroke participants and the dominant UE of unimpaired participants. The average and maximal relative spectral power (RSP) values of the EEG signals were utilized as inputs to feed the SVM model. The model's

generalization exhibited noteworthy accuracy variances when evaluating fabric stimulations within higher frequency bands, specifically the beta/gamma range. The EEG-based SVM-ML model aligned with the manual assessment of cortical responses to textile stimulations, indicating its potential for the automatic evaluation of fine tactile sensations following a stroke.

The second section examined the immediate effects of tsES on the cortical and muscular signals during voluntary UE contractions in chronic stroke patients. Twelve patients performed wrist-hand motion tasks at submaximal levels with tsES applied to the cervical spinal cord. Data acquisition involved collecting both EEG and EMG data from the sensorimotor cortex and the distal and proximal muscles of the UE. The cortico-muscular coherence (CMCoh), laterality index (LI) of peak CMCoh, and EMG activation level parameters were compared between non-tsES and tsES conditions. The results showed that tsES significantly increased the CMCoh and LI in the agonist distal muscles, decreased the activation levels of EMG in the antagonist distal muscle and proximal UE muscles, and increased the LI of the proximal UE muscles.

The third section investigated how cervical tsES training affects the patterns of cortico-muscular descending signals during voluntary movements in chronic stroke patients. Twenty patients were divided into tsES and control groups. They underwent twenty sessions of tsES with VPT or VPT alone. The evaluation outcomes, including clinical scores, CMCoh, LI, and EMG activation level, were measured before, after, and three months after the training. The tsES group showed significant differences in the

outcomes across the sessions. The clinical scores, such as FMA and MAS, improved significantly. The laterality index of distal and proximal muscles increased significantly. The CMCoh and EMG activation levels of antagonist distal and proximal muscles decreased significantly.

In conclusion, the EEG-based SVM-ML model exhibited outcomes that closely resembled the manual assessment of cortical responses to fabric stimulations; this could help to automate the measurement of fine tactile sensations in individuals who have experienced a stroke. In addition, the non-invasive cervical tsES combined with VPT in chronic stroke patients enhanced upper limb functional outcomes and reduced muscular spasticity. It also enhanced the responsiveness of residual descending pathways by increasing spinal cord excitability while reducing compensatory effects in proximal upper limb muscles. These findings suggested that tsES could be used as an adjunct to physical rehabilitation to facilitate long-term recovery of upper limb motor function in individuals with chronic stroke.

PUBLICATIONS ARISING FROM THE THESIS

Journals:

(1) **J.N. Zhang**, Y.H. Huang, F.Q. Ye, B.B. Yang, Z.Y. Li, X.L. Hu. Evaluation of Post-Stroke Impairment in Fine Tactile Sensation by Electroencephalography (EEG)-Based Machine Learning. Applied Sciences, 2022, 12, 4796.

(2) **J.N. Zhang**†, S. Zhou†, F. Chen, T.W. Wong, S. Ng, Z.Y. Li, Y.J. Zhou, S.M. Zhang, S. Guo, X.L. Hu. Automatic theranostics for long-term neurorehabilitation after stroke. Frontiers in Aging Neuroscience, 2023, 15, 1154795.

(3) **J.N. Zhang**, M.E. Wang, M. Alam, Y.P. Zheng, F.Q. Ye, S. Zhou, X.L. Hu. Effects of Non-invasive Cervical Cord Neuromodulation by Trans-spinal Electrical Stimulation on Cortico-muscular Descending Patterns in Upper Extremity of Chronic Stroke Survivors. Journal of Neural Engineering, 2023, under review.

(4) **J.N. Zhang**, M.E. Wang, M. Alam, Y.P. Zheng, K.L. Wan, F.Q. Ye, S. Zhou, X.L. Hu. Rehabilitative Effects of Non-invasive Cervical Trans-Spinal Electrical Stimulation (tsES) on Upper Limb Rehabilitation in Chronic Stroke. Journal of NeuroEngineering and Rehabilitation, 2023, to be submitted.

(5) F.Q. Ye, W. Rong, W.M. Li, K.T. Wong, M.K. Pang, H.W. Wai, L. Li, Z.C. Hong, S. Guo, Z.H. Ma, Y.P. Zheng, M. Zhang, N. Chow, S. Zhou, **J.N. Zhang**, X.L. Hu*, F.Chen*, W. Poon. Unilateral Ankle-foot Exoneuromusculoskeleton with Balance-sensing Feedback for Self-help Telerehabilitation after Stroke. Journal of NeuroEngineering and Rehabilitation, 2023, under review.

Conference papers:

(1) **J.N. Zhang**, Y.H. Huang, X.L. Hu. Trans-spinal Electrical Stimulation-induced Sensorimotor Rehabilitation of the Upper Extremity after Stroke with EEG-based Machine Learning. Hong Kong Medical and Healthcare Device Industries Association Student Research Award, 2023, Hong Kong SAR, P. R. China.

(2) **J.N. Zhang**, Y.H. Huang, X.L. Hu. Evaluation of Post-stroke Impairment in Fine Tactile Sensation by Electroencephalography (EEG)-based Machine Learning. 1st Asia-Pacific Neuroscience Student Congress and HKSAN 2nd Annual Conference, 2021, Hong Kong SAR, P. R. China.

ACKNOWLEDGEMENTS

First and foremost, I am profoundly grateful to my supervisor, Dr. HU Xiaoling. Your exceptional expertise and meticulous attitude in scientific research have shaped my research career. Thank you for your constant encouragement and tremendous patience over the past three years. I am truly fortunate and honored to have worked under your supervision.

I also sincerely thank my joint supervisor, Dr. ZHOU Yongjin. Your constructive feedback and insightful suggestions were essential for my research. I want to thank my cooperators, Prof. ZHENG Yongping, Dr. Alam, Dr. Ciaran, and Miss. Lyn. You have provided me with valuable technical support.

I am grateful to my lab colleagues, Dr. HUANG Yanhuan, Dr. YE Fuqiang, Dr. ZHOU Sa, Dr. GUO Ziqi, Miss. WANG Maner and Mr. WAN Kalim for their assistance in clinical assessments, patient training, and data processing; Dr. NAM Chingyi, Miss. QING Wanyi, Mr. LIN Legeng, Mr. Pan Changjie, Dr. YANG Bibo, and Mr. ZENG Qingtang for their suggestions and support.

I want to thank all the experimental participants. Their willingness to participate and provide invaluable data has been the cornerstone of this research.

Finally, I would like to express my heartfelt appreciation to my family. You are always my strongest supporter and cheerleader. You have given me your unconditional love, care, and encouragement. You have also sacrificed a lot for me. I dedicate this research to them.

TABLE OF CONTENTS

LIST OF FIGURES

LIST OF TABLES

LIST OF ABBREVIATIONS

ANCOVA	Analysis of Covariance
ANOVA	Analysis of Variance
ANN	Artificial Neural Network
APB	Abductor Pollicis Brevis
ARAT	Action Research Arm Test
BIC	Biceps Brachii
CBF	Cerebral Blood Flow
CL	Confidence Level
CMC	Cortico-muscular Coupling
CMCoh	Cortico-muscular Coherence
$CMRO_2$	Cerebral Metabolic Rate of Oxygen
CNS	Central Nervous System
CONSORT	Consolidated Standards of Reporting Trials
CV	Cross-validation
DALYs	Disability-adjusted Life-years
DBS	Deep Brain Stimulation
ECU	Extensor Carpi Ulnaris
ED	Extensor Digitorum

EEG	Electroencephalography
EMG	Electromyography
ERP	Event-related Potential
ES	Electrical Stimulation
eSCS	epidural Spinal Cord Stimulation
FCR	Flexor Carpi Radialis
FD	Flexor Digitorum
FIM	Functional Independence Measurement
FMA	Fugl-Meyer Assessment
fMRI	Functional Magnetic Resonance Imaging
FTT	Fabric Touch Tester
HSESC	Human Subjects Ethics Sub-committee
iMVC	isometric Maximal Voluntary Contraction
LDA	Linear Discriminant Analysis
LI	Laterality Index
MAS	Modified Ashworth Scale
MEPs	Motor Evoked Potentials
MMSE	Mini-Mental State Examination
ML	Machine Learning

MSS	Motor Status Score
NSA	Nottingham Sensory Assessment
QST	Quantitative Sensory Testing
RASP	Rivermead Assessment of Somatosensory Performance
RCT	Randomized Controlled Trial
PAD	Post-activation Depression
PET	Positron Emission Tomography
PSD	Power Spectral Density
RBF	Radial Basis Function
RSP	Relative Spectral Power
rTMS	repetitive Transcranial Magnetic Stimulation
SA	Affected Sides of Individuals after Stroke
SD	Standard Deviation
SE	Standard Error
SU	Unaffected Sides of Individuals after Stroke
SCI	Spinal Cord Injury
SWM	Semmes–Weinstein Monofilament
SVM	Support Vector Machines
TBI	Traumatic Brain Injury

TMS	Transcranial Magnetic Stimulation
TRI	Triceps Brachii
tsES	Trans-spinal Electrical Stimulation
UE	Upper Extremity
UD	Dominant Sides of Unimpaired Participants
VPT	Voluntary Physical Training
WMFT	Wolf Motor Function Test
WSO	World Stroke Organization
3MFU	3-month Follow-up

LIST OF APPENDICES

CHAPTER 1

INTRODUCTION

1.1 Stroke

1.1.1 Upper Extremity Sensorimotor Impairments

Upper extremity (UE) sensorimotor impairments are one of the main causes of post-stroke disability. These impairments include muscle weakness, spasticity, synergies in motor control, and somatosensory impairments [1]. Within the first 72 hours after stroke, upper limb function deficits are observed in 48% to 77% of individuals. At the chronic stage, motor impairments affect 33% to 66% of survivors, while somatosensory impairments affect 21% to 54% [1, 2]. The motor impairments are due to disrupted transmission of signals from the sensorimotor cortex, the region responsible for generating impulses to the spinal cord, which carries out the movement by signaling the upper limb muscles [3]. Consequently, individuals experience delays in initiating and ceasing muscle contractions, as well as a slow development of force, resulting in limited ability to move quickly and negative functional consequences [4].

Somatosensory impairments refer to deficiencies in sensation arising from skin, muscles, or joints, including light touch, pressure, temperature, or pain perception [5]. The extent of weakness and stroke severity often correlate with these impairments. Prolonged loss of sensation further contributes to motor dysfunction by distorting

internal task representations and impeding precise control of motor output [4]. Thus, somatosensory deficits can impact motor outcomes and hinder participation in daily activities. Despite extensive research on motor recovery, there has been a relatively dearth of studies focusing on the investigation of somatosensory functions following a stroke. Consequently, the rehabilitation of sensory functions has not received adequate attention within conventional approaches, and the intricate mechanisms governing sensory recovery and its interaction with motor recovery remain elusive [6]. This knowledge gap primarily arises from ineffective assessments for assessing somatosensory impairments following a stroke [7].

1.1.2 Stroke Prevalence

According to the latest data from World Stroke Organization (WSO) Global Stroke Fact Sheet 2022, stroke continues to rank as the second most prevalent cause of mortality globally and the third leading cause when considering the combined impact of death and disability [8]. The number of cases rose dramatically from 1990 to 2019, with a 70.0% rise in incident strokes, a 43.0% increase in stroke-related deaths, and a 143.0% increase in DALYs [9, 10]. In particular, in mainland China, the age-adjusted incidence rate of stroke was recorded at 297 per 100,000 individuals, which stands as the highest among studies employing similar methodologies [11]. While the overall incidence of stroke has declined in high-income countries, there has been a rising trend in stroke incidence among younger populations worldwide [12]. In Hong Kong, the report from

the LKS Faculty of Medicine, HKUMed, shows that the incidence of 'young stroke' (stroke individuals aged 18 to 55 years) has increased by 30% from 2001 to 2021 [13]. The economic costs associated with post-stroke care are huge, with around 34% of the total global healthcare expenditure allocated to addressing the consequences of stroke [14]. In the United States, the average healthcare expenditure per individual for stroke-related services is estimated to be USD 140,048 [15]. These alarming statistical findings highlight the widespread prevalence of stroke, the increasing incidence among younger individuals, and the significant burden it imposes on society.

1.2 Evaluation of Post-Stroke Sensory Impairments

1.2.1 Clinical Assessment

Standardized clinical assessments are commonly used in clinical practice to evaluate post-stroke somatosensory impairments [6]. It includes the Fugl-Meyer Sensory Scale, Nottingham Sensory Assessment (NSA), Erasmus-modified NSA, Rivermead assessment of somatosensory performance (RASP), and Quantitative sensory testing (QST) [6, 16]. These tools aim to evaluate various facets of sensation and establish uniform metrics free from subjective interpretations by stroke patients [6]. Although healthcare professionals and therapists acknowledge the significance of assessing somatosensory function, the assessment process relies on the assessor's individual experiences, making it challenging to achieve consistency in measurements, especially when dealing with a larger stroke population over an extended period [17]. In routine

clinical care, the testing of somatosensory deficits is often conducted superficially, following poorly standardized protocols that may raise concerns about the reliability and reproducibility of the results [18].

1.2.2 Neuroimaging-based Quantitative Evaluation

The advent of neuroimaging techniques, enabling comprehensive in vivo mapping of brain function, has revealed that behavioral impairments and potential recovery are intricately associated with intricate and widespread alterations in brain functional activity [19]. These techniques provide valuable imaging biomarkers to predict post-stroke sensorimotor impairments [20]. Prominent neuroimaging methods utilized in this context encompass functional magnetic resonance imaging (fMRI), positron emission tomography (PET), and electroencephalography (EEG), etc. [21-23]. Different modalities facilitate the examination of alterations in neural circuitry throughout the process of sensorimotor recovery following a stroke [24]. For instance, findings from fMRI have revealed that cortical reorganization, which is closely linked to motor recovery, is associated with task-induced activation not only in the remaining ipsilesional cortex but also in contralesional regions during motor tasks in unimpaired individuals [25, 26]. PET studies can identify the ischemic penumbra in stroke individuals, indicating the need for intervention when cerebral blood flow (CBF) values drop below 60% and cerebral metabolic rate of oxygen ($CMRO_2$) values exceed 40% of the normal range [27]. EEG measurements have been utilized to document brain

reorganization, suggesting that motor impairment following stroke may be associated with inhibitory effects induced by the affected motor cortex [28]. Among these neuroimaging techniques, EEG analysis stands out because it captures detailed information about the timing of neural responses, facilitating a deeper understanding of the cortical processes associated with post-stroke sensory deficits [28]. However, despite significant research efforts to understand changes in brain function, neuroimaging-based assessments often yield extensive data, which rely heavily on human experts, leading to time-consuming and labor-intensive processes [29].

1.2.3 Machine Learning Model-based Automatic Evaluation

Machine learning (ML) has emerged as a powerful method in neuroimaging data interpretation by delivering accurate and quick prediction outcomes with reduced workforce workload [30]. Supervised ML, which generalizes rules or patterns from labeled input data to generate predictions or classifications on unseen data, has been widely utilized in post-stroke sensorimotor impairments [31]. Commonly used supervised ML algorithms for classifications include linear discriminant analysis (LDA), artificial neural network (ANN), and support vector machines (SVM) [32, 33]. In the context of post-stroke sensorimotor impairment evaluation using neuroimaging data, ML algorithms have been applied to EEG information as input features [34]. These features can be EEG spectra, EEG waveform features, or EEG time-frequency features [7]. Once the EEG features are computed, they are fed into the ML algorithm to learn

patterns associated with sensorimotor impairment [35]. LDA has shown limited classification accuracies among recent ML studies due to its simple linear transformation for feature mapping, which may not efficiently construct the optimal classification boundary for multi-dimensional EEG data [36]. Models based on ANN provide nonlinear feature space transformation capabilities, but overfitting can be a challenge when determining hyperparameters [36]. In contrast, SVM-based models address the overfitting issue using kernel functions and have shown promise in reducing classification errors [37]. Nevertheless, the comprehensive exploration of SVM-ML techniques for automatically evaluating post-stroke sensory impairment data remains uncharted, mainly territory within the existing literature.

1.3 Electrical Stimulation-based Sensorimotor Recovery

1.3.1 Conventional Physical Therapy Programs

Regarding post-stroke sensorimotor recovery in stroke patients, conventional physical therapy rehabilitation programs are commonly employed in clinical settings as standard therapies [38]. These programs encompass various rehabilitation strategies, such as Bobath, proprioceptive neuromuscular facilitation, motor relearning, and functional strengthening approaches [39-41]. These programs involve activity-based physical therapy that could provide intensive and high-repetition training to assist the sensorimotor recovery of stroke individuals [42]. While these approaches were developed early and predominantly rely on empirical rather than scientific evidence,

their concepts are widely adopted in routine rehabilitation programs for stroke patients seeking to regain motor functions [43]. Several studies have demonstrated the positive effects of these interventions on motor function recovery following strokes [44-46]. However, there were no significant differences in the functional outcomes achieved through conventional rehabilitation strategies over a 4-year follow-up period [47]. Moreover, traditional rehabilitation often incorporates a compensatory strategy to promote some degree of independence among stroke patients [48]. The insufficient intervention of central nervous system (CNS), necessary for inducing neuronal changes, can give rise to the development of "learned disuse" issues and a progressive decline in latent function, resulting in a deterioration in disability [49, 50]. Therefore, conventional physical therapy rehabilitation programs highlight the necessity for enhanced CNS activation to facilitate long-term changes in motor function.

1.3.2 Neuromodulation Interventions

In recent decades, there have been advancements in utilizing neuromodulation interventions within rehabilitation technologies to facilitate and maximize sensorimotor recovery for stroke patients [51]. Most of these techniques are grounded in neuroscientific evidence, particularly in relation to the association with neural reorganization [52]. Researchers have proposed implanted CNS electrical stimulation (ES) as a potential option to deliver neural modulation intervention by involving the surgical placement of a small array of electrodes in specific regions of the brain or

spinal cord, such as deep brain stimulation (DBS) and epidural spinal cord stimulation (eSCS) [53, 54]. Researchers have shown that cervical epidural spinal cord stimulation alone could promote upper limb motor movements. It can improve functional abilities combined with intensive physical therapy training [55]. Additionally, long-term eSCS with training has demonstrated the potential to recover voluntary movement in chronic neurological diseases, even without ongoing stimulation [56]. However, it is essential to acknowledge that these improvements through implanted CNS ES come with inherent risks, including infection, bleeding, and potential patient injury resulting from interactions between the stimulation devices and other therapeutic instruments like ultrasound and MRI [57].

1.3.3 Trans-spinal Electrical Stimulation (tsES)

In contrast to the surgically implanted techniques, noninvasive electrical stimulation techniques for the spinal cord, such as trans-spinal electrical stimulation (tsES), offer a safer, more affordable, and easily portable alternative [58]. The spinal cord modulation via tsES utilizes a unique waveform of high-frequency electric current to reach the spinal networks from the skin surface [59]. Previous studies suggested that transcutaneous stimulation to the spinal cord can activate spinal circuitry resembling that of eSCS and could enhance functional recovery comparable to the results of eSCS when paired with physical therapy training [49]. Utilizing computational modeling and EMG research, noninvasive spinal cord stimulation has been proven effective in

augmenting the excitability of local spinal networks through the activation of dorsal root afferents, further enhancing signal transmission [60]. Noteworthy observations from case studies and clinical trials have shown that tsES has led to improvements in hand and arm function, reduction in muscular spasticity, as well as enhanced walking ability among individuals with neurological impairments, including those with spinal cord injury (SCI) and traumatic brain injury (TBI) [59]. Despite the limited research on the application of tsES for motor restoration in stroke patients, recent preliminary findings have shown positive outcomes of spinal cord electrical stimulation in enhancing motor control of the upper limb and releasing muscle spasticity after stroke [61][62]. A single study demonstrated the potential of epidural cervical electrical stimulation in an immediate enhancement of force for hand grip among individuals with chronic stroke [61]. The influences of electrical stimulation in C6 spine were evaluated by another research, and it revealed a tendency towards decreasing flexor muscular spasticity poststroke. This reduction was achieved by decreasing extra excitation of alpha motoneurons in the spinal cord [62]. These studies have demonstrated the potential effectiveness of spinal cord stimulation, which involves modulating the excitation state of intact spinal circuitry to improve the responsiveness to the residual neural pathways [63]. However, the current scientific literature exhibits a dearth of studies that have comprehensively assessed the immediate influence of tsES in cortical descending patterns on peripheral muscles during UE voluntary movements after stroke, which may potentially affect brain neuroplasticity in rehabilitation.

Early reports of clinical trials on tsES also demonstrated its potential to impact CNS excitability and facilitate functional change in patients with neurological deficits when paired with conventional physical therapy training [64]. It represents that tsES is a clinically powerful assistant to physical therapy, mitigating the risks and accessibility concerns associated with surgical procedures [49]. Understanding the mechanisms that tsES on the cortical, spinal cord circuitry, and muscle activities is crucial to ensure the stimulation is precisely applied to therapeutically relevant sites for enhancing upper limb motor function in post-stroke rehabilitation [65]. Additionally, optimal stimulation parameters are paramount in maximizing the rehabilitative effects. However, the training effects of the tsES-based neuromodulation technique in cortical, spinal cord circuitry, and muscle activity coupling patterns after stroke have not been fully explored.

1.4 Objectives

As previously mentioned, assessing post-stroke sensory impairments through neuroimaging generates vast data, necessitating costly manual evaluation. To address this challenge, ML algorithms can be employed to develop an automated predictive model. SVM-based models are particularly effective in minimizing complexity and mitigating overfitting issues through kernel functions. However, the literature lacks a comprehensive exploration of ML techniques for automatic evaluation of neuroimaging data of sensory impairments, particularly about fine tactile sensation, a fundamental somatosensory function for acquiring external information through touch. Moreover,

non-invasive spinal cord stimulation using tsES has shown promising rehabilitative effects in enhancing motor functions following stroke. Nevertheless, there is a lack of studies examining the immediate influence of tsES on cortical descending patterns affecting peripheral muscles during voluntary UE movements after stroke. This investigation holds the potential to impact brain neuroplasticity during rehabilitation. Finally, a comprehensive clinical trial was undertaken to evaluate the enduring ramifications of tsES training when coupled with physical training. It explored the effects of tsES on cortico-muscular coupling patterns in the affected upper limb by comparing measurements between stroke subjects who received tsES along with voluntary physical training (VPT) and age-matched stroke individuals who solely underwent VPT. In summary, this study has three primary objectives:

(1) Development of a novel EEG-based SVM-ML model with kernel functions to automatically evaluate fine tactile sensation impairments in post-stroke individuals.

(2) Investigation of the immediate effects of tsES on cortico-muscular descending patterns during voluntary contractions of upper extremity muscles by analyzing cortico-muscular coherence (CMCoh) and electromyography (EMG) in individuals with chronic stroke.

(3) Examination of the training effects of tsES on cortico-muscular coupling patterns during upper limb movements on the affected side of individuals with chronic stroke.

CHAPTER 2

EVALUATION OF POST-STROKE IMPAIRMENT IN FINE TACTILE SENSATION BY ELECTROENCEPHALOGRAPHY (EEG)-BASED MACHINE LEARNING

2.1 Introduction

Roughly half of individuals who have experienced a stroke have reported enduring sensory deficits pertaining to both somatosensation and proprioception, as supported by studies [67, 68]. For instance, stroke patients may struggle with sensing pressure, pain, temperature, and gentle touch [69]. These impairments can restrict their day-to-day activities and functional autonomy while impeding their post-stroke motor recovery [70, 71]. Fine tactile sensation is a basic somatosensory function that enables the acquisition of touch-based information [72]. Moreover, research has demonstrated that fine tactile sensation plays a role in maintaining body posture by providing spatial cues [73] and facilitating position control by improving sensory feedback [74, 75]. However, sensory rehabilitation has received less attention than motor rehabilitation in conventional practice due to the absence of reliable assessment methods for sensory deficits [76].

Accurate and efficient evaluations of sensory impairments play a crucial role in the ongoing rehabilitation of stroke survivors, requiring repeated measurements during

follow-up [66]. Nevertheless, traditional assessments of sensory impairments have been subjective and manual [67]. For instance, the FMA [68] and Semmes–Weinstein monofilament (SWM) test [69] are widely applied to evaluate fine tactile sensations, as the assessment results are easy to interpret. Nevertheless, the measurement process heavily relies on the assessor's expertise, making it challenging to maintain consistency in measurements as the number of stroke patients grows over time [70].

A growing body of research is developing neuroimaging-based methods to assess sensory impairments objectively, and neuroimaging refers to the use of various techniques to visualize and study the structure, function, or activity of the brain [71]. These innovative technologies involve PET, fMRI, and EEG [23, 72-77]. These approaches reveal changes in neural circuits during post-stroke sensorimotor recovery; however, they require expensive and complex medical equipment and preparations during comparison with the conventional professionals' evaluation [78]. In those methods, EEG falls under the category of functional neuroimaging because it provides functional information about brain activity and allows researchers and clinicians to study brain function, cognitive processes, and neurological disorders through the measurement and analysis of electrical signals generated by the brain [78]. EEG stands out due to its high resolution in temporal patterns and ability to capture fast sensory responses during fine textile stimuli [79, 80]. For instance, a study used EEG to compare the impact of various tactile stimuli missions, such as passive or active movement of a board, on cortex activation following a stroke [81]. The results revealed that the rhythm of sensory, as through the EEG relative powers in right hemisphere, exhibited a significantly greater magnitude during the activation of tactile perception compared to passive tactile perception in the affected left hemisphere [81]. Our previous study [81] used EEG to quantify sensory deterioration in delicate tactile

sensation after stroke during textile fabric stimulation, which emulates the typical interaction between fabric and skin. We detected disparities in the intensities of EEG relative spectral power (RSP) across various frequency ranges between the healthy and cohorts of stroke [82]. Nevertheless, measurements based on neuroimaging generate substantial amounts of material, necessitating the involvement of experts for interpretation, thus leading to extended processing time and high workload processes [83, 84].

Machine learning (ML) is a promising technique for interpreting neuroimaging data with less human effort [30]. It possesses the capability to construct an automated predictive model by acquiring knowledge of the correlations between attributes and targets from a given dataset of historical records. Subsequently, this model can be utilized to conduct repetitive analyses on extensive datasets [85]. Researchers are currently exploring diverse machine learning (ML) algorithms for the identification, categorization, and characterization of neuroimaging material [30]. For example, in a particular study, the EEG frequency spectra were employed as input features for an LDA (linear discriminant analysis) model to successfully classify various types of hand grasps based on the intentions of single trials [86]. An alternate investigation utilized the waveform characteristics of EEG as inputs for an artificial neural network (ANN) model to discern between right and wrong feedback during movements of the arm and foot [87]. However, both studies reported limited classification accuracies ranging from 41% to 86% [86, 87]. These suboptimal results could be attributed to the limitations of simple linear transformation employed by LDA for feature mapping, resulting in the establishment of non-efficiency final classification functions for EEG with multiple channels [88, 89]. While ANN-related methods possess non-linear capabilities of feature mapping, they often encounter overfitting issues, particularly when confronted

with numerous hyperparameters that require optimization during network training, such as the number of hidden layers and nodes [89]. Conversely, models based on support vector machines (SVM) address the overfitting issue using kernel functions [90]. Kernel functions could decrease the complexity of models by enabling implicit nonlinear transformations of feature spaces, eliminating the necessity for explicit mathematical expressions. Hence, during model development, Optimization is primarily required for specific hyperparameters associated with the kernel functions of SVM models [91]. SVM-ML models commonly employ diverse kernel functions, such as linear, polynomial, and radial basis function (RBF) kernels. For instance, in one particular investigation, SVM with a linear kernel was employed in classifying motor imagery based on EEG data specific to individual subjects, utilizing spectrum characteristics derived from frequency bands and channels [92]. One study evaluated the prediction results of SVM classification model with polynomial kernel in EEG data related to motor imagery [93]. Another study employed an RBF kernel in SVM classification model to distinguish EEG data related to imagined upper limb motions [94]. These investigations explored determining accuracies ranging from 67% to 92.8% [92-94]. Among the mentioned kernel functions, the RBF kernel is commonly preferred in SVM algorithms due to the superior results in handling nonlinearities during feature transformation, requiring fewer hyperparameters in comparison to other two kernels [95, 96].

The literature has not extensively investigated the utilization of SVM-ML techniques for automatic evaluations of neuroimaging data, particularly in fine tactile sensation. In a study conducted by Kim et al., they focused on extracting features related to alpha and gamma band powers from EEG data during touch interactions with various objects

[97]. Nevertheless, their evaluation was limited to the tactile perception of individuals without impairments, and they reported modest distinguishing results (68.1%) with the application of LDA classification algorithm [97]. Therefore, we aimed to develop a novel SVM model with EEG data to assess the deficiency in fine tactile sensation after stroke automatically.

2.2 Methodology

By utilizing EEG to assess cortical responses to precise tactile stimuli on the upper extremities, we built an SVM-ML model. The study involved two groups of participants: stroke survivors and healthy individuals. Our study involved the application of various fabric materials, including cotton, nylon, and wool, to elicit sensory stimulation on their skin. As a reference point for model development and optimization, we employed the RSP features obtained from the fabric stimulation of cotton as the input of baseline. The principal objective of the model was to classify the responses observed among different groups, specifically: 1) the stroke survivors' affected sides (SA), 2) the stroke survivors' unaffected sides (SU), and 3) the healthy individuals' dominant sides (UD). To assess the model's performance in a broader context, we subsequently evaluated its ability to generalize using the RSP features obtained from stimulations with various fabrics. During the evaluation process, we considered arm differences, both with and without involving them.

2.2.1 EEG Acquisitions during Fabric Stimuli

Prior to commencing the research, ethical approval was obtained from the Human

Subjects Ethics Sub-committee (HSESC) of the Hong Kong Polytechnic University. Subsequently, twelve individuals with chronic stroke were recruited as the "stroke group," while fifteen healthy individuals were enlisted as the "control group". Comprehensive demographic information for both groups can be found in **Table 2.1**. In order to be eligible for inclusion in the stroke group, individuals needed to fulfill specific criteria, which consisted of the following: (1) having singular and unilateral brain damage resulting from a stroke that had occurred at least six months prior and (2) having the stroke impairments in subcortical-related region to assure measurable EEG signals in the cortical region. The statistical analysis, conducted using an independent t-test, indicated no significant difference in age between the two groups ($P > 0.05$). To assess the normality of the data, the Shapiro-Wilk test [98] was employed.

Figure 2.1 illustrates experimental arrangement and procedure in the tactile stimulation involving fabric materials. The study encompassed three distinct fabric types (cotton, nylon, and wool) of equal dimensions but possessing different textural characteristics. We placed the fabrics alternatively on the ventral forearm of the upper limb (**Figure 2.1(c)**). The ventral forearm of the upper limb was selected as our main stimulation area was primarily based on the presence of the FCR-FD muscle in that region. The sensory function of the FCR-FD muscle is closely associated with eliciting motor function in the wrist and hand, which are the specific areas of investigation in Chapter 3 and Chapter 4. Every trial included a 30-second initial assessment without tactile stimulation, succeeded by 13-second stimulation periods with each fabric in a random

order, with 60-second intervals between them. This stimuli trial was done three times for every arm. We recorded the EEG data using a 64-channel whole brain system [99] at a 1000 Hz sampling rate. During the data measurements, each subject was instructed to remain awake while wearing earplugs and an eye mask to minimize noise from the surrounding visual and auditory stimuli. Further details of the study setup can be found according to [82].

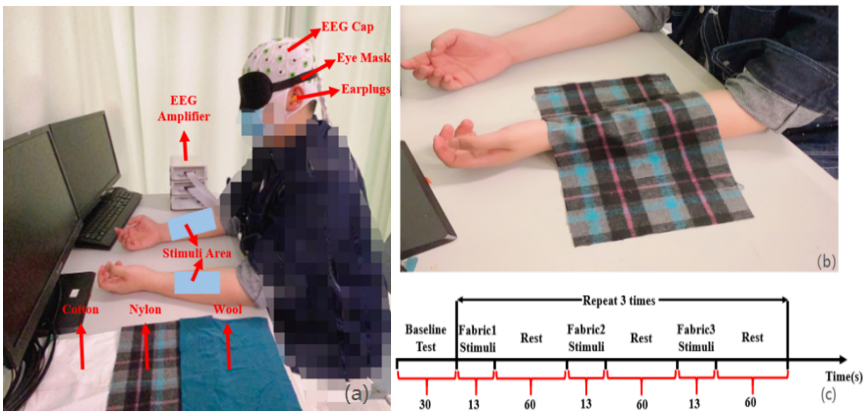

Figure 2.1 EEG experimental setup and protocol.

Table 2.1 The demographic attributes and clinical assessments for both stroke and control cohorts are outlined in [82].

Measure	Stroke group (n=12)	Control group (n=15)
Age in years	55.1±16.0	46.4±17.4
Gender (male/female)	11/1	5/10
Stroke type (ischemic/hemorrhagic)	10/2	--
Affected side (right/left)	6/6	--
Years since stroke	14.9±5.8	--
FMA (upper extremity)	42.5±15.2	--
FMA (light touch on forearm)	1±0	--
MAS (elbow)	1.1±0.7	--

Note: Data are given as mean ± SD.

2.2.2 Feature Extraction for SVM Classification Model

An SVM model was utilized to analyze features from EEG, specifically the RSP_{mean} and RSP_{max} values in various frequency bands, as inputs. These features correspond to the average and maximum cortical alterations observed during tactile stimulations. These alterations were identified manually based on former research findings [82]. The data from EEG was recorded in real-time at 1000 Hz. To prepare the RSP features of EEG data, a Butterworth bandpass filter was applied in the frequency range of 0.1 to 100 Hz to remove irrelevant high-frequency components from the EEG. Then, a Butterworth notch filter was employed to minimize 50 Hz noise originating from the environment, specifically targeting frequencies between 49 Hz and 51 Hz. After the filtering process, the trial data was divided into epochs, consisting of a 30-second baseline before stimulation and three 13-second stimulations with various textile types. The SA group yielded a total of 108 EEG samples, obtained by multiplying 12 participants by three trials and then by three fabric stimuli. Similarly, the SU group produced 108 EEG samples calculated using the same formula. On the other hand, the UD group generated 135 EEG samples, consisting of 15 participants undergoing three trials with three fabric stimuli each. Afterward, the EEG samples were converted using the Pwelch estimation method to obtain power spectra. This method is commonly employed to estimate the power spectral density of a given signal [100]. The frequency range of 0.1-100 Hz for every epoch of EEG was further divided into five distinct ranges: delta frequency range of 0.5-4 Hz, theta frequency range of 4-8 Hz, alpha frequency

range of 8-12 Hz, beta frequency range of 12-30 Hz, and gamma frequency range of 30-100 Hz [101]. Lastly, the RSP [102] of every band and textile stimulation were obtained using the specific equations, which are outlined as follows:

$$P(f_1, f_2) = \int_{f_1}^{f_2} p(f)df \qquad (2.1)$$

$$RSP(f_1, f_2) = \frac{P(f_1,f_2)}{P(0.1,100)} - \frac{P_{baseline}(f_1,f_2)}{P(0.1,100)} \qquad (2.2)$$

Where $p(f)$ denotes the density of power spectral; f_1 , f_2 represent the low cutoff frequency and high cutoff frequency, respectively; $P(f_1, f_2)$ denotes the power spectrum within the frequency range from f_1 to f_2; while $P_{baseline}$ represents EEG data's power spectrum before stimulation in every experiment. The spectrum processing of the obtained data was conducted offline using a toolbox of EEGLAB on MATLAB (Natick, MA, USA).

RSP features of multichannel EEG were represented by the RSP_{mean} and RSP_{max} values obtained by each channel of EEG, where RSP_{mean} signifies average RSP value across all channels within a specific frequency band in a data trial, while RSP_{max} corresponds to the most considerable RSP value in all channels of EEG. Subsequently, to obtain the RSP_{mean} and RSP_{max} values, values, we performed calculations on EEG data with 62 channels. These channels involve the entire brain cortex region. The calculations were conducted separately for each frequency band. We further normalized the original values using z-score normalization to reduce the variation of the ranges for the RSP_{mean} and RSP_{max},. This normalization technique scales all the RSP_{mean} and

RSP_{max} values to have a zero average and unit standard deviation, resulting in a consistent range for comparison purposes [103]:

$$RSP_i' = \frac{RSP_i - \mu_{RSP}}{\sigma_{RSP}} \qquad (2.3)$$

where RSP_i represents the original spectral feature, which can be either RSP_{mean} or RSP_{max}. The μ_{RSP} denotes the mean of RSP_i, while σ_{RSP} represents the standard deviation of RSP_i. To normalize the spectral features, we calculate RSP_i', which represents the normalized feature of spectrum. These features are subsequently utilized as features feeding into the ML classification model.

2.2.3 SVM-ML Model Configuration

The SVM-ML model's configuration is depicted in **Figure 2.2**, showcasing the process of optimizing the RBF kernel function, as well as implementing a k-fold cross-validation (CV) strategy. The features (such as RSP_{mean} and RSP_{max}) obtained during cotton textile stimulation, were utilized as benchmark inputs. The choice of cotton fabric as the stimulus for model establishment stems from its widespread use in daily life, as it comes into direct contact with the skin. Cotton fabric is known to provide a comfortable feeling with minimal stimulation intensity compared to other materials [104]. Additionally, cotton fabric demonstrates neutral textile physical properties when quantitatively assessed using the fabric touch tester (FTT) [105]. These properties, including smoothness and thickness, are comparable to nylon and wool fabrics [82].

Consequently, the RSP features of EEG triggered by the cotton textile were considered suitable benchmark inputs for configuring the ML classification model.

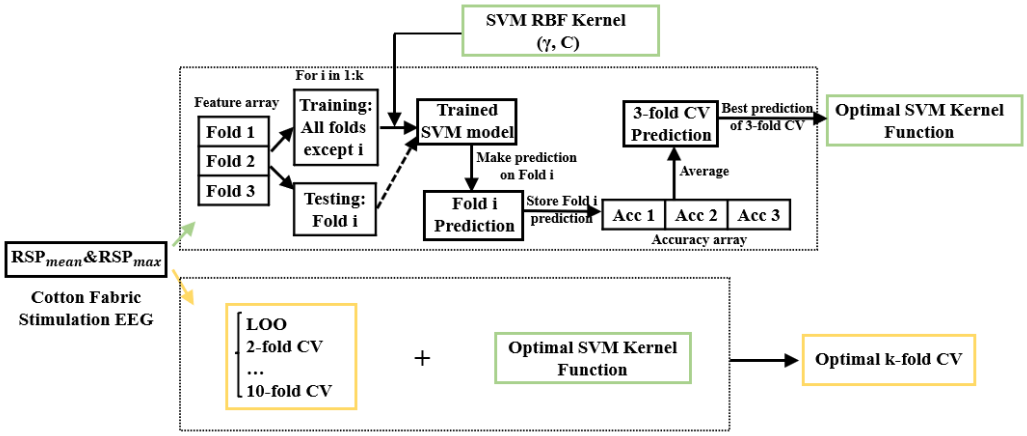

Figure 2.2 Flowchart for parameters optimization in ML classification model.

The primary objective of optimizing the RBF in the ML classification model was to determine the decision function which yielded highest classification precision when applied to RSP features associated with cotton textile stimuli. During the development of the ML classification model, two hyperparameters were optimized: scaling hyperparameter γ and the regularization hyperparameter C [106]. To explore the best (γ, C) parameters, we implemented a technique known as "grid exploration" [107]. This method entailed generating a series of candidate values for (γ, C) in sequences that exponentially increased. These values ranged from γ = 2^(-15), 2^(-13), ..., 2^(9), and C = 2^(-5), 2^(-3), ..., 2^(15), which are frequently employed intervals in SVM-ML investigations centered around EEG data for the purpose of discovering the most optimized hyperparameters [95, 108, 109]. Using these pre-defined scales, we generated a total of 143 pairs encompassing (γ, C). Every pair was subsequently utilized

for the construction of RBF kernel. To assess classification performance of every pair, we employed a three-fold cross-validation (CV) approach, considering the largest common divisor of both the twelve stroke patients and fifteen healthy controls. The utilization of this approach aligns with a widely employed pilot estimation technique that has been observed according to previous research endeavors [110]. Following the evaluation process, we identified the pair of hyperparameters that produced the highest classification accuracy. This particular configuration was deemed the optimal choice for our model. To implement the SVM algorithm, we utilized the toolbox of Scikit-learn, an open-source machine learning toolbox with Python language [111].

Figure 2.3 presents the outcomes of the grid search analysis conducted for (γ, C). Within this figure, **Figures 2.3(a)-(e)** exhibit the respective accuracies achieved by various pairs of (γ, C) pairs when differentiating between the groups of UD, SA, and SU, utilizing the RSP_{mean} and RSP_{max} as input features. The red dots in **Figures 2.3(a)-(e)** represent the coordinates and corresponding accuracy values attained for every band of frequency. Among the range of accuracies obtained, the model reached its highest accuracy (67.4%) within the gamma band, precisely at γ=2^(3) and C=2^(9).

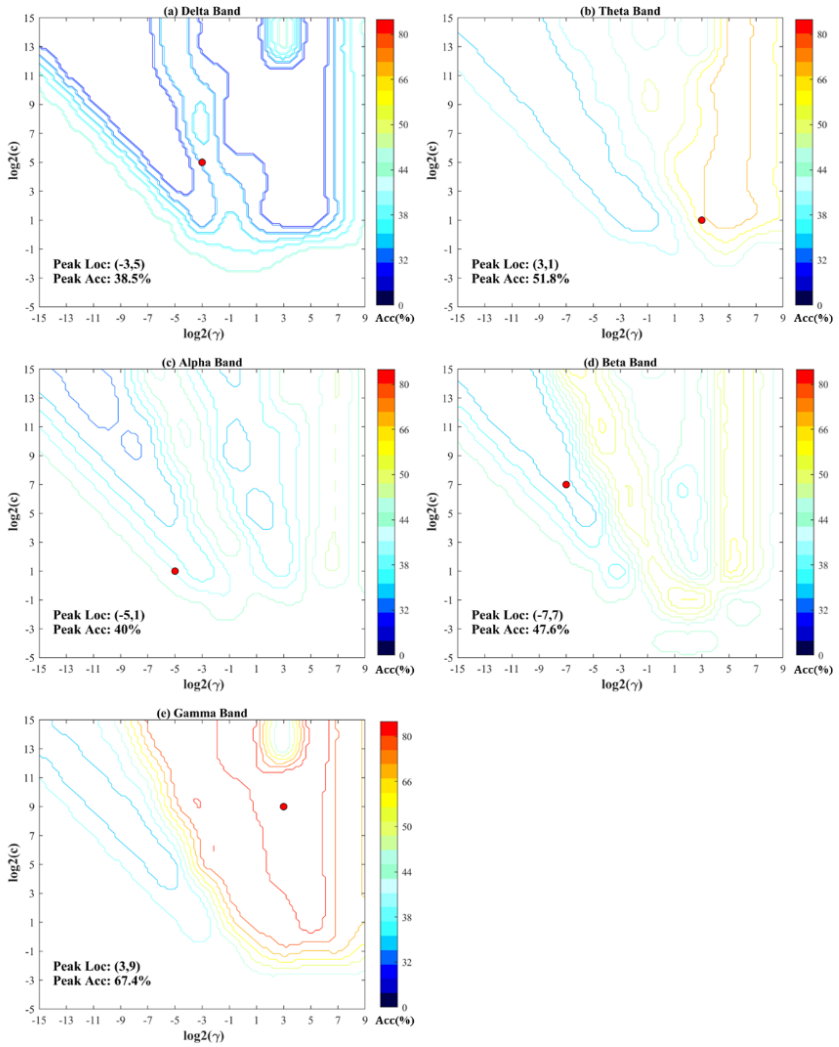

Figure 2.3 Results of grid search analysis of (γ, C) in SVM classification model with RSP features from 62-channel EEG in five frequency bands.

The sensorimotor cortex, which is the primary region responsible for reacting to sensory stimuli [112], played a crucial role in the testing of SVM classification model. During this testing phase, exclusive focus was placed on EEG channels that cover this region. The inputs to the model were the RSP_{mean} and RSP_{max} of the 21-channel EEG.

These channels, which encompass the sensorimotor area, include FC1–FC6, FCZ, C1–C6, CZ, CP1–CP6, and CPZ [113]. Results of accuracies achieved utilizing RSP characteristics with EEG of 21 channels are depicted in **Figure 2.4**. Notably, the highest accuracy of 76.8% was accomplished in the gamma band at γ=2^(1) and C=2^(3).

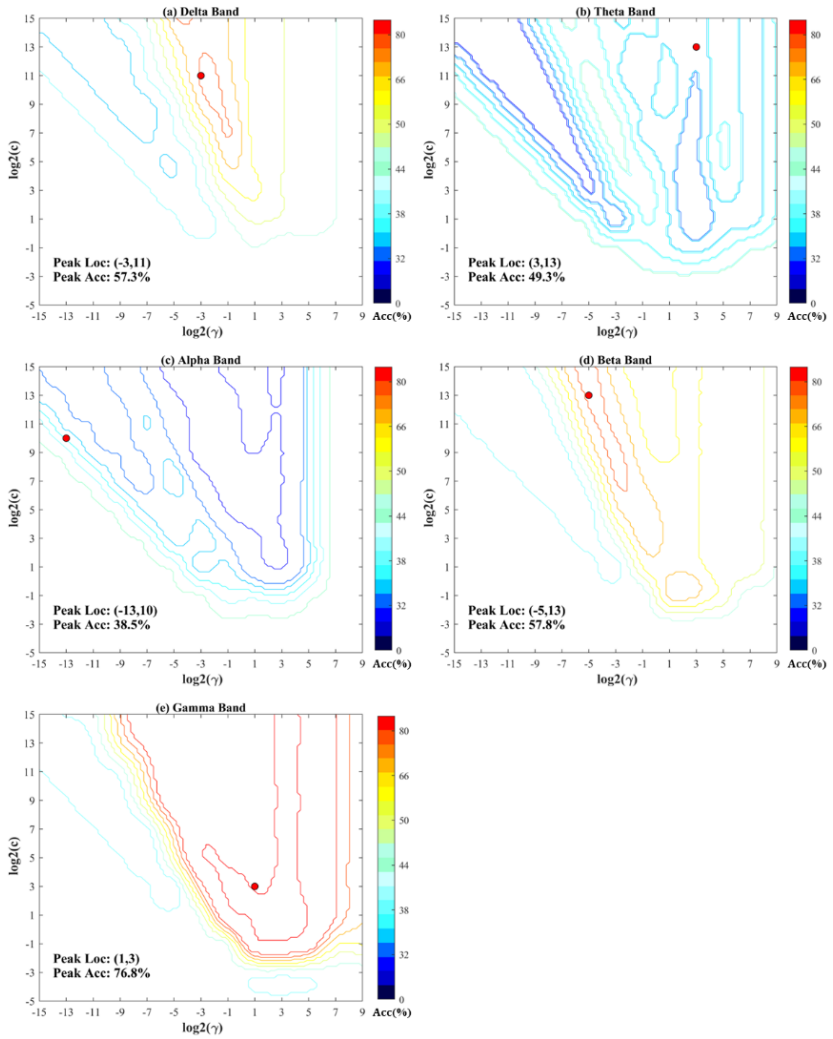

Figure 2.4 Results of grid search analysis of (γ, C) in SVM classification model with RSP features from 21-channel EEG in five frequency bands.

Table 2.2 summarizes the accuracies obtained by the SVM-ML model when employing distinct hyperparameter pairs of the RBF kernel to differentiate among three groups in different frequency bands. The table provides a comparison of the accuracy performance for both the 21-channel and 62-channel EEG channel set selections. Among the various bands of frequency, the gamma band stands out with notably high accuracy, resulting in two distinct channel sets. The accuracies of mean and peak attained in RSP features of EEG with 21 channels were superior to that obtained RSP features of EEG with 62 channels. Consequently, the pair (γ=2^(1), C=2^(3)) of RSP features with 21 channels was identified as the optimal choice for the SVM model.

Table 2.2 The classification results of SVM classification model for distinguishing three groups with different hyperparameter pairs in RBF kernel in various frequency bands.

EEG channel number		Delta	Theta	Alpha	Beta	Gamma
62	Average Acc	33.5%±0.05	37.8%±0.05	35.8%±0.03	38.2%±0.04	44.7%±0.11
	Peak Acc	38.5%	51.8%	40.0%	47.6%	67.4%
	Peak Loc (γ, C)	$(2^{-3}, 2^{5})$	$(2^{3}, 2^{1})$	$(2^{-5}, 2^{1})$	$(2^{-7}, 2^{7})$	$(2^{3}, 2^{9})$
21	Average Acc	39.1%±0.06	35.6%±0.04	33.2%±0.06	41.3%±0.07	49.2%±0.16
	Peak Acc	57.3%	49.3%	38.5%	57.8%	76.8%
	Peak Loc (γ, C)	$(2^{-3}, 2^{11})$	$(2^{3}, 2^{13})$	$(2^{-13}, 2^{10})$	$(2^{-5}, 2^{13})$	$(2^{1}, 2^{3})$

Note: Data are given as mean ± SD.

After selecting hyperparameters in RBF kernel, implementation of k-fold cross-validation (CV) followed, utilizing the RSP features calculated from the EEG data of

21 channels. The main objective of employing a k-fold CV was to improve the overall generalization performance of the SVM classification model. In comparison to a simple random split of train and test data, k-fold CV guarantees the inclusion of every data point in an original dataset in both training and testing sets. This meticulous process helps mitigate biased evaluations and promotes a more reliable assessment of the model's performance [114]. In order to reduce the fluctuation in accuracy assessments arising from a solitary execution of k-fold cross-validation, the procedure underwent replication on ten occasions, culminating in the computation of the average estimation [115-117]. Typically, values of k, such as 5 or 10, are used as they strike a balance between bias and variance in model evaluation [114, 118]. Throughout our research endeavor, we utilized a diverse set of k values spanning from 2 to 10 to scrutinize their impact on the model's performance. Furthermore, we incorporated the leave-one-out cross-validation (CV) as an additional point of reference, where k corresponds to the total quantity of data points in the whole dataset. Compared to alternative k-fold CV methodologies like five-fold and ten-fold CV, the approach with leave-one-out demands a higher computational overhead. Nevertheless, it furnishes a dependable assessment of the model's classification results because every individual sample serves as an entire test dataset [114].

Table 2.3 presents a comprehensive depiction of the performance attained by the SVM classification model, encompassing multiple frequency bands for discriminating among the groups of UD, SA, and SU. This evaluation involved the application of various k-

fold CV configurations. Utilizing a six-fold cross-validation (CV) strategy, the gamma band emerged as the most productive, leading to the attainment of the highest accuracy rate recorded at 75.4%. Notably, comparable success was observed in the leave-one-out CV, where the gamma band achieved a classification accuracy of 74.4%. Consequently, these findings led to the selection of a six-fold CV as the optimal evaluation approach when leveraging RSP features extracted from EEG with the 21 channels as input for classification model.

Table 2.3 The classification results of SVM model in distinguishing three groups with various k-fold CV configurations with various frequency bands.

CV	Accuracy				
	Delta	**Theta**	**Alpha**	**Beta**	**Gamma**
2-fold	49.6%±0.07	38.1%±0.06	27.6%±0.06	50.7%±0.07	73.8%±0.05
3-fold	49.1%±0.06	33.3%±0.07	26.0%±0.05	51.0%±0.05	74.5%±0.04
4-fold	49.7%±0.06	34.7%±0.06	23.9%±0.05	50.1%±0.05	74.8%±0.04
5-fold	49.7%±0.06	32.4%±0.05	26.1%±0.05	51.2%±0.04	75.0%±0.03
6-fold	53.2%±0.05	35.0%±0.06	22.2%±0.05	50.8%±0.05	75.4%±0.04
7-fold	46.7%±0.06	32.6%±0.05	32.9%±0.05	48.2%±0.06	72.6%±0.04
8-fold	47.0%±0.07	31.3%±0.06	28.9%±0.06	47.2%±0.06	74.8%±0.04
9-fold	49.5%±0.07	31.4%±0.06	27.8%±0.06	49.1%±0.06	74.7%±0.05
10-fold	51.7%±0.07	33.0%±0.06	25.9%±0.06	50.0%±0.05	74.8%±0.05
Leave-one-out	51.3%	28.2%	12.8%	53.8%	74.4%

Note: Data are given as mean ± SD.

2.2.4 Generalization Performance of SVM Classification Model

We established the SVM-ML framework by utilizing RSP characteristics acquired

while subjecting the cotton fabric to stimulation. Consequently, we proceeded to explore the model's capability to generalize and distinguish upper-limb groups employing inputs from various fabric types, namely nylon, wool, and cotton. The model was provided with the recorded RSP features obtained from each stimulation, and the outcomes are presented in **Table 2.4**. The distinguishing results of the diverse fabric stimulations did not conform to a normal distribution ($P < 0.5$) within every band of frequency. Remarkably, notable distinctions between groups were observed in the performance ($P < 0.001$) across stimulations of fabric in all five bands. The model demonstrated exceptional performance in the gamma band, exhibiting the highest classification accuracies across different fabric stimulations. Specifically, the cotton stimulation yielded an impressive accuracy of 75.4%, while the nylon stimulation achieved a remarkable accuracy of 83.5%. Notably, the wool stimulation surpassed both with an outstanding accuracy of 84.3%.

A comprehensive analysis of the SVM-ML model's overall accuracies across various fabric stimulations within each frequency band is presented in **Figure 2.5**. Significant differences were obtained in all five frequency bands when comparing the three stimuli of textile ($P < 0.001$), with one exception: gamma band where no significant difference was found between the stimulations of nylon and wool ($P > 0.05$). Furthermore, SVM model utilizing stimuli of nylon and wool exhibited higher results of accuracy with significance in frequency bands of beta and gamma compared to the model using stimulation of cotton ($P < 0.001$). All statistical results were obtained using Kruskal-

Wallis with Bonferroni post-hoc test.

Table 2.4 The comprehensive classification accuracies of SVM model for distinguishing various textile stimulations.

Fabric stimulation	Accuracy				
	Delta	Theta	Alpha	Beta	Gamma
Cotton	53.2%±0.05	35.0%±0.06	22.3%±0.05	50.8%±0.05	75.4%±0.04
Nylon	21.0%±0.04	40.6%±0.05	51.4%±0.04	63.2%±0.03	83.5%±0.02
Wool	30.3%±0.04	25.6%±0.06	43.0%±0.05	69.2%±0.04	84.3%±0.03
Significance (p-value)	<0.001***	<0.001***	<0.001***	<0.001***	<0.001***

Note: Data are given as mean ± SD.

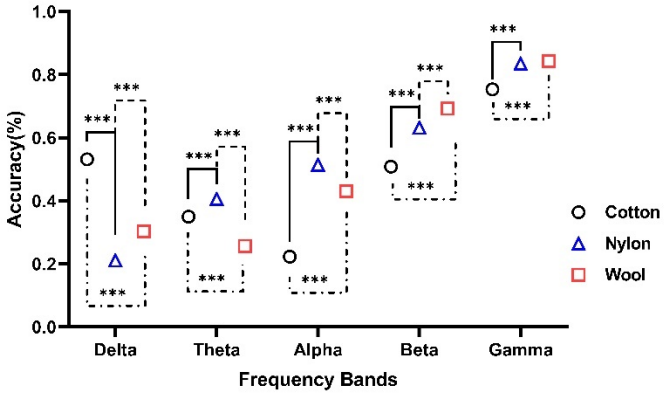

Figure 2.5 The comprehensive classification performance of SVM classification model with respect to textile stimulus in five different bands.

Table 2.5 provides an evaluation of the model's generalized performance, taking into consideration the variations in arm responses during stimulations with various fabrics. The distinguishing results of each group for different fabric stimulations deviated from normal distribution (P<0.5). Significant distinctions were observed in classification

accuracies ($P<0.001$) for each textile stimulation in every frequency band, with one exception: the SU group in the gamma band did not exhibit the statistically significant difference ($P>0.05$). Impressively, gamma band consistently demonstrated the highest distinguishing results in every group. All statistical results were obtained using Kruskal-Wallis test.

Figure 2.6 provides a comprehensive visual comparison of classification performance achieved by the SVM classification model for each textile stimulation, taking into account the arm differences, as derived from accuracies presented in **Table 2.4** and **Figure 2.5**. For the group of SA, we obtained significant variations in accuracies for the fabric stimulations within the beta band ($P<0.001$) and gamma band ($P<0.05$). However, when comparing nylon textile and wool textile across all bands, except for the beta and gamma bands, no significant differences were found ($P>0.05$). For group of SU, we identified significant disparities in the textile stimulations within the delta, alpha, and beta frequency bands ($P<0.05$). Nevertheless, in the theta band, no statistically significant disparities were found among cotton textile and nylon textile ($P>0.05$). For group of UD, we detected statistically significant variations at accuracy results for the textile stimulus across all bands of frequency ($P<0.001$), except for the gamma band, where the distinction between nylon textile and wool textile did not yield statistically significant results ($P>0.05$). All statistical results were obtained using Kruskal-Wallis with Bonferroni post-hoc test.

Table 2.5 The comprehensive classification performance of SVM model in distinguishing three groups with various textile stimulations.

Fabric stimulation		Accuracy				
		Delta	Theta	Alpha	Beta	Gamma
SA	Cotton	47.9%±0.09	28.8%±0.11	28.5%±0.10	48.9%±0.10	59.7%±0.08
	Nylon	26.8%±0.09	31.9%±0.08	54.1%±0.11	64.3%±0.10	76.2%±0.06
	Wool	22.9%±0.09	21.7%±0.08	51.1%±0.11	53.6%±0.08	78.9%±0.04
	p-value	<0.001***	<0.001***	<0.001***	<0.001***	<0.001***
SU	Cotton	48.3%±0.08	40.9%±0.13	27.0%±0.09	69.3%±0.05	91.0%±0.04
	Nylon	15.5%±0.07	40.5%±0.13	61.7%±0.04	74.9%±0.01	91.2%±0.03
	Wool	50.3%±0.03	27.8%±0.08	40.1%±0.04	84.9%±0.04	91.6%±0.01
	p-value	<0.001***	<0.001***	<0.001***	<0.001***	>0.05
UD	Cotton	51.4%±0.14	31.6%±0.10	22.0%±0.12	35.3%±0.12	78.0%±0.10
	Nylon	24.0%±0.09	51.9%±0.07	39.2%±0.10	53.7%±0.05	83.4%±0.01
	Wool	19.8%±0.09	30.0%±0.11	36.9%±0.10	71.9%±0.08	84.1%±0.06
	p-value	<0.001***	<0.001***	<0.001***	<0.001***	<0.001***

Note: Data are given as mean ± SD.

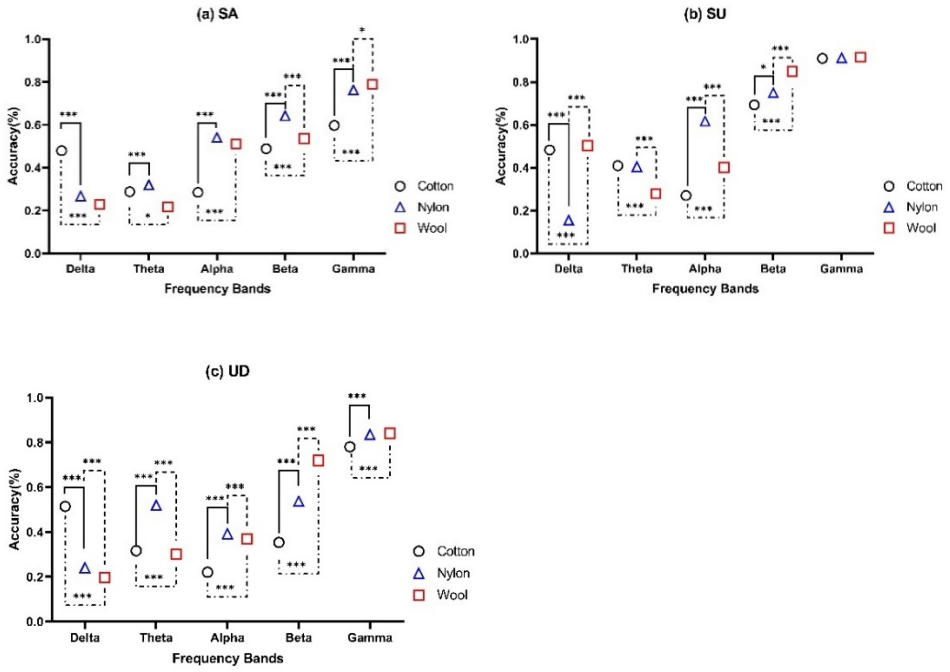

Figure 2.6 The comprehensive classification performance of SVM classification model regarding textile stimulus in five different bands involving the upper limb differences.

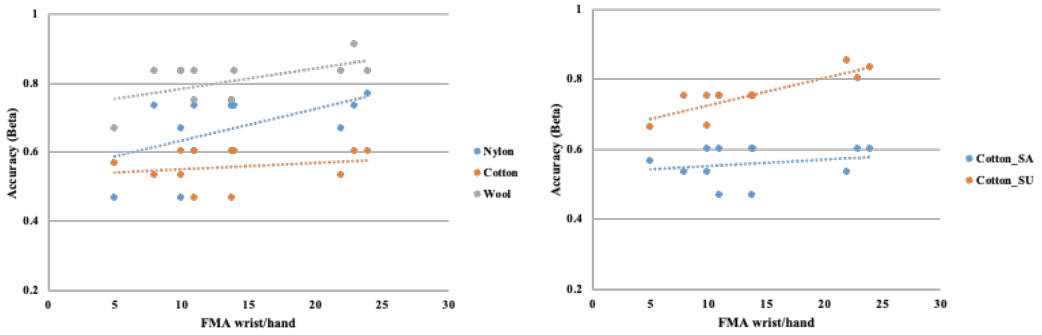

(a) (b)

Figure 2.7 The difference of classification performance of SVM classification model regarding (a) impairments' level and (b) affected side/unaffected side in beta band.

The effects of impairment level and the affected/unaffected side on classification accuracy was summarized in Figure 2.7. Specifically, Figure 2.7(a) depicted the classification accuracies of Leave-one-out cross-validation for each stroke subject under different fabric stimulations at the beta frequency band. Figure 2.7(b) displayed the classification accuracies of Leave-one-out cross-validation for each stroke subject when considering the affected/unaffected side at the beta frequency band. Notably, it was observed that the accuracy increased with higher FMA wrist/hand values (Figure 2.7(a)). Moreover, nylon and wool exhibited a more pronounced increasing trend compared to cotton for the same stroke patient, resulting in better accuracy (Figure 2.7(a)). Additionally, in the case of the same stroke patient, the unaffected side achieved higher classification accuracy than the affected side.

2.3 Discussion

We constructed the SVM classification model with EEG data that the RSP features were extracted from cotton textile stimuli as the benchmark. We evaluated the generalization results of the model by the comparison of the distinguishing results for different fabric stimuli.

2.3.1 The Configuration of SVM Classification Model

RBF Kernel Configuration

In order to optimize the performance of our SVM-ML model, we conducted a grid search for the pair of parameters (γ, C) specifically for the kernel of RBF. **Figures 2.3** and **2.4** illustrate the results of this grid search, showcasing the highest classification results achieved within the defined scale for the pair. Other SVM-based studies used similar boundaries for the pair, such as one study utilized the range (γ: e^(−8) - e^(8), C: e^(−8) - e^(8)) [119], while another study used (γ: 2^(−15) - 2^(3), C: 2^(−5) - 2^(15)) [95]. These observations suggest that the most effective values for the (γ, C) resided within the conventional exploration range. Furthermore, our SVM classification model, equipped with a more comprehensive exploration space, proved effective in accurately classifying the RSP of EEG data gathered during sensation evaluation. It is crucial to note that classification boundary complexity utilized by model for classification purposes is greatly influenced by the kernel scaling parameter γ [120]. The decision function is more linear for smaller γ values and curved for larger γ values [120]. The

model chose the optimal γ value (2^(1)) near the upper limit of predefined range of γ, implying that the EEG data from various upper-limb groups had a relatively strong nonlinearity in their original space of feature vectors. To capture these nonlinear relationships, the model successfully mapped the original EEG data to a higher-dimensional space, resulting in a decision function with a distinct "curved" shape. In the context of the SVM-ML model, the regularization parameter C plays a critical role in determining the penalty imposed for distance from the correct classification of the trained EEG sample [120]. With higher values of C, the penalty degree increases, leading to a smaller percentage of data with misclassified in the phase of training. SVM model opted for a relatively lower value of C (2^(3)) in contrast to predefined range, which indicated that established model was more tolerant of percentage of data with misclassified while striving to discover the optimal classification boundary. Such tolerance suggested the presence of potential overlapping in the various groups of training dataset close to the classification function, indicating the intricacies in the classification task. Remarkably, the model, equipped with the best pair of hyperparameters (γ, C), attained a commendable classification accuracy (76.8%). This level of accuracy aligns with prior studies that have concentrated on the SVM algorithm for the multifaceted differentiation of EEG signals, where reported accuracies exceeded 71.0% [121, 122].

EEG Channel Selection

Our observations showed that the model utilizing the EEG with 21 channels outperformed the model utilizing the EEG with 62 channels in terms of overall accuracies, disregarding discrepancies related to the arms (as shown in **Table 2.2**). Specifically, the EEG with 21 channels focuses on encompassing sensorimotor brain region, serving as the primary region in the brain responsible for processing sensory stimulations [123, 124]. The accuracies from the EEG of 21 channels indicated that the sensorimotor region's ability to directly process cortical signals, enabling SVM classification model to capture sensory distinctions presented by various fabric samples effectively. Notably, prior investigations have also substantiated the notion that the sensorimotor cortex predominantly captures significant variations in RSP across different frequency bands during stimulations of sensory, irrespective of whether individuals are unimpaired or belong to the stroke population [82, 125, 126]. However, passive fabric stimulation experiments involved non-voluntary activities extending the sensorimotor region [82]. Such a circumstance potentially poses an obstacle to the SVM-ML model's ability to discern brain responses to textile stimulations accurately. Voluntary cognitive activities also interfered with the measurement of responses of brain to sensory stimuli [127]. A prime example of this can be observed in the context of sensory evaluation after stroke, where individuals affected by sensory impairments displayed the capacity to distinguish various textile stimulations owing to compensatory cognitive processing. This compensation arises from factors such as

individual experiences and the preservation of residual sensory neural tracts [82]. This study aimed to minimize the impact of voluntary cognitive activities by instructing subjects to maintain wakefulness while refraining from mental engagement in textile stimulations. The objective was to concentrate on capturing the direct brain cortex responses evoked by subtle textile sensations. By utilizing a 21-channel EEG to detect the RSP (repetitive sensory stimulation) features of the sensorimotor cortex, the study deemed these features adequate for discerning variations in the direct brain cortex responses to sensory stimuli.

The findings revealed that the model obtained superior accuracies in the beta and gamma bands' frequency bands when differentiating between textile stimulations without considering differences in arm positions (**Table 2.2**). This was in line with the prior research in neurophysiology that delved into the intricate responses of the brain to tactile stimuli induced by textiles [126, 128]. Neural responses to textile sensations within the brain cortex arise from the intricate interplay between the skin and fabric interactions, featured by activations in the beta and gamma frequency bands of the EEG [129]. The oscillations of beta band are thought to play a role in the process of phasic synchronization in primary sensory cortex and secondary sensory cortex during the processing of fine sensory [130]. Furthermore, researchers have made noteworthy observations regarding the synchronization of neuronal assemblies in the sensorimotor brain region. These assemblies demonstrate expansive neural synchronization, oscillating within the frequency band of beta during prolonged hand lever press

activities [131]. These findings provide compelling evidence that primary sensory and motor cortex are intricately linked within a cortical network synchronized in the beta frequency range [131]. These findings suggest a strong association among primary sensory and motor brain regions, forming a cortical network that is synchronized in the beta band. Additionally, a study has provided evidence indicating that oscillations in beta band in brain region of sensorimotor play a crucial role in featuring affective textile stimulation through intricate interactions with diverse fabric types [132]. Furthermore, another study has proved distinct beta-oscillation patterns for pleasant and unpleasant fine senses [126]. In the context of tactile stimuli, gamma oscillations have also been observed in the sensorimotor cortex. These oscillations serve as a temporal code, playing a vital role in orchestrating the temporal organization of higher-order processing of somatosensory information. This temporal organization is of utmost significance for seamlessly integrating sensory information [133, 134]. Furthermore, Aya et al. have revealed that oscillations of gamma frequency band are simultaneously induced in both the primary and secondary sensory brain regions when the sensory stimulations input, underscoring their significance in establishing functional cortico-cortical relationships and transferring sensory potentials [135]. In a study conducted by Bauer et al., it was demonstrated that spatial tactile attention enhances and prolongs gamma oscillations elicited by tactile stimuli in sensorimotor cortex [136]. The study highlighted the significance of gamma-band synchronization in processing behaviorally relevant stimulations within the somatosensory system [136]. As a result, RSP changes

within the frequency bands of beta and gamma serve as highly informative input features for the SVM classification model, enabling effective classification of different fabric stimulations in both individuals without impairments and stroke patients.

K-Fold CV

In the process of determining the most suitable value for k in CV, the SVM-ML model demonstrated remarkable accuracy when employing a six-fold CV approach within the gamma band, as evidenced by the data presented in **Table 2.3**. The accuracies of different k values within the band of gamma were also similar, indicating the SVM-ML model's consistent and reliable classification performance across different split strategies of datasets [137]. Furthermore, the model's performance, assessed through leave-one-out CV technique, demonstrated performance comparable to that of the k-fold CV approach, specifically within the frequency band of gamma. This finding signifies the model's ability to provide unbiased assessment, showcasing the leave-one-out CV as a unique variant for k-fold CV, where every individual data point effectively serves as a whole testing dataset [138]. Nevertheless, leave-one-out CV had a higher computational cost than other k values in the CV during assessing the performance of SVM model, aligning with similar findings in previous studies [138, 139]. Consequently, our preference lies in utilizing the six-fold CV, as it enables us to conduct comprehensive evaluations of the model.

2.3.2 The SVM Classification Model Generalization

Various Textile Stimulations

We evaluated the model's performance of generalization by comparing accuracies for different fabric stimulations in the gamma band (**Table 2.4**, **Figure 2.5**, and **Figure 2.7(a)**). The accuracy levels observed for wool and nylon fabrics exhibited a notable increase compared to that of cotton textiles. The divergence can be attributed to the varying degrees of stimulation intensity these fabrics exert on the skin. Chen et al. conducted a study demonstrating that higher frequency bands' neural oscillations, such as the gamma band, were comparatively lower during the execution of easier tasks [140]. However, as the difficulty of the task increased, these oscillations intensified, indicating an adaptive response aimed at extracting additional patterns via the sensation environment. Regarding fabric stimulation, cotton is ubiquitous in everyday activities which typically generates least intense stimuli in the passive tactile sensation [82]. Conversely, other two fabrics contribute to a more considerable pronounced tactile sensation owing to the distinctive material characteristics. The interaction with these fabrics may necessitate increased neural effort and cortical capacities to elicit corresponding responses for the provided stimuli [82]. This notion finds further support in the research conducted by Jiao et al., where it was observed that wool evoked a relatively vigorous tactile stimulation resembling scratching, thereby giving rise to a sensation of discomfort [141]. The findings of Jiao et al. provided further evidence to

support the notion that wool fabric triggers a comparatively intense tactile stimulation resembling scratching, leading to a sensation of discomfort. Moreover, their research revealed that woolen textiles induced larger RSP characteristics in EEG compared to nylon and cotton textiles [141]. Furthermore, one study was conducted where they observed significantly elevated event-related potential (ERP) in response to nylon fabric compared to cotton fabric. This observation suggests that tactile sensation with nylon fabric resulted in reduced distraction and improved allocation of cortical resources [129]. Consequently, the model obtained higher accuracies when utilizing the EEG features of nylon and wool fabrics instead of cotton fabric.

Various Upper-Limb Groups

The performance of our model was evaluated in terms of classifying fabric stimulations while involving upper limb differences. The results of this evaluation are presented in **Table 2.5**, **Figure 2.6,** and **Figure 2.7(b)**. We observed significant differences in accuracy when classifying post-stroke stimulations with various textiles, particularly in the higher bands of frequency, when contrasted with unimpaired individuals. The discrepancy obtained when distinguishing different fabric stimuli among the various upper-limb groups aligns with the findings from manual measurements that compared the distinctions on RSP features of EEG among individuals affected by stroke with those without any impairments. The manual evaluations indicated that the power spectra for fine touch stimulation in post-stroke individuals were higher during the

frequency bands of beta/gamma [82]. SVM classification model effectively detected comparable patterns to manual evaluations by leveraging the utilization of EEG's RSP characteristics and RBF kernel's characteristics transformation capability. The incorporation of the mean and maximum values of the RSPs as input characteristics in the SVM model demonstrated an efficient ability to capture noteworthy variations observed in RSP features across various arm cohorts. Previous manual investigations have highlighted the association between EEG RSP patterns elicited by fabric stimulations and neuroplastic changes post-stroke [142]. Specifically, these investigations have indicated that damage to brain neurons resulting in sensorimotor function impairments after stroke can lead to cortical rewiring within various neural subsets [143, 144]. In response to such lesional functions, the brain can exhibit neural compensation, which manifests as a redistribution of the patterns of brain cortex reactions to stimuli [145]. Leveraging its exceptional characteristics' transformation ability, SVM algorithm with RBF kernel demonstrates the ability to determine the best classification boundary among multiple arm groups. Through implicit transformation of the original RSP feature space into a higher dimensional space of feature, the SVM effectively reduces the number of hyperparameters that need to be determined. Consequently, this feature mapping procedure ensures the model's ability to generalize well when presented with new input data [90]. In diverse clinical settings, prior research has consistently shown that SVM with a kernel of RBF exhibits low misclassification rates. Importantly, this SVM model effectively handles the intricacies involved in the

classification process [89, 146, 147]. Due to intricate nature of EEG RSP characteristics and characteristics transformation ability of kernel function in RBF, it could be anticipated that the proposed model would exhibit comparable performance to that of manual inspection in distinguishing individuals without impairments from those who have experienced a stroke.

2.4 Periodic Summary

Our study involved the development of an SVM classification model with EEG signals, specifically focusing on the RSP features (RSP_{mean} and RSP_{max}) derived from cotton fabric stimulation. These features were found to be highly responsive to textile stimulus, which were served as indicative input characteristics for the established model. To assess model's performance in generalization, we conducted a comparative evaluation of classification accuracies for different fabric stimulations, taking into account differences in arm conditions. The model demonstrated significant variations in accuracy when considering fabric stimulations after a stroke, particularly in higher frequency bands such as beta and gamma bands. These results mirrored the RSP patterns observed in manual investigations, where distinctions between post-stroke individuals and those without impairments were evident. This finding indicated that our model could effectively emulate manual assessments of cortical reactions to textile stimulus, thereby facilitating automated assessments of fine tactile sensation in post-stroke individuals.

CHAPTER 3

EFFECTS OF NON-INVASIVE CERVICAL CORD NEUROMODULATION BY TRANS-SPINAL ELECTRICAL STIMULATION ON CORTICO-MUSCULAR DESCENDING PATTERNS IN UPPER EXTREMITY OF CHRONIC STROKE SURVIVORS

3.1 Introduction

Stroke stands as a prominent contributor to enduring motor impairments, and around 3/4 of people having motor deficiencies in the upper limbs [148]. Motor deficits in individuals may potentially arise from lesions that impact both the sensorimotor cortex and the neural descending pathways [149]. These lesions can disrupt the relations of excitation and inhibition potentials between brain and prefrail muscles, resulting in altered descending patterns. This alteration often manifests as muscle spasticity and compensation on the contralesional side [150]. Muscle spasticity refers to involuntary muscle contractions that emerge due to a loss of inhibitory control over the spinal cords alpha motoneurons in the poststroke [151]. Consequently, stroke survivors in chronic stages commonly experience extra excitability of α motor neurons, leading to involuntary muscle contractions [151]. For the muscles responsible for UE movements, the distal UE muscles, which control hand and wrist joints, are particularly easy to the disturb of muscular spasticity and poststroke cortical compensation. This susceptibility

arises from the requirement of a higher precision and control degree in distal movements compared to proximal UE movements involving the shoulder and elbow joints [152]. However, the compensatory rehabilitation approaches typically used in routine practice offer limited benefits to wrist-hand motor functions. These interventions often encourage compensatory motions involving the shoulder and elbow joints once the desired daily task is achieved [153, 154]. Moreover, the motor neural tracts responsible for the distal muscles primarily originate from the lesioned side of hemisphere, and only few motor neural tracts originating from the contralesional hemisphere compared with those serving the proximal UE muscles [155]. Consequently, in neuroplasticity from brain to the muscles, poststroke 'learned disuse' can easily affect wrist-hand muscular functions. This occurs due to the lack of effective controls of excitation or inhibition specifically targeted at the distal UE muscles [156].

The strength of residual motor neural pathways from lesioned brain to the distal muscles of wrist and hand can vary according to the poststroke lesions impairments' level [157]. MEPs obtained through TMS or CMCoh assessed using EMG/EEG in voluntary muscular contractions provide insights into this assessment [158, 159]. Stroke survivors often exhibit significantly decreased CMCoh and MEPs. These findings are related with impairments in offering useful neural potentials in the brain cortex and transmitting residual motor neural drives [160, 161]. Restoring the center of cortex in the lesioned brain poststroke currently lacks immediate methods. This process relies on Hebbian neuroplasticity, which can be strengthened by repeatedly exciting the neurocircuitries

by repetitive training in long-term [162, 163]. However, when the ipsilesional neural tracts remain weak poststroke, facilitating the transferring efficiency of remaining motor neurons innervated the upper limb muscles can be achieved by the modulation of spine's excitation [164]. Trans-spinal electrical stimulation (tsES) emerges as a non-invasive technology that can modulate excitatory thresholds in circuitries of spine through applying transcutaneous current [61, 165]. Researchers have explored tsES application in individuals with spinal cord injury (SCI) to enhance neural pathways across lesioned locations and restore upper limb motor function [166]. For instance, previous research showcased the immediate modulation of spine circuits' excitability and improved motor control for proximal UE muscles in SCI patients via tsES. This was achieved by employing rectangular shape of waveforms with 1 ms from C5 to C6 spincal cord [167]. In addition, tsES has been utilized from C3 to C6 spinal cord for aiding the enhancement of UE in the motor control, including UE tasks like finger grip and pinch, among participants experiencing SCI in spinal cord [168]. These applications have the objective of providing motoneurons' activation within circuits in spine, taking them closer to the activation threshold. This, in turn, facilitates the propagation of impulses through the motor neurons via the remaining motor control tracts via brain [169, 170]. Moreover, tsES has proven to be effective in reducing UE muscular spasticity in SCI patients. Various parameters of electrical stimulation have been used, including pulses of biphasic rectangular at 30 Hz [171]. The primary mechanism behind this effect involves current stimulation of local neural tracts in spine,

achieved through dorsal column neural tracts, as well as engagement of the processes that activate presynaptic inhibition [172].

Despite the limited research conducted on the application of tsES for motor restoration in stroke patients, recent preliminary findings have shown positive outcomes of spinal cord electrical stimulation in enhancing motor control of the upper limb and releasing muscle spasticity after stroke [61, 62]. In a specific study, it was revealed that the electrical stimulation administered in cervical spine led to immediate enhancements in grip force of hand poststroke [61]. However, the invasively implanted electrodes are associated with inherent risks, such as infection and bleeding [173]. Another research endeavor examined the impact of direct electrical stimulation targeting the C6 spine segment, which yielded noteworthy findings. A potential trend was observed, indicating a reduction in spasticity within the wrist flexor muscles. This reduction was achieved by lowering the extra excitation present in α motor neurons of spine subsequent to a stroke [62]. These studies have demonstrated the potential effectiveness of spinal cord stimulation, which involves modulating the excitation state of intact spinal circuitry to improve the responsiveness to the residual neural pathways [62]. However, there is a lack of research assessing the instant influence of tsES in cortical motor neural patterns on peripheral muscles during UE voluntary movements after stroke, which may have the potential to affect brain neuroplasticity in rehabilitation. Consequently, the primary aim of the research was examining the instant influences of tsES in cortico-muscular descending motor patterns in voluntary movements of UE, focusing specifically on

lesioned side of chronic stroke patients.

3.2 Methodology

In this particular study, the primary focus was to investigate the influences of tsES on cortico-muscular motor neural tracts in poststroke patients' UE. The research employed measurements of EEG/EMG to evaluate influence of tsES in lesioned side, with a specific emphasis on extension/flexion tasks of wrist and hand. The analysis involved utilization of CMCoh to examine related coupling among the cortex and upper limb's muscles, thereby facilitating the evaluation of motor control. To assess compensation from the contralesional hemisphere, peak CMCoh's laterality index (LI) was employed. Furthermore, the acquired activation level of EMG was utilized to assess couplings of muscular activation within the UE.

3.2.1 Experimental Setup

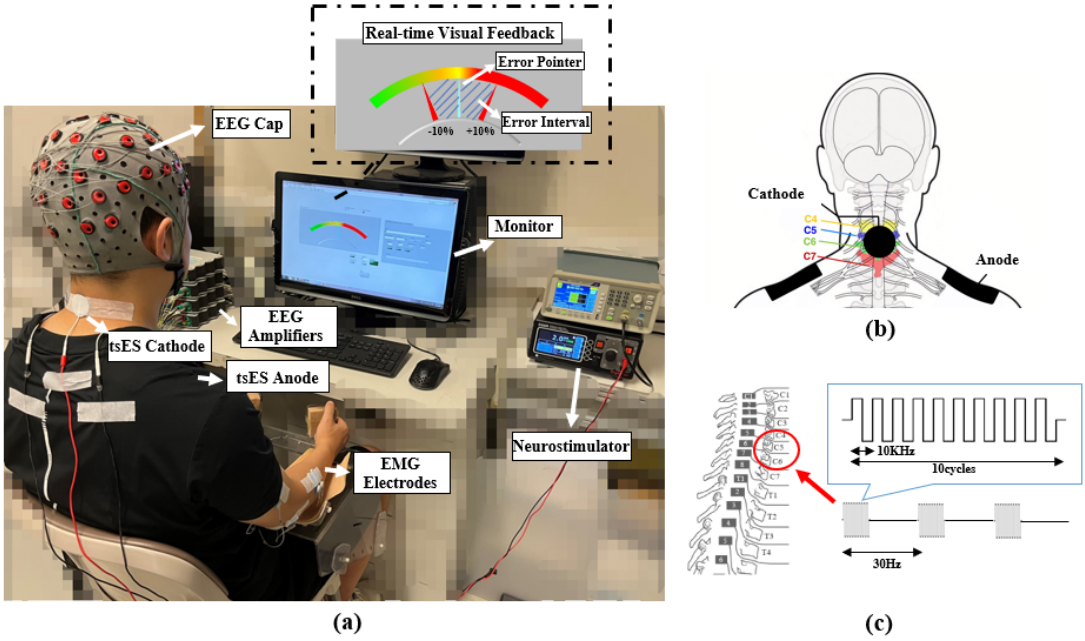

Figure 3.1 The tsES experimental setup. (a) A stroke patient with application of tsES in cervical spine; An illustration of tsES electrodes (b) and electrical stimulation (c).

The experimental setup was demonstrated in **Figure 3.1**, encompassing the placement of cervical spine stimulation site, configuration of electrical current, and the selection of electrodes. Within this setup, a subject poststroke was comfortably sit in a chair, while their lesioned upper limb remained in a silent state (**Figure 3.1(a)**). To ensure proper alignment, the forearm of the affected upper extremity was positioned neutrally on the horizontal plastic slab, confirming that hand's strength exertion was perpendicular to gravity [174]. The configuration of tsES in cervical spine was carried out by an electrical neurostimulator (DS8R). As illustrated in **Figure 3.1(b)**, the circular cathode electrode, measuring 3 cm in diameter, was accurately placed within C4 to C6. In addition, two anode electrodes, sized 8.5 × 6 cm, were interconnected, and positioned bilaterally over the acromioclavicular joints. The choice of C4 to C6 for electrical stimulation was based on the specific involvement of the cervical spinal nerves at different spinal levels in providing muscular control and sensory function of upper limb muscles [22]. More precisely, the nerves from C4 to C5 are responsible for controlling proximal muscles in the UE, as well as those from C5 to C6 govern distal muscles in the UE [23, 24]. The electrical stimulation in this study was applied in the waveform of alternating current, by using rectangular biphasic pulses with 30 Hz, where the direction

of flow changes cyclically over time. The designation of anode and cathode is merely a matter of terminology and was determined based on previous studies [175, 176]. Once the area of electrical stimulation was determined, the current was administered in bursts comprising of ten pulses of rectangular (100 μs for each pulse). The electrical stimulation were transferred at 30 Hz (**Figure 3.1(c)**) [175, 176]. This choice of waveform helps maintain a balanced electrical charge during the stimulation process, promoting the safe and effective delivery of electrical stimulation without causing harm to the tissue in the stimulated area [177, 178]. A 10 kHz was employed as the carrier frequency to avoid perception of pain sensation. The choice of frequency helps reduce the discomfort associated with the stimulation, thereby enabling the use of larger electrical current [59]. It's important to note that the selection of tsES employed in the research was successfully used in SCI and TBI patients, who suggested reasonable levels of pain during the stimulation process [166, 179].

Figure 3.2 shows the procedure of setting the stimulation current intensity (measured in mA) through feedback provided by stroke participants. Initially, the stimulation current intensity was set at 0 mA while gradually increased in increments of 5 mA from 5 to 50 mA, with smaller 1 mA increments used between 50 and 80 mA to minimize discomfort [176]. Before each increment, participants confirmed their tolerance of the sensation for at least half minute. In cases where the current was considered not tolerable, it was then decreased with one increment and subsequently utilized as the optimal intensity for subsequent motor control tasks. A maximum stimulation intensity

threshold of 80 mA was implemented for all participants to ensure safety. This threshold was continuously monitored throughout the experiment to maintain safe stimulation levels on the skin of the cervical spine, based on previous studies involving human subjects [180]. Moreover, participants' physiological responses, including pressure of blood and rate of heart, were supervised real-time at three-minute intervals in process of determining stimulation current.

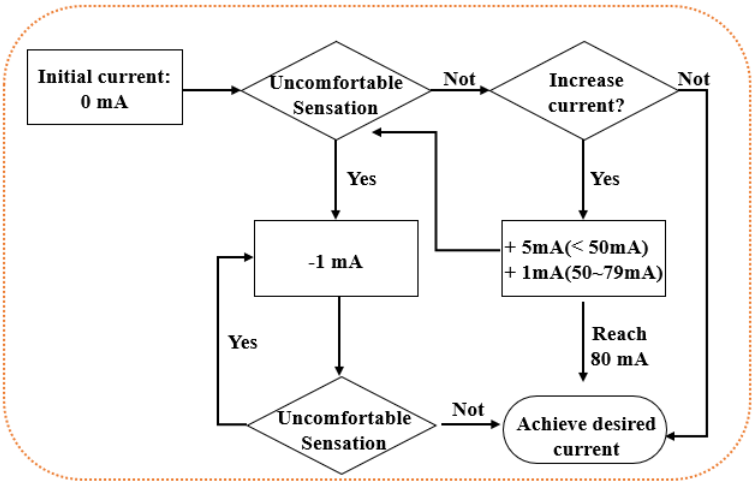

Figure 3.2 The confirmation of stimulation electrical current.

To attach electrodes of EEG, a cap of 64 channels was placed on stroke subject's scalp. Reference electrodes were placed at left earlobe, while the ground electrode was situated at AFz electrode, following the 10-20 standard system. A total of 21 channels were utilized to obtain signals of EEG, specifically targeting the cortex of sensory and motion. These channels covered the following areas: C1, C2, C3, C4, C5, C6, CZ, CP1, CP2, CP3, CP4, CP5, CP6, CPZ, FC1, FC2, FC3, FC4, FC5, FC6, and FCZ. The

sensorimotor cortex was specifically chosen for electrode placement due to its role as the main source of cortico-muscular motor neural tracts [181]. For the collection of EMG signals, five UE muscles were targeted: ECU-ED, FCR-FD, APB, BIC and TRI. The bipolar determination with a 20 mm inter-electrode space was used to capture the signals of EMG for every muscle of upper limb. The olecranon of the elbow was selected as the reference electrodes. Prior to attaching these electrodes, the surface of skin was thoroughly cleaned via abrasive gel and cotton pads to maintain the impedance below five kΩ. For amplification of the EEG signals, the g.USBamp amplifier was employed, providing a 10,000-fold amplification. Subsequently, the signals were subjected to filtering using the bandpass filter spanning in 2-100 Hz. Similarly, the signals of EMG were augmented via the identical amplifier, providing the 1000-fold amplification. These signals were further filtered using a bandpass filter range of 10-500 Hz. Additionally, both EEG and EMG underwent further filtering with a 50 Hz filter to eliminate any interference. In order to obtain the synchronized EMG/EMG data, a DAQ board was selected. The DAQ board operated at the 1200 Hz's sampling frequency, enabling acquisition of high-resolution data. For visual feedback of motor control of wrist and hand, online processing utilized data of EMG obtained specifically from the distal UE muscles. These signals were processed in real-time to provide feedback through a custom interface made via LABVIEW. The interface allowed for interactive control and visualization of the wrist-hand motion based on the acquired EMG signals. As shown in **Figure 3.1(a)**, the interface displayed a color range spanning

from left side to the right side, serving as a visual representation to the progressive levels of agonist muscle contraction. This color range depicted the spectrum from 0-100% of the iMVC in extension/flexion of wrist and hand. For instance, the extension task utilized EMG data of ECU-ED muscle, while the flexion task employed EMG data of FCR-FD muscle. The process of performing iMVC was described in **Section 3.2.3 Evaluation Protocol**. Throughout measurement process, the movement of the blue pointer responsible to the instantaneous changes in the agonist muscles' contraction levels. Simultaneously, the interface featured two constant red pointers that denoted reasonable range of 10% error in the motion control. These red pointers served as visual indicators, ensuring that the measured contraction levels remained within the designated range [182]. The real-time contraction levels of the agonist muscle i were obtained as follows [183]:

$$\mathrm{EMG}_{\mathrm{contraction(i)}} = \frac{\mathrm{EMG_i} - \mathrm{EMG}_{\mathrm{baseline(i)}}}{\mathrm{EMG}_{\mathrm{max(i)}} - \mathrm{EMG}_{\mathrm{baseline(i)}}} \times 100\% \qquad (3.1)$$

Where EMG_i is the mean value in rectified envelope of EMG in muscle i within a window of 100 ms; $EMG_{max(i)}$ denotes the mean value of the rectified envelope of instant EMG for muscle "i" during maximal force. $EMG_{baseline(i)}$ represents the mean value of the rectified envelope of instant EMG for muscle "i" in the state of relax.

3.2.2 Subject Recruitment

Following the acquisition of ethical clearance from the HSESC, recruitment of chronic

stroke individuals was initiated, adhering to the inclusion criteria: (i) Age from 30-70 years old; (ii) Minimal six months since experiencing a unilateral brain damage; (iii) Adequate cognitive abilities to understand experiment's content and fundamental suggestions (MMSE > 21); (iv) appropriate muscle tone in upper limb (MAS < 3); (v) Moderate to severe motor impairments on the affected side of the upper limb (15 < FMA-UE < 55); (vi) detectable voluntary EMG signal; (vii) Ability to sit up for a minimum of 60 minutes. The exclusion criteria consisted of the following: (i) Musculoskeletal dysfunction in upper limb; (ii) Recent botulinum toxin injection in last six months in UE muscles; (iii) Presence of any implanted metal or electronic stimulator, such as a cardiac pacemaker, cochlear implant, etc.; (iv) Use of medications that affect neural excitability, such as antidepressants, antipsychotics, etc.; (v) History of epilepsy or current pregnancy. Finally, a total of 12 individuals who had survived chronic stroke were recruited, with an average age of 51.7 ± 11.3 years. The average time since stroke occurrence was 8.8 ± 5.9 years. **Table 3.1** summarizes the demographic information of involved subjects.

Table 3.1 Demographic information of stroke participants.

Subject	Age (years)	Gender (male/female)	Stroke type (H/I)	Affected side (right/left)	Years since stroke	FMA-UE	MAS-wrist
1	63	M	H	Left	6	39	2
2	65	F	I	Right	13	50	1.4
3	51	F	H	Left	8	36	1
4	54	M	H	Left	3	21	3
5	37	M	H	Right	19	45	1.4
6	41	F	H	Right	7	55	1
7	50	F	H	Left	3	49	1
8	59	M	I	Right	11	50	2
9	41	F	H	Right	10	19	2
10	67	M	I	Left	19	35	3
11	34	M	H	Left	3	43	1.4
12	58	F	H	Right	3	43	1.4
Overall	51.7±11.3	6/6	9/3	6/6	8.8±5.9	40.4±11.2	1.7±0.7

Note: H: Hemorrhagic; I: Ischemic.

The stroke participants in Chapter 3 were distinct from those in Chapter 2 due to differences in the experimental procedures. Ethical approval from the university is required for experiments involving human subjects. Both Chapter 2 and Chapter 3 received separate ethical approvals, resulting in a time delay between the two experiments. In Chapter 2, we initially conducted the experiment focused on assessing fine tactile sensation through fabric stimulation after obtaining the necessary ethical approval. Subsequently, in Chapter 3, we performed the tsES experiment by recruiting new stroke subjects from our pool of patients. This was necessary because some stroke patients from study I either declined participation or were not available due to personal reasons.

3.2.3 Evaluation Protocol

Prior to the sessions, an initial measurement of iMVC was performed to establish the relaxed and maximal levels of EMG data for visual feedback in the perform of motor control tasks involving five specific muscles. The iMVC assessment of agonist muscle followed the protocol outlined in reference [27] and involved three repetitions with the following steps: (i) The subject maintained the upper limb in a resting state for five seconds to obtain the relaxed signal of EMG; (ii) The subject was then instructed to fastly generate maximal strength with muscle and sustain contraction for 5 seconds. To impede fatigue of muscles, a 5-minute break was provided between consecutive contractions. The highest value among three iMVC assessments was chosen as the maximal level of EMG for every muscle in upper limb.

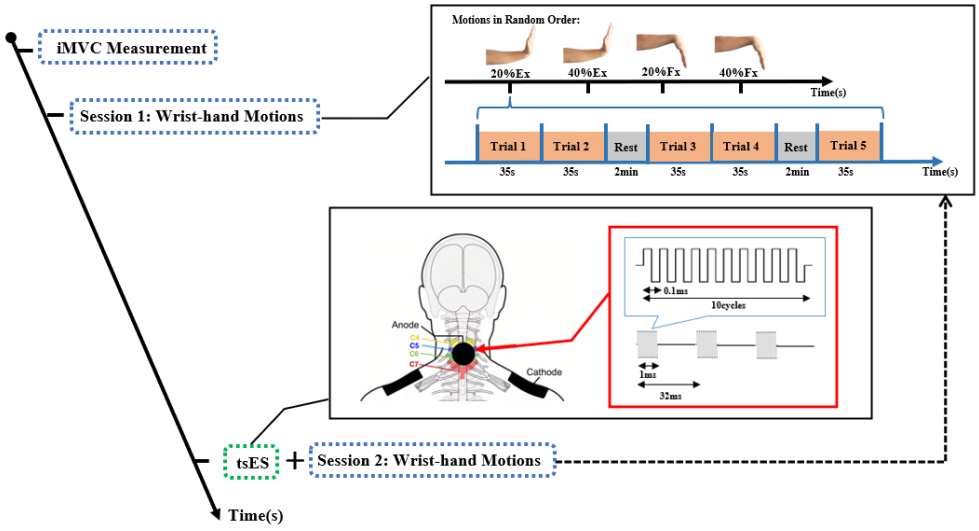

Figure 3.3 The protocol for motions tasks with tsES in the wrist and hand.

Following measuring iMVC, motion tasks were conducted in two sessions in lesioned side of patients poststroke (**Figure 3.3**). The 1st session focused on extension/ flexion in wrist and hand, without employing tsES. Two distinct degrees of muscular contraction, representing twenty percent and forty percent of each subject's iMVC, were utilized and labeled as 20% Ex, 40% Ex, 20% Fx, and 40% Fx. The participants poststroke followed randomly presented motion task names displayed on a monitor screen to perform the wrist-hand contractions. The objective was to achieve best muscular control, defined as maintaining a zero percent deviation from central line for thirty-five seconds, with fluctuations within an error of -10% to +10%. To prevent muscle fatigue, each motion task was repeated five times, with a 2-minute rest period between each repetition. Muscle fatigue was assessed by monitoring the average EMG power spectrum's frequency, considering a 10% reduction as an indication of fatigue [184, 185]. No signs of muscle fatigue were observed throughout the entire duration of the wrist-hand extension and flexion.

After completing the 1st session of motion, the neurostimulator was activated. Based on stroke participant's feedback following the procedure outlined in Section 3.2.1 of the Experimental Setup, the optimal current of current was confirmed. Across all participants, the mean value of the optimal electrical current was 42.9 ± 13.9 mA, ranging from 12-70 mA. Following the confirmation of the optimal electrical current, tsES was applied on cervical spine. The stroke patient was then asked to conduct 2nd session of motion, which had the identical procedures as 1st session. The tsES duration

matched the duration of motor functions in UE, totaling 1660 seconds. This duration was derived from four motion tasks, each comprising five 35-second trials, along with two 2-minute rest periods. To ensure the accuracy of signals of collected EEG/EMG, stroke participants were advised to avoid head movements and eye blink, prior to every trial in two sessions of motions.

3.2.4 EEG and EMG Processing

To assess impact of tsES on cortico-muscular interactions, several factors were examined, involving CMCoh, LI, and activation levels of EMG. A comparison was made between the phenomenon of not involving tsES and involving tsES to assess any differences or effects. The captured EEG signals underwent a filtration process employing a 3rd-order Butterworth bandstop filter. This filtering step aimed to remove any potential artifacts caused by the applied stimulation during the task involving movement of the wrist and hand. Specifically, a band-stop filter with a range of 29-31 Hz was applied to effectively attenuate the artifacts of stimulation occurring at a frequency of 30 Hz, thus minimizing their impact on obtained EEG, as practiced in [186]. The application of electrical stimulation resulted in a noticeable and consistent results in obtained EEG data for time domain, as depicted in **Figure 3.4(a)** to **(b)**. In the domain of frequency, PSD of EEG exhibited a prominent peak at 30 Hz, as shown in **Figure 3.4(c)**. However, upon implementing band-stop filter, spectra of EEG exhibited a similarity to those obtained in the absence of electrical stimulation. This

observation indicates that the effectiveness of band-stop filter in eliminating the artifacts from the EEG.

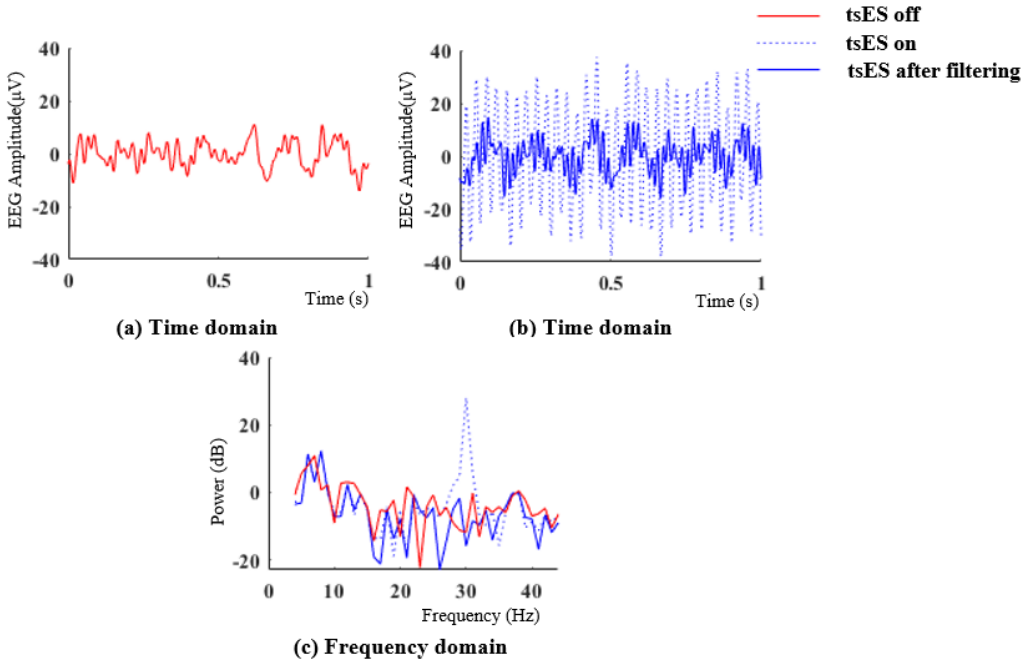

Figure 3.4 EEG signals from CZ channel for a 1s' interval of upper limb flexion at 20% iMVC when activating tsES. The time domain representation of the EEG amplitude is depicted in (a)~(b). The EEG PSD in domain of frequency is shown in (c).

To estimate the cortico-muscular coupling patterns, coherence among EEG via sensorimotor cortex and EMG via five upper limb muscles were analyzed. The CMCoh was specifically calculated within the beta frequency band, ranging from 13-29 Hz. It is worth noting that the beta frequency band is known to exhibit the most pronounced CMCoh during steady and moderate isometric muscle contractions [187, 188]. The calculation of CMCoh values was performed using the following method:

$$\mathrm{CMCoh}_{\mathrm{EEG,EMG}}(\mathrm{f}) = \frac{|\mathrm{P}_{\mathrm{EEG,EMG}}(\mathrm{f})|^2}{\mathrm{P}_{\mathrm{EEG}}(\mathrm{f})\cdot\mathrm{P}_{\mathrm{EMG}}(\mathrm{f})} \qquad (3.2)$$

$$\mathrm{P}_{\mathrm{EEG,EMG}}(\mathrm{f}) = \frac{1}{\mathrm{n}}\sum_{i=1}^{n} \mathrm{EEG_i}(\mathrm{f})\mathrm{EMG_i^*}(\mathrm{f}) \qquad (3.3)$$

Where $P_{EEG,\ EMG}(f)$ represents cross-spectrum density, $P_{EEG}(f)$, $P_{EMG}(f)$ are auto-spectrum densities of the data of EEG/EMG. The coupling estimation offers a standardized assessment for magnitude of CMCoh patterns, shown as a continuous numerical value within the range of 0 to 1. A value of 0 signifies a total absence of connection, while a value of 1 signifies a perfect correlation [160]. The statistical significance of the CMCoh value was determined based on a threshold of $P < 0.05$. This significance level was established by comparing the CMCoh value to the confidence level (CL), and it could be obtained by Equation (3.4):

$$\mathrm{CL} = 1 - 0.05^{1/(L-1)} \qquad (3.4)$$

Where the parameter L represents epochs of trial. For every EEG/EMG trial, the duration was thirty seconds. Initially, the trials were 35 seconds long, but the final 5 seconds were removed. Each trial was then divided into 1200 data points, representing 1-second segments, with a 50% overlap between adjacent segments. A total of 275 trial epochs were obtained, resulting from 55 trial segments multiplied by 5 trial numbers. These trial epochs provided the EEG/EMG data for evaluation. To determine statistical significance of the CMC values, a confidence level (CL) of 0.011 was utilized. This CL served as the threshold to assess whether the CMC values exceeded the expected level of chance occurrence. The maximal CMCoh were measured for every muscle in UE.

This measurement aimed to obtain the most significant CMCoh among EEG/EMG signals for motion tasks of UE. By identifying the peak CMCoh values, the specific instances of high coherence between the cortical EEG activity and the corresponding muscle activation were determined for each UE muscle [189]. To visualize activation region in the cortex with the highest CMCoh, the topography of the peak CMCoh was employed. Additionally, LI was employed to evaluate the relative hemispheric lateralization of the peak CMCoh in all stroke participants, as shown in Equation (3.5):

$$\text{Laterality Index} = \frac{\text{Coh}_{\text{ipsilesional}}}{\max(\text{Coh}_{\text{contralesional}}, \text{Coh}_{\text{midsagittal}})} \qquad (3.5)$$

Where CMCoh in the ipsilesional, contralesional, and midsagittal hemispheres are represented by $\text{Coh}_{\text{ipsilesional}}$, $\text{Coh}_{\text{contralesional}}$, and $\text{Coh}_{\text{midsagittal}}$. The LI values, which indicate hemisphere dominance of peak CMCoh, are assessed based on whether they are smaller than 1 (indicating contralesional hemisphere dominance) or larger than 1 (indicating ipsilesional hemisphere dominance) [190].

To assess the results for muscle activation in motion tasks of wrist and hand, the normalized EMG activation levels were utilized [191]. The initial EMG for a specific muscle, denoted as muscle i, was first standardized via relaxed and maximal levels in the period of iMVC. This normalization process was achieved using Equation (3.6). Subsequently, the activation level of EEG for muscle i was determined using Equation (3.7):

$$\mathrm{EMG_{Normalized(i)}} = \frac{\mathrm{EMG_{origin(i)} - EMG_{baseline(i)}}}{\mathrm{EMG_{max(i)} - EMG_{baseline(i)}}} \times 100\% \qquad (3.6)$$

$$\mathrm{EMG_{ActLevel(i)}} = \frac{1}{\mathrm{T}} \int_0^{\mathrm{T}} \mathrm{EMG_{Normalized(i)}}(\mathrm{t})\mathrm{dt} \qquad (3.7)$$

Where standardized EMG of muscle i is represented as $EMG_{Normalized(i)}$, $\int_0^{\mathrm{T}} \mathrm{EMG_{Normalized(i)}}(\mathrm{t})\mathrm{dt}$ is envelope of muscle i's EMG during T. After normalization, the activation level of muscle i's EMG is computed as $EMG_{ActLevel(i)}$. The evaluation of EEG/EMG data was performed by applying customized code based on FieldTrip in MATLAB R2019b, which can be found at http://www.fieldtrip.fcdonders.nl. This customized code facilitated the analysis and processing of the EEG and EMG data, enabling the acquisition of the evaluation outcomes.

3.2.5 Statistical Analysis

Figure 3.5 presents the statistical analysis to compare the obtained CMCoh-related parameters without tsES and with tsES. The normality of these measurements was assessed via Shapiro-Wilk test. Regarding the CMCoh values, it was found that both groups displayed a normal distribution at both iMVC levels of every motion ($P > 0.05$). However, exceptions were observed in TRI (40% Ex), BIC (20% Fx), APB (20% Ex & 40% Fx), where the distribution deviated from normality ($P < 0.05$). Regarding the LI, it was observed that both groups exhibited a normal distribution in ECU-ED at both iMVC level of Ex, as well as 20% Fx's FCR-FD. However, in 40% Fx of FCR-FD, the distribution deviated from normality ($P < 0.05$). The activation levels of EMG in two groups exhibited the normal distribution ($P > 0.05$), except for FCR-FD (20% Ex), BIC

(40% Ex), TRI (20% & 40% Fx), where distribution deviated from normality. For the parameters that exhibited a normal distribution (P > 0.05), a paired t-test was employed to assess the differences without tsES and with tsES. On the other hand, for parameters that did not follow a normal distribution (P < 0.05), Wilcoxon signed-rank test was utilized for assessing conditions' variations without and with tsES. In this study, a statistical significance level of 0.05 was predetermined.

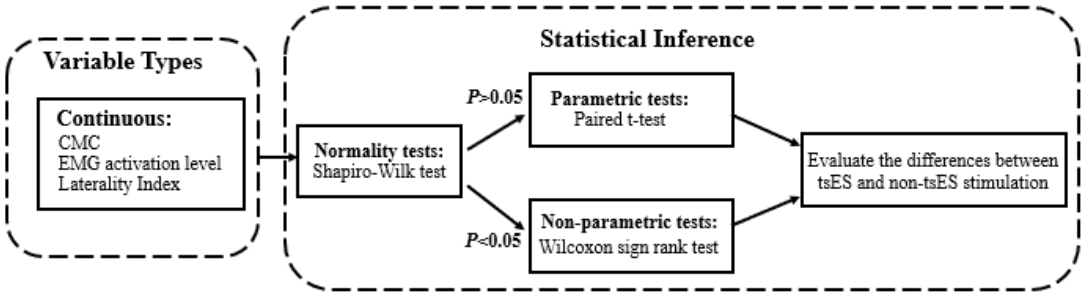

Figure 3.5 The flowchart of the statistical analysis.

3.3 Results

3.3.1 Cortico-muscular Coherence

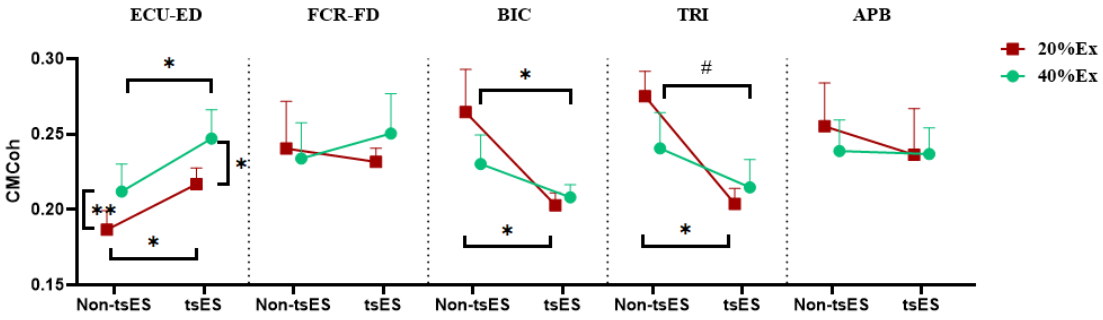

(a)

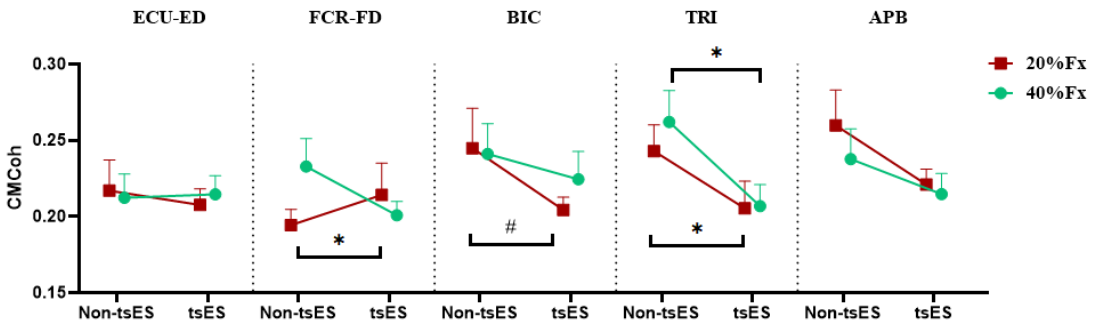

(b)

Figure 3.6 CMCoh during (a) extension and (b) flexion in wrist and hand without tsES and with tsES. The observed differences were indicated follows: '*': $P < 0.05$ and '**': $P < 0.01$ (Paired t-test), '#': $P < 0.05$ (Wilcoxon signed rank test).

In **Figure 3.6**, the CMCoh values are presented for wrist-hand motions, comparing without tsES and with tsES. **Table 3.2** and **Table 3.3** provide the detailed conclusion of the statistical findings considering CMCoh. Specifically, during extension motion, the ECU-ED's CMCoh statistically increased under tsES in two levels of extension contraction ($p < 0.05$). In contrast, BIC exhibited the statistical reduction in CMCoh with tsES at two levels of extension contraction ($p < 0.05$). Similarly, TRI showed a notable reduction in CMCoh at both contraction levels ($p < 0.05$). Furthermore, it was found that ECU-ED's CMCoh statistically increased from twenty to forty percent extension at two conditions. During flexion tasks of wrist and hand, muscle of FCR-FD showed a statistically increase in CMCoh at twenty percent of flexion ($p < 0.05$). Conversely, the CMCoh values of TRI and BIC showed a significant decrease at two

levels of agonist muscles during tsES ($p < 0.05$), other than BIC at forty percent of flexion. Nevertheless, no statistical variations observed when comparing CMCoh values of other upper limb muscles within and with group comparisons.

Table 3.2 CMCoh of upper limb muscles during extension of wrist and hand without tsES and with tsES.

Muscle		20%Extension	40%Extension	P (Partial η^2)
		CMCoh (Mean±SD)		
ECU-ED	Non-tsES	0.187±0.009	0.212±0.011	**0.009****(0.457)
	tsES	0.217±0.011	0.247±0.019	**0.023***(0.618)
	P (Partial η^2)	**0.030*** (0.801)	**0.036*** (0.767)	
FCR-FD	Non-tsES	0.240±0.031	0.233±0.024	0.846(0.063)
	tsES	0.232±0.020	0.239±0.018	0.321(0.127)
	P (Partial η^2)	0.829(0.070)	0.590(0.061)	
BIC	Non-tsES	0.265±0.028	0.230±0.019	0.285(0.340)
	tsES	0.203±0.013	0.208±0.008	0.749(0.202)
	P (Partial η^2)	**0.048***(0.686)	**0.041***(0.397)	
TRI	Non-tsES	0.275±0.037	0.241±0.024	0.878(0.048)
	tsES	0.204±0.010	0.215±0.018	0.799(0.081)
	P (Partial η^2)	**0.010***(0.579)	**0.047#** (0.629)	
APB	Non-tsES	0.255±0.029	0.239±0.020	0.612(0.166)
	tsES	0.236±0.031	0.237±0.017	0.610(0.161)
	P (Partial η^2)	0.241(0.371)	0.907(0.038)	

Note: The observed differences is indicated: '*': $P < 0.05$ and '**': $P < 0.01$ (Paired t-test), and '#': $P < 0.05$ (Wilcoxon signed-rank test).

Table 3.3 CMCoh of upper limb muscles during flexion of wrist and hand without tsES and with tsES.

Muscle		20%Flexion	40%Flexion	*P* (Partial η^2)
		CMCoh (Mean±SD)		
ECU-ED	Non-tsES	0.217±0.020	0.212±0.015	0.820(0.074)
	tsES	0.208±0.011	0.215±0.012	0.603(0.170)
	P (Partial η^2)	0.717(0.118)	0.921(0.032)	
FCR-FD	Non-tsES	0.194±0.010	0.233±0.018	0.376(0.670)
	tsES	0.214±0.021	0.201±0.009	0.462(0.155)
	P (Partial η^2)	**0.043***(0.070)	0.206(0.430)	
BIC	Non-tsES	0.245±0.026	0.241±0.019	0.878(0.050)
	tsES	0.204±0.008	0.224±0.018	0.304(0.345)
	P (Partial η^2)	**0.045**#	0.538(0.202)	
TRI	Non-tsES	0.243±0.017	0.262±0.020	0.346(0.315)
	tsES	0.205±0.017	0.207±0.014	0.869(0.054)
	P (Partial η^2)	**0.016***(0.477)	**0.023***(0.671)	
APB	Non-tsES	0.260±0.023	0.221±0.018	0.445(0.242)
	tsES	0.238±0.020	0.215±0.013	0.575(0.117)
	P (Partial η^2)	0.219(0.417)	0.445(0.278)	

Note: The observed differences is indicated: '*': $P < 0.05$ (Paired t-test), and '#': $P < 0.05$ (Wilcoxon signed rank test).

3.3.2 Cortico-muscular Coherence Topography

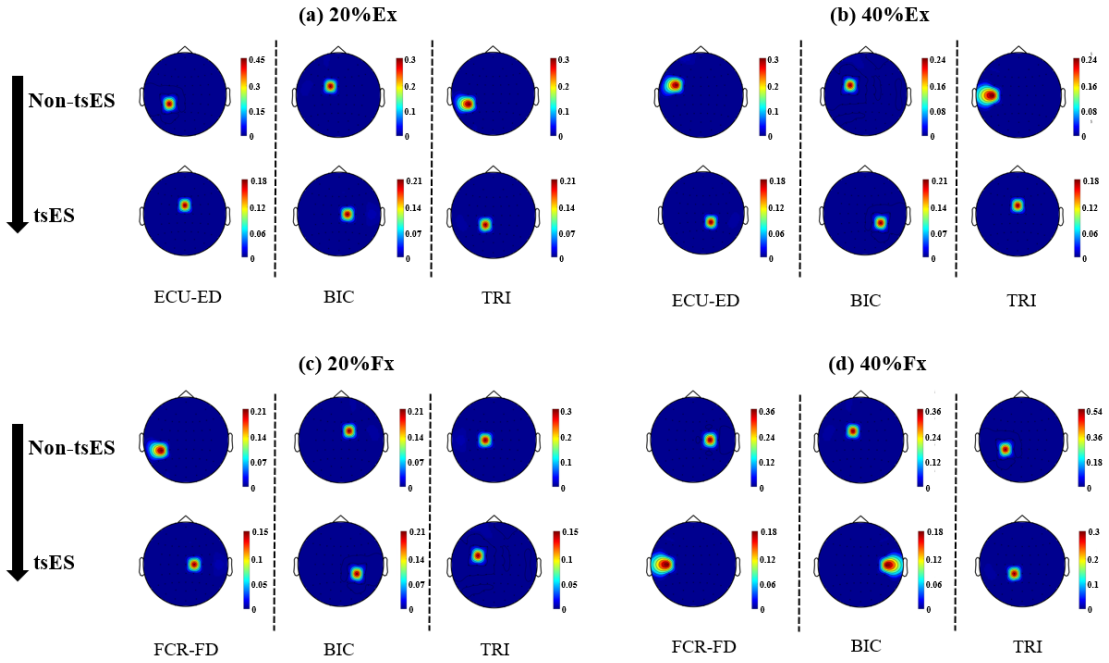

Figure 3.7 Topographies of CMCoh in a stroke subject (left hemiplegia) during wrist-hand motions. The muscles included are ECU-ED, BIC, and TRI for (a) 20% and (b) 40% Ex. The muscles included are FCR-FD, BIC, and TRI for (c) 20% and (d) 40% Fx. The topographies are presented for both without tsES and with tsES.

In **Figure 3.7**, we observe the topographies of CMCoh in the stroke patient (left hemiplegia). The visual representation illustrates the effect of applying tsES, which seemed to induce a shift in the peak CMCoh channel. Specifically, during the extension of upper limb, there is a distinct shift in the CMCoh channel of peak value from the non-lesion side to lesioned side of cortex. Specifically, at 20% Ex (**Figure 3.7(a)**), we observe the following shifts in the peak CMCoh channel for the corresponding muscles:

for ECU-ED, the CMCoh moves from CP3-FCZ; for BIC, the CMCoh shifts from FC1-C1; for TRI, the CMCoh transitions from CP5-CP1. For forty percent of extension (**Figure 3.7(b)**), we observe further shifts in the peak CMCoh channel for the muscles involved in wrist-hand extension. The specific changes are as follows: for ECU-ED, CMCoh shifts from FC5-CP2; for BIC, CMCoh moves from FC3-CP4; for TRI, CMCoh transitions from C5-FCZ. Similarly, we observe the shift pattern at twenty percent of flexion (**Figure 3.7(c)**) during flexion of wrist and hand. CMCoh for FCR-FD shifts from CP5-C1, while for BIC, it moves from FC1-CP4. Furthermore, at forty percent of flexion (**Figure 3.7(d)**), we observed a specific shift in CMCoh of BIC. It transitions from FC1-C5.

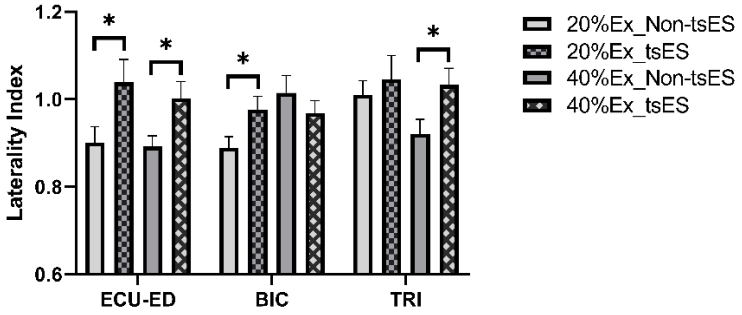

(a)

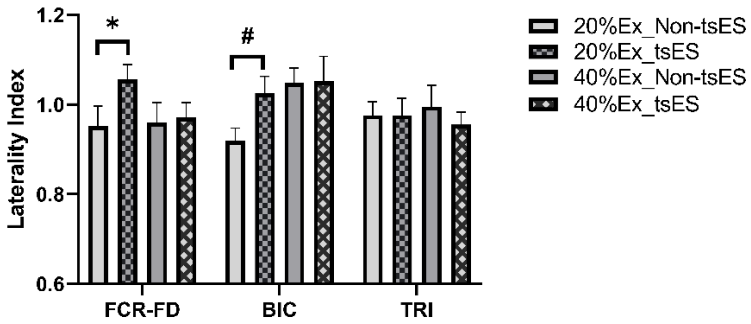

(b)

Figure 3.8 LI during (a) extension and (b) flexion of wrist and hand.

In **Figure 3.8**, the LI during extension and flexion of wrist and hand are presented. Further detailed statistical analysis of LI values could be obtained in **Table 3.4** & **3.5**. During the extension motion tasks, there were significant differences in LI in the following muscles: ECU-ED exhibited significantly higher LI values at both 20% and 40% Ex. BIC showed significantly higher LI values at 20% Ex. TRI demonstrated significantly higher LI values at 40% Ex. These differences were determined through a Paired t-test ($p < 0.05$). In the case of the flexion motion tasks, there were significant differences in LI values in the following muscles: FCR-FD exhibited significantly higher LI values at 20% Fx. BIC showed significantly higher LI values at 20% Fx. This difference was determined using a Wilcoxon signed-rank test ($p < 0.05$), whereas no statistical variation in LI was observed in FCR-FD at forty percent of flexion.

Table 3.4 LI values during extension of wrist and hand without tsES and with tsES.

Muscle		20%Extension	40%Ex Extension
		Laterality Index (Mean±SD)	
ECU-ED	Non-tsES	0.901±0.036	0.892±0.024
	tsES	1.039±0.052	1.002±0.039
	P (Partial η^2)	**0.039***(0.680)	**0.040***(0.680)
BIC	Non-tsES	0.889±0.025	1.015±0.040
	tsES	0.976±0.031	0.968±0.029
	P (Partial η^2)	**0.019***(0.796)	0.332(0.282)
TRI	Non-tsES	1.010±0.032	0.921±0.033
	tsES	1.046±0.054	1.033±0.038
	P (Partial η^2)	0.325(0.300)	**0.026***(0.742)

Note: The observed differences is indicated as follows: '*' denotes $P < 0.05$ based on Paired t-test.

Table 3.5 LI values during flexion of wrist and hand without tsES and with tsES.

Muscle		20%Flexion	40%Flexion
		Laterality Index (Mean±SD)	
FCR-FD	Non-tsES	0.952±0.044	0.960±0.045
	tsES	1.056±0.033	0.971±0.033
	P (Partial η^2)	**0.031***(0.711)	0.805(0.079)
BIC	Non-tsES	0.919±0.028	1.049±0.032
	tsES	1.025±0.038	1.052±0.055
	P (Partial η^2)	**0.023**$^{\#}$	0.951(0.014)
TRI	Non-tsES	0.976±0.030	0.995±0.048
	tsES	0.976±0.038	0.955±0.028
	P (Partial η^2)	0.988(0.000)	0.446(0.224)

Note: The observed differences is indicated as follows: '*' denotes P < 0.05 based on Paired t-test, and '#' for P < 0.05 based on Wilcoxon signed rank test.

3.3.3 EMG Activation Level

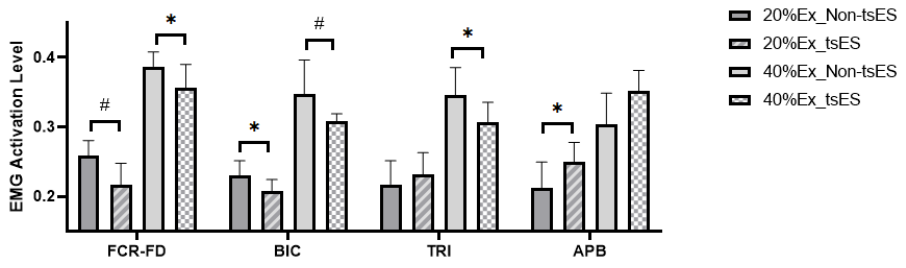

(a)

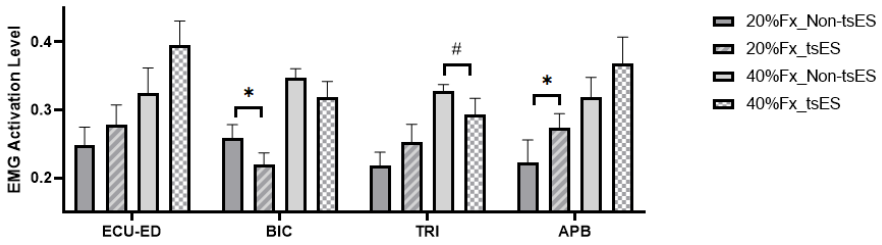

(b)

Figure 3.9 EMG activation levels during (a) extension and (b) flexion of wrist and hand without tsES and with tsES.

Figure 3.9 illustrates the EMG activation levels during motions of wrist and hand. **Table 3.6** and **Table 3.7** contain the significant details, including p-values and effect sizes, for the activation levels of EMG. In the case of the 20% Ex condition, there was a significant decrease in the EMG activation levels of the FCR-FD ($p < 0.05$) and BIC ($p < 0.05$). Conversely, the activation levels of the EMG in APB showed a significant increase ($p < 0.05$). During the 40% Ex condition, there were significant decreases in the EMG activation levels of the FCR-FD, TRI ($p < 0.05$), and BIC ($p < 0.05$). The 20% Fx condition showed a significant increase in the EMG activation level of the APB muscle ($p < 0.05$). Conversely, the BIC muscle exhibited a significant decrease in its activation level of EMG ($p < 0.05$). For the forty percent of flexion condition, the activation level of EMG for the TRI muscle demonstrated a statistical decrease ($p < 0.05$). However, no significant differences were observed in the activation levels of EMG for the other muscles when comparing between different groups.

Table 3.6 EMG activation level of upper limb muscles during extension of wrist and hand without tsES and with tsES.

Motion		FCR-FD	BIC	TRI	APB
		EMG activation level (Mean ± SD)			
20%Ex	Non-tsES	0.258±0.022	0.231±0.021	0.217±0.034	0.213±0.037
	tsES	0.217±0.031	0.208±0.017	0.232±0.031	0.250±0.027
	P (Partial η^2)	**0.041**#	**0.038***(0.292)	0.542(0.200)	**0.025***(0.385)
40%Ex	Non-tsES	0.387±0.021	0.348±0.049	0.346±0.039	0.304±0.044
	tsES	0.356±0.034	0.308±0.011	0.307±0.028	0.352±0.029
	P (Partial η^2)	**0.040***(0.757)	**0.039**#	**0.019***(0.363)	0.291(0.355)

Note: The observed differences is indicated as follows: '*' for $P < 0.05$ (Paired t-test), and '#' for $P < 0.05$ (Wilcoxon signed rank test).

Table 3.7 EMG activation level of upper limb muscles during flexion of wrist and hand without tsES and with tsES.

Motion		ECU-ED	BIC	TRI	APB
		EMG activation level (Mean ± SD)			
20%Fx	Non-tsES	0.248±0.027	0.259±0.020	0.218±0.020	0.223±0.033
	tsES	0.279±0.011	0.220±0.017	0.253±0.026	0.274±0.020
	P (Partial η^2)	0.405(0.276)	**0.043***(0.744)	0.445	**0.018***(0.458)
40%Fx	Non-tsES	0.324±0.037	0.347±0.014	0.328±0.009	0.318±0.030
	tsES	0.395±0.055	0.319±0.023	0.293±0.023	0.368±0.039
	P (Partial η^2)	0.067(0.646)	0.148(0.501)	**0.033#**	0.368(0.300)

Note: The observed differences is indicated as follows: '*' for $P < 0.05$ (Paired t-test), and '#' for $P < 0.05$ (Wilcoxon signed rank test).

3.4 Discussion

The primary objective of this study was to investigate the instant influence of tsES on cortico-muscular motor control patterns in upper limbs of individuals diagnosed with stroke during movement of wrist and hand. The study specifically focused on comparing the differences in coherence between CMCoh, the LI, and activation levels of EMG without tsES and with tsES. According to the findings of the study, it was observed that the values of coherence between CMCoh moved to the lesioned side when tsES was applied. The shift in peak CMCoh suggests that tsES has the potential to

instantly improve remaining motor control pathways that originate from the lesioned side. As a result, tsES may also help decrease compensation influences exerted by the non-lesioned brain side in motion controlling of distal muscles in the UE (Figure 3.10).

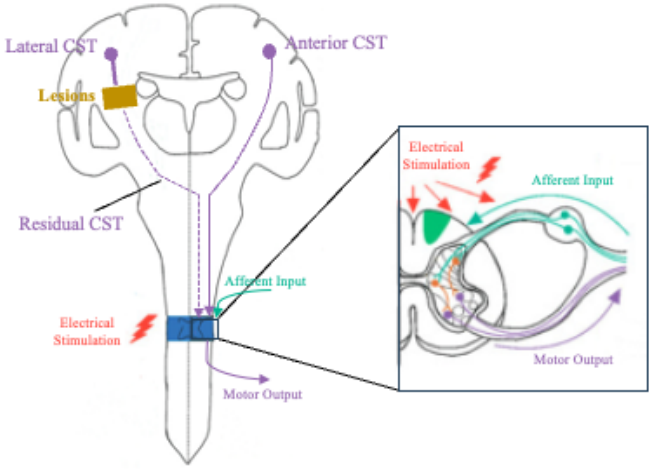

Figure 3.10 The illustration of tsES neuromodulation mechanism

3.4.1 tsES improved excitation/ inhibition control of UE muscles

The improved excitation controlling of cerebral cortex for the muscles was illustrated via substantial improvement in CMCoh of agonist UE muscles, such as ECU-ED in twenty and forty percent's extension, FCR-FD in twenty percent's flexion) (**Figure 3.6**). The changes in CMCoh provide evidence of the immediate impact of tsES on enhancing the precision for controlling motion tasks of wrist and hand at different difficulty levels. This effect is attributed to the interactions between sensory and motor neural networks in cervical spine. These networks actively regulate physiological states, resulting in an amplified responsiveness to descending neural tracts' signals originating from the

cerebral cortex [192]. The sensory pathways in the cervical spinal cord, known as ascending tracts, transmit somatosensory information from the body to the brain through the white matter of the spinal cord [192]. During tsES, the focus is primarily on providing "touch sensation" in the dorsal/posterior root, where the gracilis and cuneate fasciculi transmit this sensory information to the cerebral cortex [192]. In this study, the stroke patients actively engaged in voluntary movements, which primarily involved the descending tract known as the lateral corticospinal tract [192].

Prior research involving persons has employed PAD as a method for examining the effects in recruiting group Ia/Ib neural fibers in MEPs of cervical spine [193, 194]. The results obtained from this study provided confirmation that the application of continuous electrical stimulation exhibits a preferential activation and recruitment of proprioceptive sensory fibers with larger to medium diameters. These specific fibers are primarily situated in the dorsal root/column [195]. These myelinated axons, found within the neural tracts of the vertebral canal, exhibit greater responsiveness to external electrical stimulation due to their lower excitation thresholds compared to alpha motor fibers [196]. Located in the dorsal root of the spine, where their neuronal somas are situated, these fibers are capable of transferring potentials of excitatory to the spinal motoneurons and interneurons through both mono- and poly-synaptic proprioceptive circuits [197]. As a result, the elevation of membrane potentials in spinal neurons enhances the response for spinal neural tracts to motor control that originate from the brain [198].

In the case of stroke participants, there was no disparity in the CMCoh of antagonist muscles among the conditions without tsES and with tsES. However, activation levels of EMG in FCR-FD during wrist-hand extension exhibited a significant decrease when tsES was applied (Figure 3.9(a)). The observed decrease in muscular output implied the potential recruitment of local inhibition neural tracts in spine, leading to precise interactive inhibition [199]. Reciprocal inhibition primarily occurs through the mediation of Ia afferents, that convey inhibition potentials toward the antagonist UE muscle, suppressing the activation while in motion [200]. Nevertheless, evidence shows a decrease in transmission along the interactive inhibitory tracts in patients affected by stroke. This results in heightened excitability of the α motoneurons responsible for regulating antagonist UE muscle [201, 202]. Electrical stimulation assists in depolarizing Ia fibers located in posterior column, subsequently establishing robust synaptic connections with spinal cord's inhibitory interneurons [203]. By activating these inhibitory interneurons, it is possible to augment the inhibitory regulation of the antagonist muscle, thereby diminishing its recruitment and enhancing coordination between muscles of agonist/antagonist [204].

3.4.2 tsES decreased cortical/proximal muscular compensation influence

During execution of wrist-hand extension and flexion movements, the proximal muscles, specifically the BIC and TRI as illustrated in **Figure 3.6**, exhibited a notable

decrease in peak CMCoh when tsES was applied. The observed phenomenon indicates a relatively diminished allocation of cortical resources for the innervation of proximal muscles in the UE during distal motions of upper limb. The tsES was found to elicit a decreasing trend in activation levels of EMG in proximal muscles (**Figure 3.9**). Distal movements of the upper extremity showed a reduced reliance on proximal muscular compensation, indicating the influence of continuous spinal cord stimulation on the improved physiological condition of neural tracts in spine. This heightened physiological state increases the response of neural tracts in spine to supraspinal commands transmitted through the remaining motor pathways [205, 206]. The application of tsES resulted in a notable increase in the LI within the proximal muscles of upper limb in execution of motions in wrist and hand (**Figure 3.8**). Specifically, the BIC demonstrated a significant increase in LI in 20% extension/flexion in wrist and hand, while the TRI demonstrated a LI increase of 40% during wrist-hand extension when tsES was applied. The reorientation of lateralization in hemisphere to the ipsilesional side led to decreased control from the non-lesioned side to proximal UE muscles, consequently reducing compensation of these muscles. Prior research has examined the compensatory contractions displayed by the proximal UE muscles following a stroke, revealing a relocation of the cortical motor controlling center for these muscles to the contralesional side [183]. Furthermore, an fMRI investigation has documented heightened flow of blood for multiple cortices within the non-lesioned side when stroke patients executed gripping tasks. This finding suggests a higher level of

activation in the contralesional cortex compared to individuals without impairments serving as control participants [26]. While proximal-to-distal compensation in the UE offers an alternative for impaired distal movement following a stroke, it can also contribute to the phenomenon known as "learned disuse". Unfortunately, learned disuse can lead to additional motor deficits such as reduced dexterity and the development of abnormal muscle synergies [207]. Impairment of motor control in distal UE muscles exhibits greater severity because of the damage sustained by the main sensorimotor area and its associated motor control neural pathway after stroke, in contrast to the impairment observed in proximal UE muscles. The variation observed can be attributed to the fact that the distal muscles of the UE primarily receive innervation from the lateral CST, which was mainly from the ipsilesional side. This tract is more susceptible to damage caused by stroke, leading to the observed differences. Conversely, the anterior CST, responsible for controlling the proximal muscles of the UE, remains primarily ipsilateral in spine and is comparatively less influenced by damage resulting from a stroke [208]. In the majority of stroke patients, lesions of the motor pathways are typically partial. While some residual pathways may remain intact, these circuits are often unable to transfer an adequate level of excitability required to stimulate the motor neurons in the upper limb muscles [209, 210]. Through the utilization of electrical stimulation, tsES effectively modulates the excitability of the spinal cord. This modulation helps lower the threshold for motoneurons in transferring motor impulses. The aim is to promote the combination of residual motor control tracts from

the central nervous system [164]. As a result of this integration, there is an increased propagation signals from of motor control in residual descending neural tracts [211]. Consequently, there was a reduction in cortical compensatory effects originating from the contralesional hemisphere, which is responsible for the proximal UE muscles during movements of distal UE.

The obtained elevation in the LI within the distal muscles of the UE, specifically in the ECU-ED for 20% Extension and 40% Extension, as well as in the FCR-FD for 20% Flexion (**Figure 3.8**), serves as additional evidence supporting the presence of improved residual descending control. As previously discussed, the application of stimulation current for spinal cord has the ability to adjust the physiological state of tracts, thereby promoting relations among the motor tracts originating from the lesioned side and distal UE muscles that they innervate [208]. These findings align with previous research, which suggested that long-lasting current to cervical spine resulted in increased force and control of the hand [212]. More specifically, individuals with SCI exhibited the ability to generate higher levels of hand grip force. Moreover, the stimulation of multiple segments at the C3-C7 resulted in an increase in the evoked response of distal UE muscles, while the recruitment of UE muscles in the proximal side decreased [212]. The improvement of plasticity in synapse from lesioned side may account for the observed increased synergies of the UE during movements of distal UE muscles [213]. In the context of synaptic plasticity, there is a complex interplay and connectivity among the motor axons and neurons within spine [213]. The electrical

stimulation induces an excitability state in the corticospinal anterior horn, facilitating the strengthening of synaptic plasticity through the arrival of descending impulses from the brain [214]. In the context of the organization of motor neurons, it has been observed that the cortico-motoneurons responsible for distal upper limb muscles do not exert inhibitory control over those governing proximal muscles at the cortical level. This phenomenon can be attributed to the topographical arrangement of motor neurons of the spine, guided by two fundamental principles: the flexor/extensor and proximal/distal rule. According to the flexor/extensor rule, motoneurons innervating UD muscles are positioned posteriorly to those innervating extensor muscles. Similarly, the proximal/distal rule dictates that motoneurons responsible for distal muscles, such as hand muscles, are located laterally in relation to motoneurons controlling proximal muscles of. Consequently, this process enhances the likelihood of following neuronal firing, in accordance with the principles of the Hebbian-type learning effect. Through current stimulation of synaptic efficiency is enhanced, leading to an increased likelihood of firing [214].

One limitation in the research was small sample size of participants included. We continued collecting individuals until we observed significant differences in most of the obtained parameters. Eventually, we recruited twelve subjects with variable impairments in motor functions, and the results showed that tsES modulated neuro-muscular interactions in poststroke individuals. However, the study lacked access to neuroimaging data that would provide precise information about the location of the

participants' brain lesions. Motor impairments were solely evaluated through behavioral assessments, focusing on the paralyzed side. Despite the wide range of motor impairments observed in the participants, we obtained findings from the recruited individuals. This suggests that tsES may be an efficient method of neuromodulation for individuals with different degrees of impairment following a stroke.

In future studies, we plan to address these limitations by increasing the sample size and investigating the instant influences of tsES for various subtypes poststroke. We aim to categorize participants based on the location of their brain lesions and severity of motor impairments, which will provide further insights into the variations among different subgroups. Furthermore, the changes in CMCoh of proximal muscles, specifically the BIC and TRI, apart from wrist movement, and other single-joint movements such as elbow movement will be executed. This additional investigation aims to compare the alterations in CMCoh observed in muscles involved in single-joint movements with those occurring during multi-joint movements. Finally, we will conduct clinical trials to examine the training results of tsES in affected upper limb poststroke. These trials will involve multiple sessions of training that combine tsES with VPT exercises, allowing us to gain a better understanding of the potential benefits of this intervention.

3.5 Periodic Summary

In this study, our investigation focused on the instant impact of tsES in cortico-muscular coupling during voluntary muscular movements of the affected distal UE in individuals

poststroke. Electrophysiological measurements, such as coherence between cortex and muscles, LI, and activation levels of EMG, were utilized for the analysis. The findings of this study revealed that by providing long-lasting current stimulation to cervical spine, it is possible to improve the excitation and inhibition effects of UE muscles in UE. This stimulation technique also helps to minimize the compensatory effects in the cortical region and proximal muscles. In particular, through the modulation of sensory and motor networks tracts in the cervical spine, tsES facilitated enhancement of motor controlling excitation effects to agonist muscle, while concurrently improving local inhibition motor control to antagonist muscle. The changes in brain lateralization to the lesioned side, along with reduced activation levels of EMG in proximal muscles of UE, suggesting a decline in compensation from cortical side and proximal muscular side. The implications of these findings indicate that tsES has the potential to improve responses to motor control tracts from the lesioned brain by adjusting cervical spine excitation. This highlights the possibility of utilizing tsES as an additional input to improve motor recovery poststroke, particularly for upper extremities.

CHAPTER 4

REHABILITATIVE EFFECTS OF NON-INVASIVE CERVICAL TRANS-SPINAL ELECTRICAL STIMULATION ON UPPER LIMB REHABILITATION IN CHRONIC STROKE

4.1 Introduction

Stroke continues to be a significant factor in long-term disability, affecting around 80% of survivors with upper limb motor impairments [2, 215]. Facilitating the restoration in motor function for upper extremities is crucial in persons who have experienced a stroke, as it empowers them to engage in fundamental tasks necessary for daily living. This improvement in motor ability not only enhances their level of independence but also has a positive impact on their overall quality of life [216]. To regain motor function in stroke patients' upper extremities, current rehabilitation techniques heavily rely on intensive and repetitive occupational and physical training programs [217]. However, the effects of recovery typically diminish after six months to one year after stroke, and individuals who receive inadequate rehabilitation support may experience further deterioration [218]. Consequently, there is a pressing need for the development and implementation of enhanced rehabilitation technologies that can significantly improve the long-term motor restoration in the upper extremities following a stroke.

Over the past few years, there has been an increasing utilization of stimulation-based

neuromodulation interventions in rehabilitation technologies, including deep brain stimulation (DBS), epidural spinal cord stimulation (eSCS), repetitive transcranial magnetic stimulation (rTMS), and tsES [219-221]. This is primarily due to their association with neural reorganization, which has been recognized as a crucial factor in facilitating motor recovery [222]. Encouraging outcomes have been witnessed when employing DBS and eSCS as interventions to enhance motor recovery among individuals afflicted with central neurological conditions, including TBI, SCI, and stroke [223-225]. These relevant studies primarily focused on the surgical implantation of a small array of electrodes in specific brain or cervical spinal cord areas. The objective behind this approach was to effectively modulate the impact of electrical stimulation on the neural system [226]. Although these techniques have been demonstrated effectiveness in improving motor functions after stroke by precisely modulating the neuronal circuitry, they are associated with the risks of infection, bleeding, and the patient injury caused by the interaction between the stimulation devices and other therapeutic instruments, such as ultrasound and MRI [173].

In contrast to the surgically implanted techniques, non-invasive stimulation techniques (e.g., rTMS and tsES) could modulate the neural activity in brain or spinal cord with fewer associated side effects [227, 228]. However, the high-frequency rTMS has been reported to induce epileptic seizures in a few cases and may not be suitable for patients who had partial brain resection [229]. The utilization of tsES offers a safer, easier-to-operate, and more affordable alternative to modulate the spinal cord [230]. To achieve

this, a distinctive waveform of high-frequency electric current is utilized, which traverses from the surface of the skin to reach the spinal networks [230]. This innovative approach has shown promising results, as evidenced by recent studies demonstrating noteworthy enhancements in upper limb motor function among individuals with chronic SCI individuals who received cervical tsES intervention and voluntary physical training (VPT) [168, 212]. For example, maximum hand grip strength was improved after 4-week voluntary hand grip training combined with eight sessions of non-invasive cervical tsES (monophasic waveform at 30 Hz) delivered along the midline between C3-C4 and C6-C7 spinal levels [212]. Another study revealed that hand lateral pinch strength exhibited an increase after a four-week intervention involving combined transcutaneous spinal stimulation (biphasic and rectangular waveform with 30 Hz at C3-C4 and C6-C7 levels) and VPT. Furthermore, this functional improvement was sustained during a follow-up period of over three months without additional treatment [168]. Both studies also observed a notable augmentation in the amplitude of spinal motor evoked potentials (MEPs) for distal upper limb muscles following tsES intervention [168, 212]. These findings indicated that tsES combined with VPT could improve the effectiveness of residual corticospinal tract by augmenting the inter-neuronal spinal circuits excitability and reducing the threshold for motor impulse propagation [169]. In individuals with chronic stroke, the spinal circuits below the cortical lesion remain intact, and there has been a scarcity of studies that have specifically explored the impacts of spinal cord electrical stimulation on the process of

upper extremity motor recovery [61, 164]. For example, Powell et al. determined the immediate assistive effects of continuous cervical electrical stimulation (biphasic waveform with 40-100 Hz at C4-T1 levels) in facilitating motor function in the arm and hand [61]. Blanc et al. concluded that stroke subjects with intervention combing direct tsES and peripheral nerve stimulation achieved significant reductions in upper extremity spasticity and improvement in motor function compared to the shame condition [62]. These pilot studies showed the potential of tsES in enhancing upper limb motor function in chronic stroke. However, both studies focused exclusively on the effects of tsES and non-tsES conditions, thereby overlooking the potential combined rehabilitation effects of tsES and conventional VPT in chronic stroke. In addition, these studies solely evaluated the kinematics and functional movements, without assessing the impact of tsES on the remaining descending pathways from central nervous system (CNS) to the peripheral muscles in chronic stroke patients.

The interaction patterns between CNS activity and muscle activity could be captured through specific parameters obtained from electroencephalography (EEG) and electromyography (EMG), such as spinal MEPs and cortico-muscular coherence (CMC) [231, 232]. Previous studies on CMC in stroke patients have explored the connections between sensorimotor cortex activity and muscle activity in the upper extremities during tasks involving upper limb motion. These studies have indicated that analyzing changes in CMC can provide insights into the cortico-muscular patterns associated with upper extremity motor functions [156, 183, 233]. Therefore, the primary objective of

current research was to examine rehabilitative effects of non-invasive tsES for affected upper extremities affected by chronic stroke in individuals.

4.2 Methodology

To investigate the rehabilitation effects of tsES, a randomized controlled trial (RCT) was conducted, involving individuals diagnosed with chronic stroke. The participants were divided into two groups: one group received tsES in conjunction with voluntary physical training (VPT), while the other group solely underwent VPT. Measurements were then compared between these two groups of stroke subjects in order to assess the impact of tsES on the rehabilitation process. The evaluated outcomes included clinical scores, as well as three electrophysiology-related parameters (CMC, laterality index, and EMG activation level) at three different evaluation time points (pre-, post-, and 3MFU training).

4.2.1 Experimental Setup of Trans-spinal Electrical Stimulation

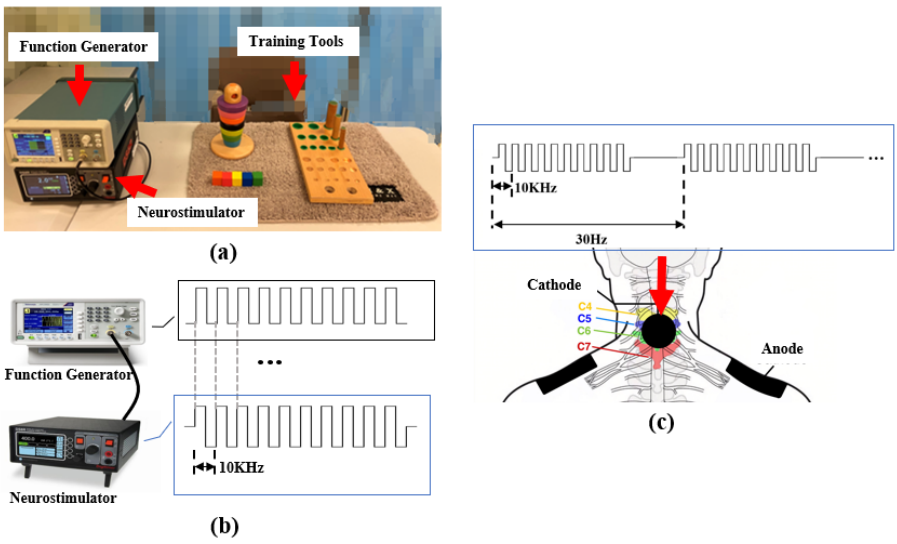

Figure 4.1 The experimental setup for trans-spinal electrical stimulation training. (a) the configurations that delivers electrical stimulation and training tools. (b) the illustration stimulation waveforms generated by function generator and neurostimulator. (c) the illustration of specific stimulation sites of cathode electrode (C4-C6) and anode electrodes (acromioclavicular joints) on a stroke subject.

Figure 4.1 depicts the experimental setup utilized for tsES training. This involved the use of the neurostimulator (DS8R, Digitimer, UK) and an arbitrary function generator (Tektronix, AFG1022, USA) to deliver non-invasive and painless cervical electrical stimulation (**Figure 4.1(a)**). The function generator and the neurostimulator were connected using a BNC cable, with the function generator supplying a monophasic and rectangular waveform signal to trigger the neurostimulator (**Figure 4.1(b)**). The trigger signal consisted of 10 cycles of rectangular, monophasic waveform. Upon detecting the ascending trend of the trigger signal, the neurostimulator emitted a biphasic and rectangular pulse, resulting in 10 cycles of pulses being generated (**Figure 4.1(b)**). The stimulation protocol involved delivering ten 0.1ms rectangular biphasic pulses at a carrier frequency of 10kHz and a burst frequency of 30Hz (**Figure 4.1(c)**). This stimulation approach leveraged the painless effects of high-frequency stimulation and the charge-balancing properties of a biphasic waveform, which helps prevent potential tissue damage [234, 235]. To apply the stimulation, a single rounded self-adhesive

hydrogel surface electrode was meticulously placed on middle line of skin surface over the C4-C6 spinous processes as the cathode. Additionally, two rectangular self-adhesive hydrogel surface electrodes were attached to acromioclavicular joints of shoulders, with one electrode per side serving as the anode. Before the electrode placement, thorough skin preparation was carried out to minimize skin impedance. This involved meticulously cleaning the skin using scrubs and 75% alcohol, followed by a drying process.

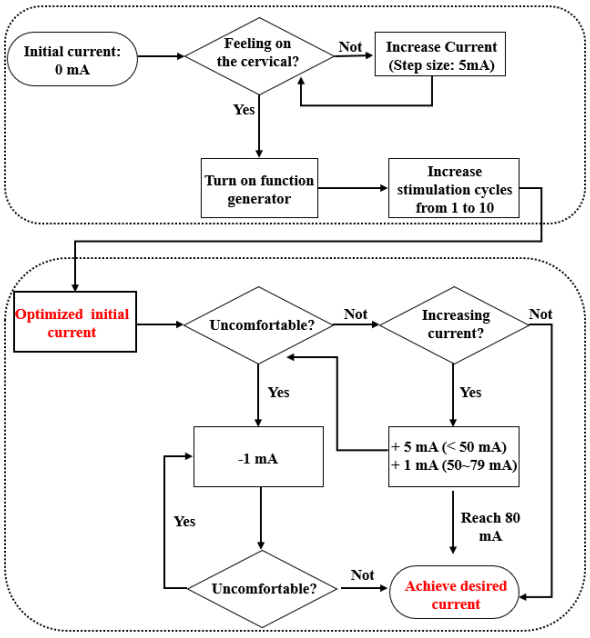

Figure 4.2 The flowchart for modulating the electrical stimulation intensity by the function generator and neurostimulator.

Figure 4.2 demonstrates how the stimulation intensity was adjusted by the neurostimulator and function generator. The process of determining the optimal stimulation intensity for a stroke individual is as follows: (1) the stimulation intensity

of the neurostimulator was initiated from 0 mA and gradually increased in 5 mA increments until the stroke patient could sense it on the cervical area; (2) the stimulation cycles on the function generator were increased from 1 to 10; (3) the intensity of the stimulation was gradually increased in 5mA increments for stimulation levels below 50mA, and in 1mA increments for stimulation levels ranging from 50mA to 79mA [236]. The maximum level of stimulation intensity was set at 80mA, which was adopted by previous studies [237]; (4) during the adjustment of the stimulation intensity, the participant was instructed to provide feedback on the comfort level of the delivered stimulation. If the intensity could not be increased further and tolerated for the duration of a 20-minute training session, the current intensity was regarded as the optimal stimulation intensity for the patient.

4.2.2 tsES Rehabilitation Program

Subjects Recruitment

Following the acquisition of ethical clearance from the HSESC, consent forms regarding the purpose of the research have been signed by participants before the experiment.

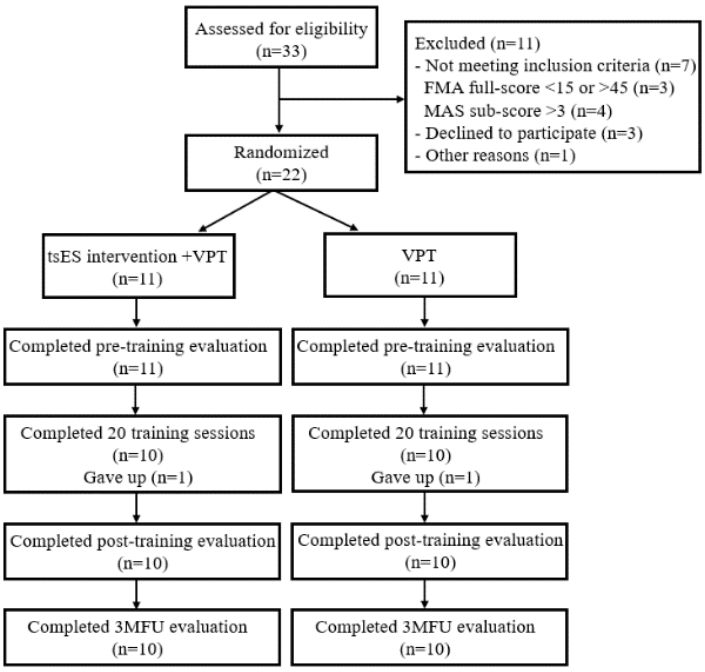

Figure 4.3 The flowchart of Consolidated Standards of Reporting Trials (CONSORT) for randomized trial design.

Figure 4.3 depicts the presentation of the flowchart adhering to the CONSORT. The inclusion criteria of this study included: (a) age (years old): 30-75; (b) stroke lasting longer than six months, with unilateral brain lesion and motor impairment; (c) sufficient cognitive ability, demonstrated by a score higher than 21 on the MMSE; (d) scores lower than 3 on the MAS for elbow, wrist, finger; (e) FMA-UE score between 15 and 45; (f) exhibiting detectable voluntary EMG signals in five upper extremity muscles, including ECU-ED, FCR-FD, BIC, TRI, APB; (g) capability to maintain a seated position for at least 60 minutes, with acceptable assistance if needed. The exclusion criteria were as follows: (a) botulinum toxin injection before six months; (b) current

use of medications or treatments that can affect muscle tone or upper limb motor function; (c) a history of substance or drug abuse; (d) participation in other studies related to upper limb motor function recovery; (e) pregnancy or plans to become pregnant during the study, or epilepsy; (f) allergies to electrodes or electrical stimulation; (g) the presence of metal implants or stimulators, including but not limited to pacemakers or deep brain stimulators. A random assignment was conducted to allocate all participants into two coherent: the tsES group and the control group. There were ten participants in each group.

Training Protocol

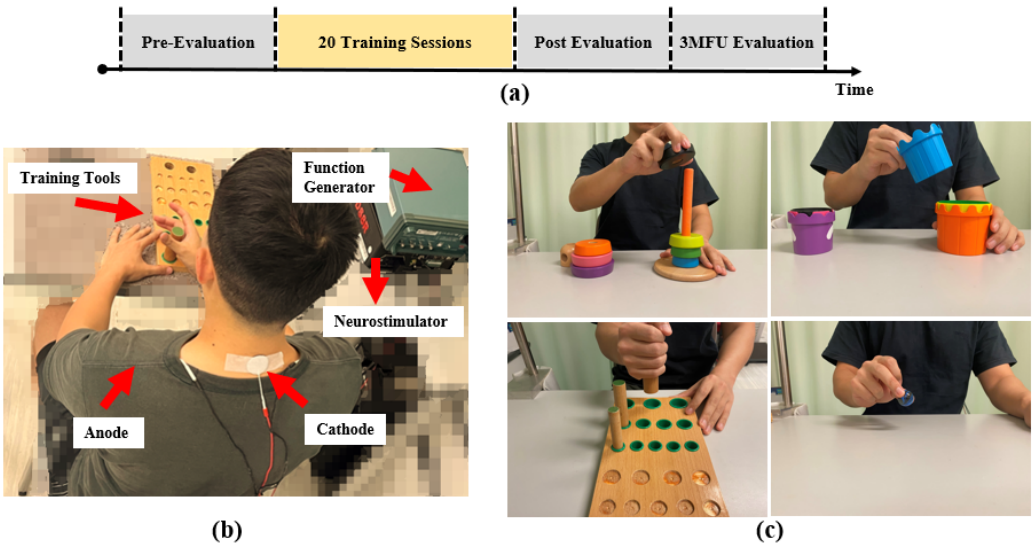

Figure 4.4 The timeline and configuration of the training protocol. (a) the timeline of the training protocol, including 20 training sessions and three evaluations at pre-, post-, and 3-month follow-up training. (b) the illustration of a stroke individual received trans-spinal electrical stimulation when performing voluntary physical training. (c) the illustration of four types of voluntary physical training.

The timeline of the training protocol for both groups is depicted in **Figure 4.4(a)**. The initial pre-training phase involved three consecutive days of clinical assessments conducted by two blinded assessors who were unaware of the group assignments. This process was to minimize any potential influence on motor performance caused by factors such as nervousness in stroke subjects, subjective judgments by the assessors, and other external factors [238]. Additionally, one CMC evaluation was performed before the training sessions. The second stage encompassed 20 training sessions. After the training, the post-training assessment stage was immediately conducted, which included one clinical assessment and one CMC evaluation. Finally, participants returned to the laboratory for a 3-month follow-up (3MFU) evaluation, which comprised one clinical assessment and one CMC evaluation.

Each training session for stroke participants in both groups had a duration of 50 minutes and was divided into three phases: (1) 20 minutes of tsES stimulation combined with VPT in the tsES group (**Figure 4.4(b)**), while the control group performed VPT along with sham stimulation; (2) a 10-minute rest period was implemented to minimize the muscle fatigue and spasticity; (3) 20 minutes of VPT training without tsES for both groups, which ensured that the stimulation intensity applied to the cervical spine in the tsES group remained within a safe range [239]. During the first and third phases of each training session, the participant was instructed to engage the affected upper limb in

tasks that involved four different types of tools (**Figure 4.4(c)**): (a) stacking towers: the participant was required to open the hand, grasp rings of various sizes, and place each ring above the central hole of a stationary pedestal before releasing their grip; (b) stacking cups: the participant needed to sequentially insert smaller cups into larger cups until the most miniature cup was correctly positioned; (c) placing sticks: the participant was instructed to open the hand, grasp three differently sized sticks, and subsequently place these sticks into the corresponding holes located on a wooden board positioned on the desk; (d) grasping cubes: the participant used their fingers to grip cubes and then release them. Each type of task needed to be used at least once in both the first and third training phases.

4.2.3 Training Effects Evaluation

Clinical Assessment

A comparative analysis was conducted between the tsES and control groups, focusing on various assessment measures. These measures encompassed the FMA in three distinct categories: full score, wrist/hand score, and shoulder/elbow score. Additionally, the MAS was utilized, which comprised three categories: finger, wrist, and elbow. Other assessment tools employed included the MSS, ARAT, FIM, WMFT scores, and WMFT time. To minimize the impact of different assessors on the clinical assessments, the same assessor was assigned to conduct the pre-, post-, and 3MFU-training assessments for each participant.

Cortico-muscular Coherence Evaluation

To assess the CMC patterns during upper limb extension and flexion tasks, a data collection process was undertaken. Specifically, the EEG was recorded via sensorimotor cortex. Simultaneously, EMG was obtained from five distinct groups of upper limb muscles. To enhance the quality of the recorded signals, both the EEG and EMG data were augmented by applying the g.USBamp amplifier. The EEG underwent amplification with a multiplication factor of 10,000, whereas the EMG was augmented using the factor of 1,000. To ensure appropriate signal processing, the bandpass filter settings were 2-100 Hz for EEG signals and 10-500 Hz for EMG signals. Synchronization and recording of both EEG/EMG was achieved using the data collecting board, specifically at 1200 Hz sampling frequency.

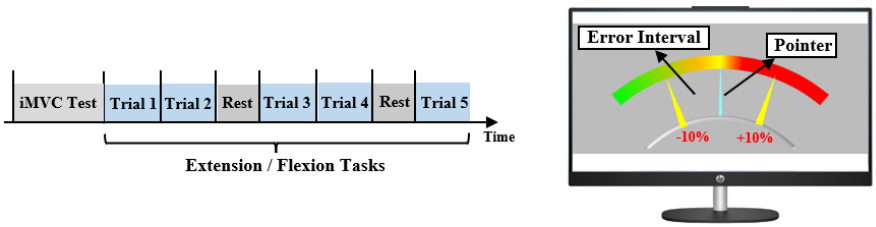

Figure 4.5 The timeline and visual interface of the wrist-hand motions for CMC evaluation.

The timeline of the wrist-hand extension and flexion tasks during pre-, post-, and 3MFU training stages was presented in **Figure 4.5(a)**. The initial step involved the acquisition of isometric maximal voluntary contraction (iMVC) EMG signals [62]. The participant received instructions to engage in iMVC for each of the five target muscles, sustaining

effort for five seconds. To minimize potential muscle fatigue, a 5-minute resting period was allowed. The iMVC EMG signals were collected three times, and the highest recorded value among the three trials was chosen as maximal EMG for every muscle. Following the iMVC acquisition, the participant randomly performed two types of tasks: extension and flexion for wrist and hand at a level in 40% iMVC level of agonist muscles (ECU-ED/FCR-FD for extension/flexion). **Figure 4.5(b)** displays the visual interface of extension and flexion tasks for wrist and hand. A customized operational interface was created using LABVIEW software (National Instruments Corp., USA). This interface displayed a colored spectrum on the computer screen, which represented the current level of EMG activation in real time. The spectrum ranged from 0% (green color) to 100% (red color), calculated using baseline and iMVC values of agonist muscles. Throughout the tasks, the contraction level of the agonist muscles (ECU-ED/FCR-FD for extension/flexion) was continuously recorded and calculated. To provide feedback to the participant, a blue pointer was used on the interface, while two yellow pointers indicated the acceptable error range (±10%) for the tasks [182]. The $EMG_{contraction(i)}$ was calculated as:

$$EMG_{contraction(i)} = \frac{EMG_i - EMG_{baseline}}{EMG_{max} - EMG_{baseline}} \times 100\% \quad (4.1)$$

Here, EMG_i represents the mean of the rectified EMG envelope of the agonist muscles i in a window of 0.1-second, while EMG_{max} and $EMG_{baseline}$ represent the corresponding average values during maximum force and at rest, respectively [183].

Each trial was performed for 35 seconds, and after completing the first and second trials of each task, a 2-minute rest period was provided. The same rest period was given after completing the third and fourth trials. To mitigate potential artifacts caused by fluctuations at the end of the task, the final 5 seconds of each trial were excluded. Each trial's data series was segmented into 1200 data points using a 1-second window with a 50% overlap. There were 55 segments within each trial, and a total of 275 trial epochs of EEG and EMG signals across the five trials for each participant. After preprocessing the EEG signals, the CMC was calculated to assess the connection pattern among the sensorimotor area with upper limb muscles. CMC value was derived using the following formulation:

$$CMC_{EEG,EMG(f)} = \frac{|P_{EEG,EMG}(f)|^2}{P_{EEG}(f) \cdot P_{EMG}(f)} \quad (4.2)$$

$$P_{EEG,EMG}(f) = \frac{1}{n}\sum_{i=1}^{n} EEG_i(f) EMG_i^*(f) \quad (4.3)$$

Here, $P_{EEG,EMG}(f)$ represents cross-spectral density of EEG and EMG data, while $P_{EEG}(f)$ and $P_{EMG}(f)$ represent the auto-spectral density of EEG and EMG data at frequency of f, respectively. The $CMC_{EEG,EMG(f)}$ value ranges from 0 to 1, indicating the strength of correlation between both signals, ranging from no correlation to a perfect correlation [160]. The preprocessing and calculation involving electrophysiological signals were executed via custom code implemented with toolbox of fieldtrip in MATLAB R2019b (http://www.fieldtrip.fcdonders.nl, The MathWorks Inc., Natick, MA, USA). To determine the statistical significance of the CMC value ($p < 0.05$), a

confidence level (CL) was obtained via the formula:

$$CL = 1 - 0.05^{\frac{1}{(L-1)}} \qquad (4.4)$$

In this formula, L represents the number of trial epochs. If the calculated CMC value exceeds the threshold of 0.011, it suggests that the value of CMC is significant at p-value < 0.05.

Laterality Index

Peak CMC values were then used to generate a hot spot map of the sensorimotor cortex to visually inspecting the brain lateralization, and the calculation of a laterality index was conducted using the following formula:

$$Laterality\ Index = \frac{CMC_{ipsilesional}}{max\ (CMC_{contralesional}, CMC_{midsagittal})} \qquad (4.5)$$

Here, $CMC_{ipsilesional}$, $CMC_{contralesional}$, and $CMC_{midsagittal}$ correspond to largest CMC in ipsilesional hemisphere, contralesional hemisphere, and midsagittal line. Laterality index provides a measure of dominance between the hemispheres. If the calculated laterality index is greater than 1, it indicates that the ipsilesional hemisphere exhibits a predominant peak CMC value. Conversely, if the laterality index is smaller than 1, it suggests that the contralesional hemisphere demonstrates a predominant peak CMC value [190].

EMG Activation Level

The normalization of raw EMG activation level of each muscle was obtained with the baseline ($EMG_{baseline(i)}$) and iMVC level ($EMG_{max(i)}$) of EMG signals of corresponding muscle. Subsequently, EMG activation level was calculated using formula (4.7):

$$EMG_{Normalized(i)} = \frac{EMG_{origin(i)} - EMG_{baseline(i)}}{EMG_{max(i)} - EMG_{baseline(i)}} \times 100\% \quad (4.6)$$

$$EMG_{ActLevel(i)} = \frac{1}{T}\int_0^T EMG_{Normalized(i)}(t)dt \quad (4.7)$$

Here, normalized EMG signals of muscle i ($EMG_{Normalized(i)}$) underwent linear envelope processing over a specific time interval (T) to produce $\int_0^T EMG_{Normalized(i)}(t)dt$, which was further calculated to obtain normalized muscle i's EMG activation level ($EMG_{ActLevel(i)}$).

4.2.4 Statistical Analysis

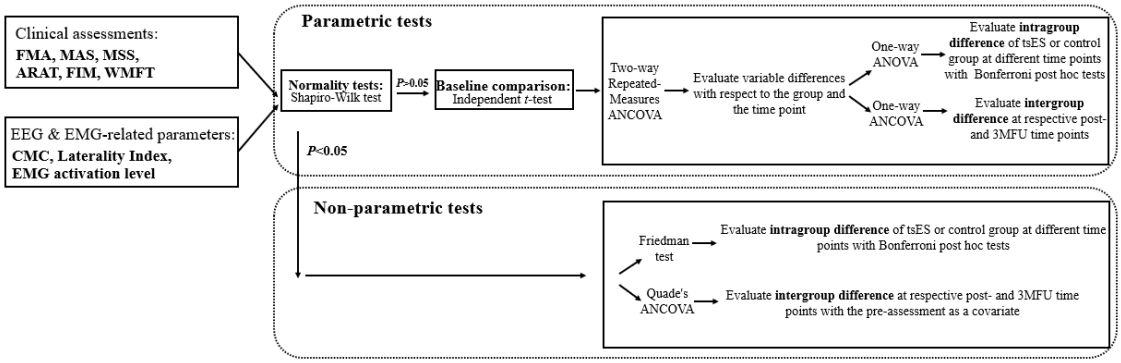

Figure 4.6 The flowchart of the statistical analysis.

The normality of the collected parameters, including clinical assessments, CMC, laterality index, and EMG activation level, was examined using the Shapiro-Wilk test.

The statistical results suggested that the FMA, MSS, ARAT, WMFT, CMC, laterality index, and EMG activation level exhibited a distribution of normality ($P > 0.05$), and the MAS and FIM scores demonstrated a distribution of non-normality ($P < 0.05$). For the parameters following a normal distribution, an independent t-test confirmed no significant difference ($P > 0.05$) in the assessments before the training intervention. To evaluate the effects of the group (experimental or control) and session (pre-, post-, and 3MFU) factors on the measured outcomes, a two-way ANCOVA was employed, with pre-intervention scores serving as covariates. To compare the differences within each group across various time points, a one-way ANOVA was conducted, and Bonferroni correction method was applied. Additionally, a post hoc between-group comparison was conducted using a one-way ANCOVA by using pre-intervention scores as the covariate, analyzing outcomes at the post-intervention and 3MFU time points. The Friedman test was applied to assess the intragroup variations at various time points for the parameters that did not exhibit a normal distribution (specifically, the MAS and FIM scores). Subsequently, we used a Bonferroni post-hoc test to examine these variations in detail. Quade's ANCOVA was performed to assess intergroup differences at the post-intervention and 3MFU time points, with pre-intervention scores utilized as covariates. A statistical significance level of 0.05 was utilized as the threshold to determine the presence of statistical significance, serving as a benchmark for evaluating the observed results.

4.3 Results

4.3.1 Clinical Assessment

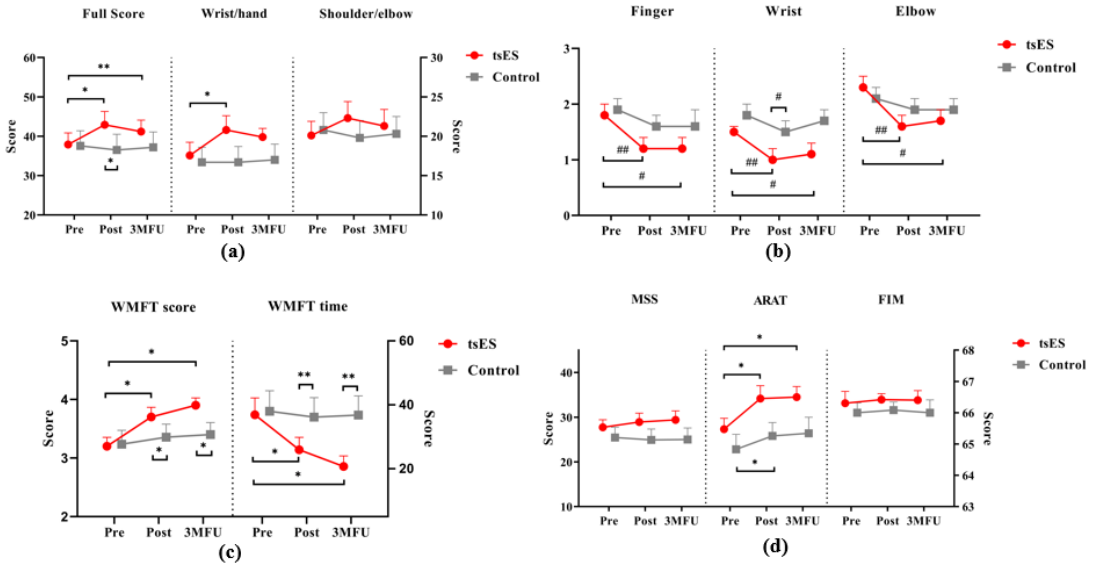

Figure 4.7 The clinical scores assessed prior to the initial training session and after the completion of 20 training sessions, as well as during 3MFU for both tsES and control groups: (a) FMA full score, wrist/hand score, and shoulder/elbow score, (b) MAS score at the finger, the wrist, and the elbow, (c) WMFT score and time, (d) MSS, ARAT, and FIM. Each evaluation session is presented with the mean value accompanied by the standard error (SE).

Figure 4.7 displays the clinical scores compared between tsES group and control group in three stages. The overall statistical data was presented in **Table 4.1**. Significant variations were evident concerning the grouping and assessment sessions in both the FMA total score and FMA wrist/hand score, as indicated by the statistical analysis ($P < 0.05$, Two-way ANCOVA, see **Table 4.1**). Within the tsES group, FMA full score showed significant differences among the different evaluation sessions ($P < 0.01$, One-

way ANCOVA, **Table 4.1**). More specifically, significant improvements were noted in both the FMA total score and FMA wrist/hand sub-scores, demonstrating a substantial increase from the pre-training to post-training session ($P < 0.05$, **Table 4.1**). Furthermore, a significant enhancement in the FMA total score was noted between pre-training session and the 3MFU evaluation ($P < 0.01$, **Table 4.1**). In contrast, within control group, no significant differences were found among the three FMA score categories in relation to the session factor ($P > 0.05$, **Table 4.1**). In addition, a statistically significant disparity in FMA total score during post-training stage was observed between two groups ($P < 0.05$, **Table 4.1**). The above pairwise comparison was conducted using One-way ANOVA with Bonferroni post hoc tests.

In **Figure 4.7(b)**, significant reductions were observed in MAS scores of fingers, wrist, elbow in group of tsES both before and after training period ($P < 0.01$, **Table 4.1**). This decline in scores was also evident when comparing the pre-training session to the 3MFU evaluation ($P < 0.05$, **Table 4.1**). Conversely, within the control group, no notable differences were found in the three MAS sub-scores based on the session factor ($P > 0.05$, **Table 4.1**). The above pairwise comparison was conducted using Friedman test with Bonferroni post hoc tests. Furthermore, when examining the MAS wrist score between the tsES and control groups at the 3MFU stage, a statistically significant distinction was observed ($P < 0.05$, Quade's ANCOVA, **Table 4.1**).

The statistical analysis revealed a significant impact of the group factor on both the

WMFT-score and time ($P < 0.05$, Two-way ANCOVA, **Table 4.1**, **Figure 4.7(c)**). When comparing the pre- and post-training assessments as well as the pre-training and 3MFU assessments, the tsES group exhibited a notable rise in WMFT-score and a fall in WMFT-time ($P < 0.05$, **Table 4.1**). Conversely, no significant differences were obtained within group of control in relation to session factor ($P > 0.05$, **Table 4.1**). There was a significant intergroup variance at both the post-training and 3MFU time points ($P < 0.05$, **Table 4.1**). **Figure 4.7(d)** illustrates the MSS, ARAT, and FIM scores. In both groups, the ARAT score increased significantly from pre-training to post-training ($P < 0.05$, **Table 4.1**). The above pairwise comparison was conducted using One-way ANOVA with Bonferroni post hoc tests. Furthermore, the results obtained from MSS and ARAT did not reveal any session- or group-specific differences ($P > 0.05$, Two-way ANCOVA, **Table 4.1**).

Table 4.1 The average and standard error, and statistical analyses of clinical assessments.

Measurement	Group	Pre	Post	3MFU	One-way ANOVA	Two-way Repeated Measures ANCOVA		
						Session	Group	S*G
		Mean ± Standard Error			*P* (Partial η^2)	*P* (Partial η^2)		
FMA-full score	tsES	37.9±3.0	42.9±3.4	41.2±2.9	**0.008****(0.354)	**0.009****(0.286)	**0.028***(0.211)	0.957(0.000)
	Control	37.6±3.8	36.5±4.0	37.2±3.9	0.861(0.013)			
	P(Partial η^2)	0.946(0.017)	**0.020***(0.231)	0.072(0.146)				
FMA-wrist/hand	tsES	17.6±1.7	20.8±1.8	19.9±1.1	0.099(0.190)	**0.009****(0.282)	0.078(0.141)	0.807(0.003)
	Control	16.7±1.9	16.7±2.0	17.0±2.0	0.830(0.017)			
	P(Partial η^2)	0.747(0.077)	0.058(0.020)	0.195(0.079)				
FMA-shoulder/elbow	tsES	20.8±2.2	19.8±2.2	20.3±2.2	0.692(0.033)	0.079(0.140)	0.065(0.153)	0.755(0.005)
	Control	20.1±1.8	22.3±2.1	21.3±2.1	0.122(0.174)			
	P(Partial η^2)	0.514(0.075)	**0.033***(0.199)	0.196(0.078)				
MAS-finger	tsES	1.8±0.2	1.2±0.2	1.2±0.2	***0.009***$^{\#\#}$	--	--	--
	Control	1.9±0.2	1.6±0.2	1.6±0.3	*0.494*			
	P	*0.523*	*0.242*	*0.198*				
MAS-wrist	tsES	1.5±0.1	1.0±0.2	1.1±0.2	***0.006***$^{\#\#}$	--	--	--
	Control	1.8±0.2	1.5±0.2	1.7±0.2	*0.486*			
	P	*0.117*	***0.043***$^{\#}$	*0.089*				
MAS-elbow	tsES	2.3±0.2	1.6±0.2	1.7±0.2	***0.010***$^{\#}$	--	--	--

	Control	2.1±0.2	1.9±0.2	1.9±0.2	*0.273*			
	P	*0.502*	*0.443*	*0.378*				
WMFT-score	tsES	3.2±0.2	3.7±0.2	3.9±0.2	**0.000****(0.745)	0.096(0.127)	**0.007****(0.296)	0.518(0.020)
	Control	3.2±0.2	3.4±0.2	3.4±0.2	0.211(0.132)			
	P(Partial η^2)	0.937(0.026)	**0.010***(0.276)	**0.016***(0.248)				
WMFT-time	tsES	36.9±5.3	25.9±3.9	20.7±3.3	**0.000****(0.621)	0.267(0.058)	**0.001****(0.418)	0.227(0.069)
	Control	38.0±6.4	36.2±6.1	36.8±6.0	0.684(0.034)			
	P(Partial η^2)	0.892(0.043)	**0.007****(0.298)	**0.002****(0.385)				
MSS	tsES	27.7±1.7	28.9±2.0	29.4±2.0	0.079(0.206)	0.875(0.001)	0.655(0.010)	0.098(0.125)
	Control	25.5±2.3	24.9±2.4	25.0±2.6	0.762(0.024)			
	P(Partial η^2)	0.435(0.191)	0.099(0.124)	0.693(0.008)				
ARAT	tsES	27.3±2.4	34.2±2.9	34.5±2.4	**0.005****(0.386)	0.392(0.035)	0.687(0.008)	0.050(0.171)
	Control	22.8±2.4	25.8±3.0	26.4±3.6	**0.042***(0.250)			
	P(Partial η^2)	0.285(0.303)	0.384(0.037)	0.077(0.141)				
FIM	tsES	66.3±0.4	66.4±0.2	66.4±0.3	*0.422*	--	--	--
	Control	66.0±0.3	66.1±0.3	66.0±0.4	*0.878*			
	P	*0.497*	*0.410*	*0.514*				

Note: The observed differences are denoted as follows: '*' for P < 0.05 and '**' for P < 0.01 (One-way ANOVA with Bonferroni post hoc tests); '$^{\#}$' for P < 0.05 and '$^{\#\#}$' for P < 0.01 (Friedman test with Bonferroni post hoc tests).

4.3.1 Cortico-muscular Coherence

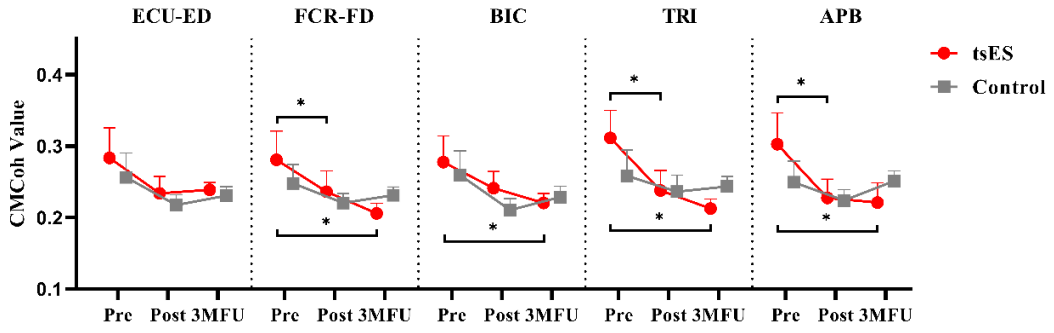

(a)

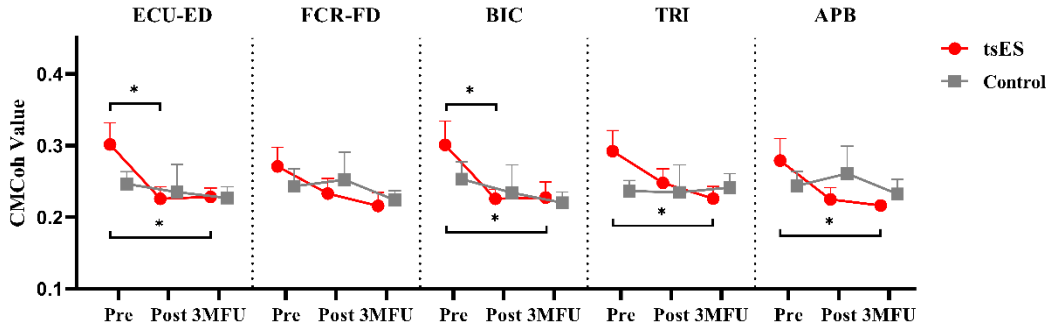

(b)

Figure 4.8 The cortico-muscular coherence during the extension (a) and flexion (b) tasks in wrist and hand before initial training sessions, after 20 training sessions, and at the 3MFU for both the tsES and control groups.

Figure 4.8 depicts the CMC values of five upper limb muscles (ECU-ED, FCR-FD, BCI, TRI, and APB) across two motion tasks (extension and flexion) during three different sessions (pre-training, post-training, and 3MFU). **Table 4.2** and **Table 4.3**

present the detailed CMC values, including the probabilities of Two-way ANCOVA (session and group factor), One-way ANOVA (session factor), and One-way ANCOVA (group factor). For wrist-hand extension task (**Figure 4.8(a)**), the study observed significant differences in the CMC values of muscles when considering the session factor (Two-way ANCOVA, **Table 4.2**). Specifically, significant disparities were detected among the FCR-FD muscle, BIC muscle, and TRI muscle regarding the session factor ($P < 0.05$). APB muscle exhibited significant differences in session factor ($P < 0.001$) and in interaction among session and group factors ($P < 0.05$). Furthermore, a noteworthy variance in CMC values across sessions for the FCR-FD muscle, TRI muscle, and BIC muscle in group of tsES ($P < 0.05$, One-way ANOVA, **Table 4.2**). Notably, a decrease in CMC values was observed when comparing the pre-training and post-training assessments for FCR-FD, TRI, and APB muscles ($P < 0.05$, **Table 4.2**). Additionally, a reduction in CMC values was noted in FCR-FD, BIC, TRI, and APB muscles between pre-training and 3MFU assessments ($P < 0.05$, **Table 4.2**). In reference to wrist-hand flexion task (**Figure 4.8(b)**), the CMC values of the ECU-ED and BCI muscles showed significant differences concerning the session factor ($P < 0.05$, Two-way ANCOVA, **Table 4.3**). Furthermore, in group of tsES, significant differences for CMC values were observed for the ECU-ED, FCR-FD, TRI, and BIC muscles across different sessions ($P < 0.05$, One-way ANCOVA, **Table 4.3**). Moreover, a significant decrease was indicated in CMC values for the ECU-ED and BIC from the pre-training to post-training assessments ($P < 0.05$, **Table 4.3**). Similarly, all five

muscles except for FCR-FD exhibited a significant decline in values of CMC when comparing pre-training and 3MFU assessments ($P < 0.05$, **Table 4.3**). However, no significant variations were observed in control group across the five muscles concerning the session factors ($P > 0.05$, **Table 4.2** & **4.3**). The above pairwise comparison was conducted using One-way ANOVA with Bonferroni post hoc tests.

Table 4.2 The mean and standard error, and the statistical analyses of cortico-muscular coherence during wrist-hand extension.

Muscle	Group	Pre	Post	3MFU	One-way ANOVA	Two-way ANCOVA		
						Session	Group	S*G
		Mean ± Standard Error			*P* (Partial η^2)	*P* (Partial η^2)		
ECU-ED	tsES	0.284 ± 0.042	0.234 ± 0.023	0.238 ± 0.010	0.161 (0.184)	0.105 (0.118)	0.525 (0.023)	0.906 (0.005)
	Control	0.256 ± 0.034	0.218 ± 0.015	0.230 ± 0.013	0.500 (0.074)			
	P (Partial η^2)	0.621 (0.225)	0.721 (0.008)	0.719 (0.008)				
FCR-FD	tsES	0.281 ± 0.040	0.236 ± 0.029	0.206 ± 0.014	**0.025*** (0.337)	**0.030*** (0.177)	0.790 (0.004)	0.239 (0.076)
	Control	0.248 ± 0.026	0.220 ± 0.013	0.231 ± 0.012	0.532 (0.068)			
	P (Partial η^2)	0.502 (0.307)	0.947 (0.000)	0.076 (0.174)				
BIC	tsES	0.278 ± 0.036	0.241 ± 0.023	0.220 ± 0.013	**0.039*** (0.302)	**0.039*** (0.164)	0.629 (0.013)	0.581 (0.030)
	Control	0.259 ± 0.034	0.211 ± 0.016	0.229 ± 0.015	0.408 (0.095)			
	P (Partial η^2)	0.718 (0.164)	0.334 (0.055)	0.460 (0.033)				
TRI	tsES	0.311 ± 0.038	0.238 ± 0.028	0.212 ± 0.013	**0.002**** (0.493)	**0.017*** (0.203)	0.797 (0.004)	0.127 (0.108)
	Control	0.258 ± 0.036	0.236 ± 0.023	0.243 ± 0.014	0.782 (0.027)			
	P (Partial η^2)	0.327 (0.451)	0.366 (0.048)	**0.046*** (0.215)				
APB	tsES	0.303 ± 0.044	0.227 ± 0.026	0.221 ± 0.028	**0.001**** (0.515)	**0.009**** (0.231)	0.799 (0.004)	**0.046*** (0.157)
	Control	0.249 ± 0.030	0.224 ± 0.015	0.251 ± 0.014	0.488 (0.077)			
	P (Partial η^2)	0.327 (0.450)	0.322 (0.058)	**0.045*** (0.216)				

Note: The observed differences are denoted as follows: '*' for $P < 0.05$ and '**' for $P < 0.01$ (One-way ANOVA with Bonferroni post hoc tests).

Table 4.3 The mean and standard error, and the statistical analyses of cortico-muscular coherence during wrist-hand flexion.

Muscle	Group	Pre	Post	3MFU	One-way ANOVA	Two-way ANCOVA		
						Session	Group	S*G
		Mean ± Standard Error			*P* (Partial η^2)	*P* (Partial η^2)		
ECU-ED	tsES	0.301 ± 0.030	0.226 ± 0.017	0.228 ± 0.013	**0.005**** (0.442)	**0.048*** (0.003)	0.524 (0.003)	0.249 (0.006)
	Control	0.246 ± 0.017	0.235 ± 0.038	0.227 ± 0.016	0.843 (0.019)			
	P (Partial η^2)	0.129 (0.712)	0.512 (0.026)	0.572 (0.019)				
FCR-FD	tsES	0.271 ± 0.026	0.233 ± 0.021	0.216 ± 0.019	**0.043*** (0.295)	0.151 (0.100)	0.997 (0.000)	0.433 (0.045)
	Control	0.243 ± 0.024	0.252 ± 0.038	0.224 ± 0.013	0.661 (0.045)			
	P (Partial η^2)	0.451 (0.345)	0.472 (0.031)	0.342 (0.053)				
BIC	tsES	0.301 ± 0.033	0.226 ± 0.013	0.227 ± 0.021	**0.026*** (0.333)	**0.040*** (0.163)	0.569 (0.018)	0.426 (0.046)
	Control	0.253 ± 0.024	0.234 ± 0.038	0.241 ± 0.020	0.621 (0.052)			
	P (Partial η^2)	0.261 (0.519)	0.730 (0.007)	0.910 (0.001)				
TRI	tsES	0.292 ± 0.028	0.248 ± 0.020	0.226 ± 0.017	**0.019*** (0.357)	0.230 (0.078)	0.519 (0.023)	0.158 (0.097)
	Control	0.236 ± 0.015	0.235 ± 0.038	0.241 ± 0.020	0.973 (0.003)			
	P (Partial η^2)	0.102 (0.771)	0.799 (0.004)	0.062 (0.190)				
APB	tsES	0.279 ± 0.031	0.225 ± 0.017	0.216 ± 0.007	0.059 (0.270)	0.260 (0.072)	0.808 (0.003)	0.263 (0.072)
	Control	0.244 ± 0.020	0.261 ± 0.038	0.232 ± 0.020	0.727 (0.035)			
	P (Partial η^2)	0.354 (0.425)	0.328 (0.056)	0.264 (0.073)				

Note: The observed differences are denoted as follows: '*' for $P < 0.05$ and '**' for $P < 0.01$ (One-way ANOVA with Bonferroni post hoc tests).

4.3.2 Cortico-muscular Coherence Topography

Figure 4.9 illustrates the CMC topographies of two left hemiplegia stroke participants, who were chosen as representative cases, during different training periods (pre-training, post-training, and 3MFU) when performing two wrist-hand motor tasks (extension and flexion). For wrist-hand extension task, it was observed that upper extremities muscles of individuals in tsES group displayed a noteworthy shift in the peak channel of CMC activation. Specifically, there was a relocation of the peak channel of CMC from left hemisphere (contralesional) to right hemisphere (ipsilesional). Specifically, the ECU-ED muscle moved from CZ to FC3 to C4, and the FCR-FD muscle moved from CP1

to FC6 to CPZ (**Figure 4.9(a)**). Furthermore, the TRI muscle moved from CP3 to FC6 to CP1 during the three phases of training. For the wrist-hand flexion task, a similar shifted pattern was also observed: the ECU-ED muscle shifted from CZ to FC6 to C1, and the FCR-FD muscle shifted from CZ to FCZ to CP4 (**Figure 4.9 (a)**). The unimpaired participant did not exhibit clear patterns of alterations in the shift of CMC peak channel (**Figure 4.9 (b)**).

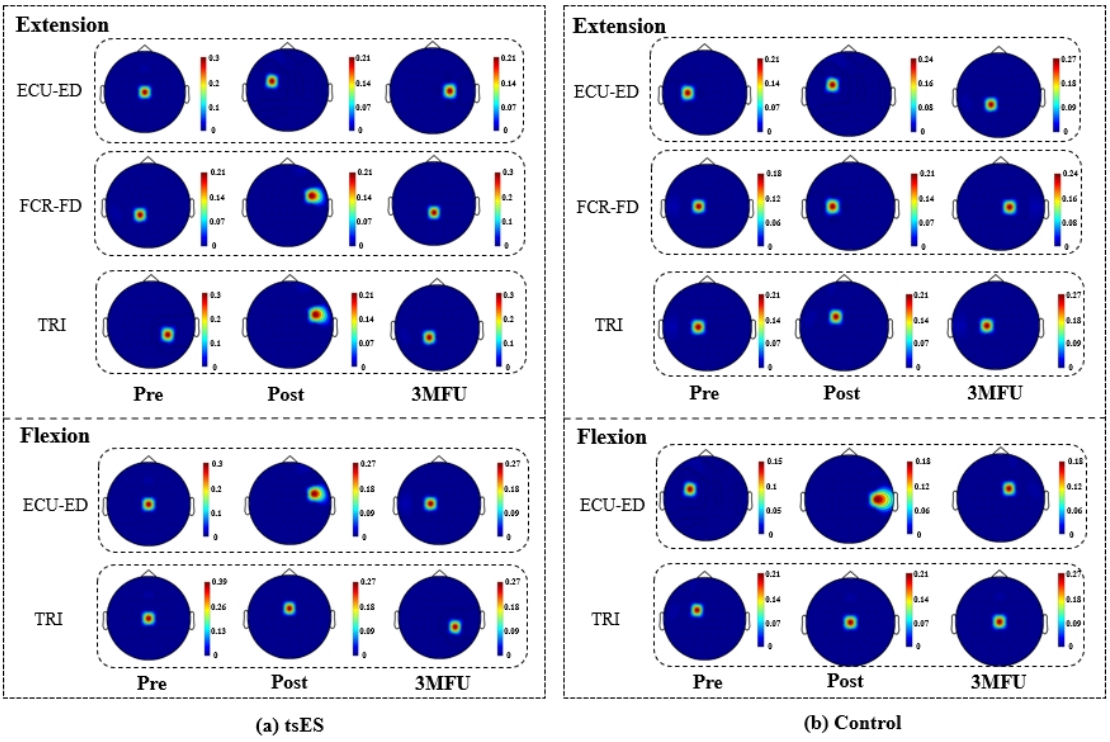

Figure 4.9 The CMC topographies of upper limb muscles during wrist-hand motions in two representative stroke subjects with left hemiplegia from (a) tsES group and (b) control group, respectively.

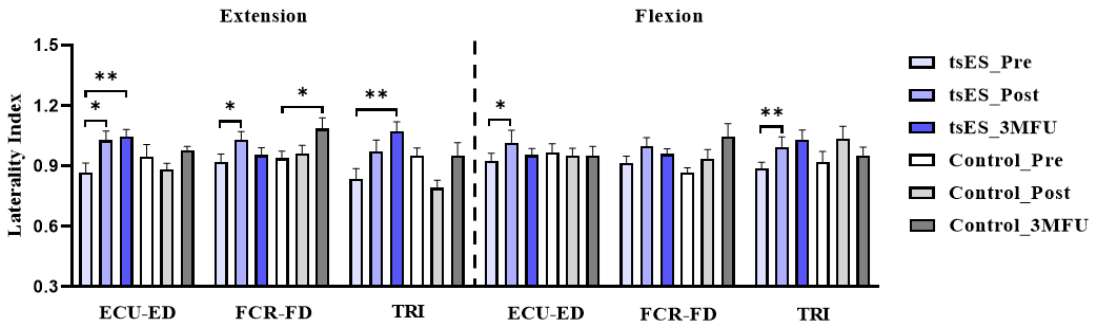

Figure 4.10 The laterality index before initial training sessions, after 20 training sessions, as well as 3MFU in both tsES and control groups during wrist-hand extension and flexion.

Figure 4.10 shows the laterality index of CMC for upper limb muscles in both tsES group and control group. **Table 4.4** presents detailed laterality index values, including two-way ANCOVA probabilities for session and group factors, one-way ANCOVA probabilities for session factor, and one-way ANCOVA probabilities for group factor. During the wrist-hand extension task depicted in **Figure 4.10**, noteworthy disparities were observed in the laterality index of three muscles: ECU-ED, FCR-FD, and TRI. These disparities were detected in relation to the session factor, as well as the interactions between session and group factors ($p < 0.05$, Two-way ANCOVA, **Table 4.4**). Significant variations in the laterality index of the ECU-ED, FCR-FD, and TRI muscles were observed across multiple sessions within the tsES group (One-way ANOVA, **Table 4.4**). These differences encompassed the laterality index values from pre- and post-training assessments for the ECU-ED and FCR-FD muscles ($P < 0.05$,

Table 4.4). Additionally, laterality index exhibited significant differences from pre-training to the 3MFU assessments for the ECU-ED and TRI muscles ($P < 0.05$, **Table 4.4**). In contrast, unimpaired participants demonstrated a significant increase solely in FCR-FD muscle when comparing pre-training and 3MFU assessments ($P < 0.05$, **Table 4.4**). Regarding flexion task in wrist and hand depicted in **Figure 4.10**, the laterality index values of the ECU-ED and TRI muscles exhibited noteworthy differences for session factor ($P < 0.05$, Two-way ANCOVA, **Table 4.4**). Overall, our findings indicate significant disparities in the laterality index of ECU-ED muscle, FCR-FD muscle, and TRI muscle across various sessions within the tsES group (One-way ANOVA, **Table 4.4**). Specifically, ECU-ED and TRI muscles experienced a significant increase in the laterality index when comparing the pre-training and post-training assessments ($P < 0.05$, **Table 4.4**). However, no significant changes in the upper limb muscles were observed between training sessions within the control group ($P > 0.05$, **Table 4.4**). The above pairwise comparison was conducted using One-way ANOVA with Bonferroni post hoc tests.

Table 4.4 The average and standard error, and the statistical analyses of laterality index during extension and flexion of wrist and hand.

Motion	Muscle	Group	Pre	Post	3MFU	One-way ANOVA	Two-way ANCOVA		
							Session	Group	S*G
			Mean ± Standard Error			*P* (Partial η^2)	*P* (Partial η^2)		
Extension	**ECU-ED**	tsES	0.868 ± 0.046	1.028 ± 0.046	1.045 ± 0.036	**0.005**** (0.442)	**0.033*** (0.172)	0.265 (0.069)	**0.018*** (0.200)
		Control	0.946 ± 0.060	0.883 ± 0.030	0.976 ± 0.021	0.256 (0.140)			
		P (Partial η^2)	0.314 (0.488)	**0.019*** (0.284)	0.060 (0.193)				
Extension	**FCR-FD**	tsES	0.919 ± 0.039	1.030 ± 0.041	0.953 ± 0.037	**0.031*** (0.320)	**0.039*** (0.164)	0.535 (0.022)	**0.026*** (0.184)
		Control	0.938 ± 0.036	0.960 ± 0.043	1.085 ± 0.053	**0.048*** (0.286)			
		P (Partial η^2)	0.727 (0.163)	0.112 (0.142)	0.067 (0.184)				
Extension	**TRI**	tsES	0.835 ± 0.052	0.973 ± 0.055	1.070 ± 0.049	**0.010*** (0.400)	**0.025*** (0.185)	0.152 (0.111)	**0.014*** (0.213)
		Control	0.949 ± 0.039	0.791 ± 0.038	0.951 ± 0.065	0.068 (0.258)			
		P (Partial η^2)	0.095 (0.813)	**0.022*** (0.272)	0.208 (0.092)				
Flexion	**ECU-ED**	tsES	0.914 ± 0.034	0.997 ± 0.044	0.958 ± 0.027	**0.043*** (0.295)	**0.028*** (0.180)	0.855 (0.002)	0.140 (0.103)
		Control	0.867 ± 0.024	0.936 ± 0.046	1.047 ± 0.062	0.343 (0.235)			
		P (Partial η^2)	0.276 (0.466)	0.512 (0.026)	0.572 (0.019)				
Flexion	**FCR-FD**	tsES	0.924 ± 0.038	1.014 ± 0.064	0.954 ± 0.033	0.633 (0.026)	0.153 (0.116)	0.408 (0.041)	0.401 (0.042)
		Control	0.967 ± 0.043	0.949 ± 0.038	0.949 ± 0.047	0.808 (0.007)			
		P (Partial η^2)	0.727 (0.339)	0.294 (0.064)	0.897 (0.001)				
Flexion	**TRI**	tsES	0.887 ± 0.032	0.994 ± 0.051	1.031 ± 0.047	**0.009**** (0.549)	**0.027*** (0.180)	0.976 (0.000)	0.282 (0.068)
		Control	0.920 ± 0.051	1.036 ± 0.061	0.952 ± 0.041	0.155 (0.187)			
		P (Partial η^2)	0.588 (0.243)	0.674 (0.011)	0.105 (0.147)				

Note: The observed differences are denoted as follows: '*' for $P < 0.05$ and '**' for $P < 0.01$ (One-way ANOVA with Bonferroni post hoc tests)

4.3.3 EMG Activation Level

Figure 4.11 visually illustrates activation levels of EMG in upper limb muscles for both groups. The comprehensive data regarding the precise values of EMG activation levels were presented in **Table 4.5** and **Table 4.6**. These values encompass probabilities for the two-way ANCOVA (session factor/group factor) and separate one-way ANCOVA probabilities (session factor/group factor). Notably, in the context of the wrist-hand extension tasks illustrated in **Figure 4.11(a)**, the session factor revealed significant discrepancies in activation levels for EMG in FCR-FD and proximal muscles (BIC and

TRI) ($P < 0.05$, Two-way ANCOVA, **Table 4.5**). Moreover, a significant distinction in activation levels for EMG in FCR-FD and proximal muscles (BIC and TRI) was observed across sessions within the tsES group ($P < 0.05$, One-way ANOVA, **Table 4.5**). Furthermore, the assessment between pre-training and post-training periods demonstrated a noteworthy decrease in activation levels for EMG for FCR-FD muscle, BIC muscle, TRI muscle, and APB muscle ($P < 0.05$, **Table 4.5**). In a similar vein, a substantial reduction in EMG activation levels of the FCR-FD muscle, BIC muscle, and TRI muscle was obtained between the pre-training and 3MFU evaluations ($P < 0.05$, **Table 4.5**).

Within wrist-hand flexion tasks (**Figure 4.11(b)**), the activation level of EMG for ECU-ED, BCI, APB displayed significant variations in relation to session factor ($P < 0.05$, Two-way ANCOVA, **Table 4.6**). Similarly, when considering tsES group, ECU-ED, BCI, and APB muscles exhibited significant differences within the session factor ($P < 0.05$, **Table 4.6**). Specifically, a significant decrease in activation levels of EMG for ECU-ED and BIC muscles was observed from pre-training phase to the post-training phase ($P < 0.05$, **Table 4.6**). Furthermore, activation levels of EMG for ECU-ED, BIC, TRI, APB muscles displayed a significant decrease from the pre-training phase to the 3MFU phase ($P < 0.05$, **Table 4.6**). Conversely, no significant variations were observed in the upper extremities' muscles of the unimpaired group by the session factors ($P > 0.05$, One-way ANOVA with Bonferroni post hoc tests, **Table 4.5 & 4.6**). The above

pairwise comparison was conducted using One-way ANOVA with Bonferroni post hoc tests.

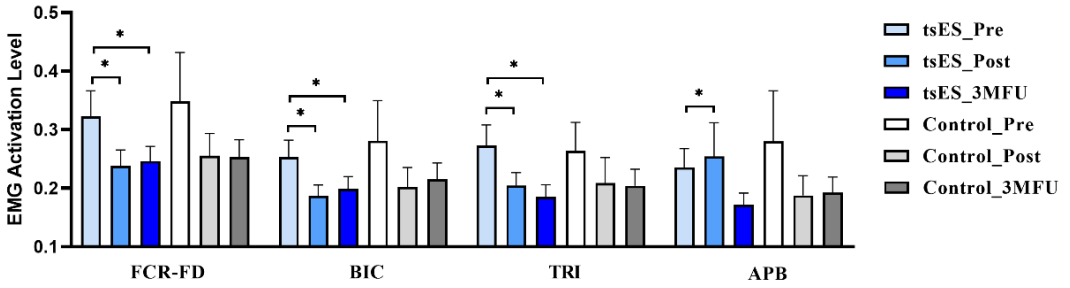

(a)

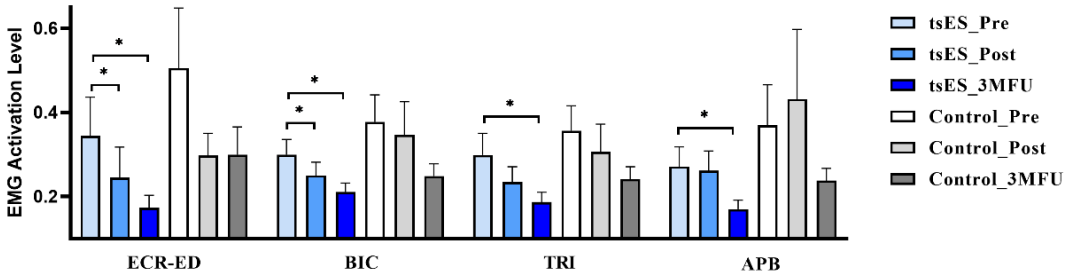

(b)

Figure 4.11 The EMG activation level during the extension (a) and flexion (b) tasks in wrist and hand before initial training sessions, after 20 training sessions, and at the 3MFU for both the tsES and control groups.

Table 4.5 The mean and standard error, and the statistical analyses of EMG activation level during wrist-hand extension.

Muscle	Group	Pre	Post	3MFU	One-way ANOVA	Two-way ANCOVA		
						Session	Group	S*G
		Mean ± Standard Error			*P* (Partial η^2)	*P* (Partial η^2)		
FCR-FD	tsES	0.323 ± 0.044	0.238 ± 0.028	0.246 ± 0.025	**0.030*** (0.390)	**0.033*** (0.156)	0.735 (0.006)	0.970 (0.001)
	Control	0.348 ± 0.083	0.256 ± 0.038	0.254 ± 0.030	0.261 (0.126)			
	P (Partial η^2)	0.792 (0.114)	0.792 (0.004)	0.884 (0.001)				
BIC	tsES	0.253 ± 0.029	0.187 ± 0.019	0.199 ± 0.021	**0.019*** (0.441)	**0.019*** (0.180)	0.653 (0.010)	0.966 (0.002)
	Control	0.272 ± 0.062	0.202 ± 0.034	0.197 ± 0.021	0.176 (0.159)			
	P (Partial η^2)	0.717 (0.114)	0.865 (0.002)	0.748 (0.006)				
TRI	tsES	0.273 ± 0.035	0.205 ± 0.022	0.186 ± 0.021	**0.034*** (0.287)	**0.035*** (0.154)	0.898 (0.001)	0.895 (0.006)
	Control	0.264 ± 0.048	0.209 ± 0.044	0.204 ± 0.028	0.412 (0.085)			
	P (Partial η^2)	0.882 (0.064)	0.884 (0.001)	0.563 (0.018)				
APB	tsES	0.236 ± 0.032	0.254 ± 0.058	0.172 ± 0.020	0.193 (0.152)	0.219 (0.073)	0.993 (0.000)	0.395 (0.045)
	Control	0.280 ± 0.086	0.188 ± 0.033	0.193 ± 0.026	0.368 (0.095)			
	P (Partial η^2)	0.634 (0.206)	0.286 (0.060)	0.637 (0.012)				

Note: The observed differences are denoted as follows: '*' for P < 0.05 (One-way ANOVA with Bonferroni post hoc tests).

Table 4.6 The mean and standard error, and the statistical analyses of EMG activation level during wrist-hand flexion.

Muscle	Group	Pre	Post	3MFU	One-way ANOVA	Two-way ANCOVA		
						Session	Group	S*G
		Mean ± Standard Error			*P* (Partial η^2)	*P* (Partial η^2)		
ECU-ED	tsES	0.345 ± 0.091	0.245 ± 0.073	0.173 ± 0.030	**0.024*** (0.312)	**0.031*** (0.160)	0.190 (0.084)	0.749 (0.014)
	Control	0.505 ± 0.143	0.297 ± 0.053	0.300 ± 0.066	0.204 (0.147)			
	P (Partial η^2)	0.385 (0.403)	0.856 (0.002)	0.121 (0.122)				
BIC	tsES	0.300 ± 0.036	0.250 ± 0.032	0.211 ± 0.021	**0.019*** (0.329)	**0.013*** (0.195)	0.211 (0.077)	0.697 (0.018)
	Control	0.378 ± 0.064	0.347 ± 0.079	0.249 ± 0.029	0.141 (0.178)			
	P (Partial η^2)	0.303 (0.451)	0.625 (0.013)	0.427 (0.034)				
TRI	tsES	0.299 ± 0.051	0.235 ± 0.036	0.187 ± 0.023	**0.005**** (0.411)	**0.002**** (0.267)	0.290 (0.056)	0.954 (0.002)
	Control	0.357 ± 0.059	0.307 ± 0.066	0.242 ± 0.029	0.105 (0.201)			
	P (Partial η^2)	0.468 (0.315)	0.564 (0.018)	0.234 (0.074)				
APB	tsES	0.271 ± 0.047	0.261 ± 0.047	0.170 ± 0.021	**0.039*** (0.278)	0.052 (0.137)	0.257 (0.064)	0.685 (0.019)
	Control	0.370 ± 0.096	0.432 ± 0.166	0.238 ± 0.029	0.242 (0.132)			
	P (Partial η^2)	0.367 (0.394)	0.724 (0.007)	0.133 (0.115)				

Note: The observed differences is denoted as follows: '*' for P < 0.05 and '**' for P < 0.01 (One-way ANOVA with Bonferroni post hoc tests).

4.4 Discussion

The primary objective for this research endeavor was to examine the impact of integrating tsES with VPT in the upper limb motor rehabilitation among chronic stroke individuals. To achieve this objective, a clinical trial was implemented, employing a comparative analysis of the effects produced by the combination of tsES and VPT versus the use of VPT alone. Various parameters were measured during different evaluation sessions, namely before training, after training, and 3MFU. These measurements encompassed clinical assessments, CMC, laterality index, and activation level of EMG. The findings revealed that the group receiving tsES with VPT demonstrated more favorable outcomes in terms of motor performance and muscle tone. This combined intervention improved the cortical and muscular control of distal muscles while reducing the compensatory use of proximal muscles. The mechanisms underlying these improvements involved enhanced excitability of spinal neural circuits due to cervical tsES, as well as increased responsiveness of residual excitatory and inhibitory pathways from the ipsilesional hemisphere.

4.4.1 Training Effectiveness on Upper Limb Motor Functions

The effectiveness of tsES training was indicated by the improvements in upper limb functional outcomes and releasement in muscular spasticity. Our findings showed that the stroke individuals who received tsES exhibited elevated motor performance based on clinical evaluations, including FMA, WMFT, and ARAT. More specifically, the

FMA-full score was increased significantly across different evaluation time points (**Figure 4.7(a)** & **Table 4.1**). The FMA graded selective upper limb movements, ranging from abnormal voluntary synergy movements to fractionated and isolated joint movements [240]. It has been consistently recognized as a reliable indicator of motor impairment severity after stroke [240]. Higher FMA motor scores in the upper limb for the tsES group were associated with reduced motor impairments and increased ability to perform isolated joint movement [241]. Notably, significant differences were observed in both intra-group comparisons across evaluation time points and inter-group comparisons across the group factor for WMFT-time and WMFT-score (**Figure 4.7(c)** & **Table 4.1**). The WMFT measures post-stroke upper limb motor abilities through time-based and multiple-joint functional tasks [242]. The significant decrease in WMFT-time indicated that stroke patients with tsES were able to complete complex motions and functional tasks at a higher movement speed compared to the participants without tsES [243, 244]. Although the ARAT scoring of control group with VPT showed a similar significant increase from pre-training to post-training evaluation, similar to the tsES group, it is noteworthy that the tsES group demonstrated an additional significant increase in ARAT scores from the post-training to the 3MFU evaluation (**Figure 4.7(d)** & **Table 4.1**). This finding suggests the presence of significant and enduring effects resulting from the integration of tsES in the rehabilitation process. The ARAT used standardized equipment (e.g., woodblocks, alloy tubes, and marbles) to assess the hand and arm movements (e.g., grasp, grip, and pinch)

[245]. The significant increase in the ARAT scores of 3MFU evaluation demonstrated that the stroke participants with tsES achieved sustained improvement in the performance of purposeful upper limb motor activities [246]. In addition to the functional outcomes' improvement, stroke individuals who received tsES experienced a significant reduction in muscular spasticity in the upper limb, as indicated by decreased MAS scores in the finger, wrist, and elbow (**Figure 4.7(b)** & **Table 4.1**). The MAS could evaluate the reflex activities elicited in specific muscles during resistance to the passive movement [247]. The significant decrease in MAS scores after intervention with tsES indicated that the stroke patients had lower muscle tone. This reduction in muscle tone facilitated smoother and more effortless movement of affected upper extremity throughout its entire motion range, as compared with control group [248]. The observed motor recovery and muscle spasticity releasement revealed by these clinical assessments could be attributed to the cortical reorganization in and around lesion areas. This cortical reorganization could involve an increase in both the quantity and density of dendrites' synapses, as well as the unmasking of latent neural networks [249]. The functional recovery indicated by these clinical assessments suggested that cervical spinal electrical stimulation assisted stroke individuals in enhancing the effectiveness of regaining independence in activities of daily living [250, 251].

4.4.2 Improved Cortical and Muscular Control of Distal Upper Limb

The Inhibitory Control of Antagonist Muscles

In the stroke participants who received tsES, an improvement in inhibitory control from the sensorimotor cortex to the antagonist muscles was observed, as evidenced by a significant decrease in CMC (e.g., FCR-FD in extension and ECU-ED in flexion) during post-training and 3MFU evaluations (**Figure 4.8**, **Table 4.2** & **4.3**). The primary neurophysiological mechanism driving the improvement was the increased excitability of the spinal neural circuits due to the cervical tsES [194]. This excitation provided additional neuromodulatory input to the motor recovery, complementing the effects of pure physical therapy interventions [252]. Previous studies utilizing computational modeling to construct the induced electric field by the spinal current stimulation have demonstrated that the increased excitability of spinal networks occurs through the activation of dorsal root afferents [253, 254]. The activation of sensory afferents via dorsal roots could recruit spinal interneuronal circuitry across the multiple segments of the spinal cord, augmenting the responses from the "silent" residual descending inhibitory pathways [255]. Our findings align with this observation, as our results demonstrated a significant elevation in the laterality index within the antagonist muscles (**Figure 4.8** & **Table 4.4**), indicating the relocation in the cortical control center from the contralesional side to the ipsilesional side (**Figure 4.8**). Moreover, empirical studies utilizing EMG in human subjects have provided evidence that the targeted

dorsal root activation through cervical tsES could increase the motor axons' excitability in ventral roots by trans-synaptic transmission [256]. This direct activation of motor pools that innervate the upper extremity muscles plays a significant role in modulating the sensory-motor pathways [256]. Therefore, the inhibitory control toward antagonist muscles during voluntary motions was increased. This aligns with the distinct reduction in activation levels of EMG for distal antagonist muscles in extension and flexion motion tasks of wrist and hand (**Figure 4.11**, **Table 4.5** & **4.6**).

The Excitatory Control of Agonist Muscles

Although the cortical control to the agonist muscles did not show a significant increase in CMC after tsES, the laterality index of these muscles significantly increased after 20 training sessions following tsES (**Figure 4.8** & **Table 4.4**). This suggested that cervical spinal circuitry stimulation also amplifies the responsiveness of residual excitatory control signals from the ipsilesional hemisphere to the agonist muscles. However, the insufficient activation of alpha motoneurons limited the effects of the cortical control from the cortex to the agonist muscles, resulting in a failure to induce the muscle responses [257]. Alpha motoneurons in the upper limb muscles were affected by the chronic stroke, including factors such as the location and severity of the stroke, the type and duration of the rehabilitation [151]. In uninjured individuals, there is a balance between the activation of alpha motoneurons in agonist and antagonist muscles, allowing for smooth coordination of upper limb movements [258]. Stroke lesions could

damage the connection between alpha motoneurons and the descending neural tracts, leading to reduced activation of agonist alpha motoneurons and increased activation of antagonist alpha motoneurons (i.e., muscle weakness and spasticity) [151, 258]. The abnormal structural changes and degeneration of alpha motoneurons would occur in the process of chronic stroke, particularly in the agonist muscles [259]. These agonist alpha motoneurons experience impaired abilities to generate action potentials and transmit contraction signals to the corresponding muscles [260]. Consequently, the agonist muscles became less sensitive to the residual excitatory control signals from the ipsilesional hemisphere, even when amplified by the non-invasive cervical spinal cord electrical stimulation.

4.4.3 Reduced Compensatory Effects from Proximal Upper Limb

The stroke participants with tsES demonstrated a reduction in reliance on compensatory effects during extension and flexion motions of wrist and hand. This was evidenced by a significant reduction in the levels of activation obtained in proximal muscles (TRI/BIC muscles), as measured by parameters: CMC and activation levels of EMG. (**Figure 4.8, Table 4.2** & **4.3**). The compensation strategies from the proximal upper limb muscles occur because of stroke-related damages to the ipsilesional brain regions responsible for executing motor control of distal muscles such as primary motor cortex [49]. Compared to distal upper extremities muscles, the proportion of descending neural pathways originating from the hemisphere opposite to the side of the stroke and

innervating proximal upper extremity muscles is more significant [261]. It indicated that proximal muscles were less affected by stroke lesions [261]. However, proximal compensation strategies could have negative consequences for long-term upper limb motor function recovery, such as joint deformities, nerve compression [4]. With the application of cervical tsES, the remaining descending inhibitory control from the ipsilesional hemisphere to the motor pools of proximal muscles was augmented via activating the preferentially sensory and motor roots in the intact spinal circuits [262]. The significantly increased laterality index observed in this study (**Figure 4.8** & **Table 4.4**) provided evidence that the descending neural tracts innervating the proximal muscles have shifted to the ipsilesional hemisphere. This observation aligns with prior research studies that have consistently shown the effectiveness of cervical tsES in enhancing wrist-hand function and reducing shoulder compensatory movements in SCI people by modulating the corticospinal tract (CST) and augmenting the responses from the cortex [263]. Consequently, the application of cervical tsES can effectively engage sensory-motor pathways, leading to the activation of motor pools that innervate the proximal muscles of the upper limb.

4.5 Periodic Summary

In this study, the rehabilitation effects of combining non-invasive cervical spinal cord electrical stimulation with physical therapy on the motor restoration of affected upper limbs in chronic stroke individuals were investigated. The clinical scores indicated the

effectiveness of tsES training by the improvement in upper limb functional outcomes and releasement in muscular spasticity. The relocation of the peak CMC to the ipsilesional sensorimotor cortex in the distal upper limb muscles demonstrated that tsES could augment the responsiveness from residual excitatory and inhibitory descending pathways by elevating the excitability of spinal cord. The observed decrease in CMC and activation levels of EMG in upper limb muscles of proximal side suggested a decrease in compensation influence of cortical and muscular side. The improved outcomes proved the advantage of tsES as an assistant approach to physical rehabilitation interventions in facilitating long-term upper limb motor recovery among chronic stroke individuals.

CHAPTER 5

CONCLUSIONS

Post-stroke rehabilitation places significant emphasis on evaluating and recovering sensorimotor function in the upper limb. One potential approach to assess post-stroke sensory impairments is through the use of neuroimaging data-driven machine learning, which can help reduce the labor-intensive workload associated with manual evaluation conducted by healthcare professionals. Furthermore, non-invasive neuromodulation techniques targeting UE motor function could offer a novel assistive strategy to enhance neuro-reorganization in the affected side of the brain. To explore these possibilities, three experiments were conducted in this study: (i) development of a novel EEG-based SVM-ML model to automatically evaluate fine tactile sensation impairments in post-stroke individuals; (ii) evaluation of instant influences of tsES in cortico-muscular control coupling in voluntary contractions of upper limb muscles; (iii) investigation of the rehabilitation influences of tsES on UE motor recovery in affected side stroke patient.

The initial experiment carried out in this study involved the development of an EEG-based SVM-ML model specifically designed to evaluate impairments in fine tactile sensation. The SVM-ML model utilized average and maximal RSP values extracted from the EEG signals as inputs. The results demonstrated significant differences in accuracies across fabric stimulations in higher frequency bands (beta/gamma),

indicating the potential of the SVM-ML model for automatically evaluating post-stroke fine tactile sensations and its alignment with a manual assessment of cortical responses for textile stimulations.

In the second experiment of the study, the instant influences of tsES in cortical and muscular signals of voluntary upper limb movements were investigated in individuals with chronic stroke. The findings revealed that tsES results in a statistically increase in CMCoh and LI for agonist distal muscles, a decrease in activation levels of EMG in antagonist distal muscle and proximal UE muscles, and an increase in the LI of the proximal UE muscles.

The third experiment of the study involved the implementation of a randomized clinical trial to explore training influences of tsES on upper limb motor recovery for individuals poststroke. The tsES group demonstrated significant differences in the evaluated outcomes throughout the training sessions. There were significant enhancements observed in the clinical assessments, including FMA and MAS, indicating enhanced motor function and released muscle spasticity. The laterality index of distal and proximal muscles also showed a significant increase, while the CMCoh and EMG activation levels of antagonist distal muscles and proximal muscles decreased significantly.

In conclusion, the EEG-based SVM classification model demonstrated potential for automating the assessment of fine tactile sensations after stroke, offering a more

efficient and objective assessment method. The combination of non-invasive cervical tsES with VPT in chronic stroke patients resulted in significant improvements in upper limb functionality and reduction in muscular spasticity. The tsES intervention facilitated enhanced responsiveness of residual descending pathways, increasing spinal cord excitability, and mitigating compensatory effects in proximal upper limb muscles, suggesting its potential as an adjunctive approach for long-term upper limb motor function recovery in chronic stroke rehabilitation.

We will undertake further research focusing on the following four aspects:

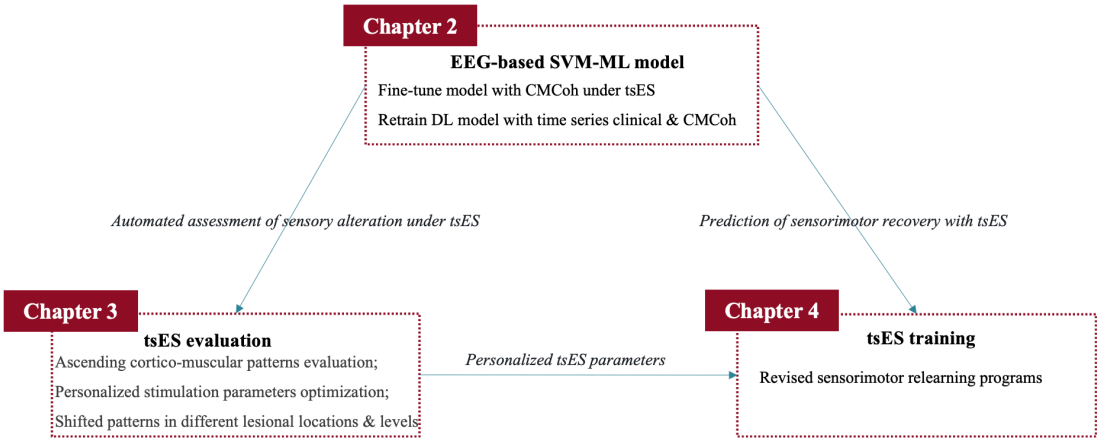

(1) Investigation of fine-tuned SVM-ML models (Chapter 2) that facilitate the automatic evaluation of sensory functions alteration under tsES (Chapter 3).

(2) Implementation of deep learning methods to analyze the time series data obtained during the evaluation of the rehabilitative effects of tsES combined with VPT (Chapter 4). By leveraging these advanced techniques, we aim to extract valuable insights and make accurate prognosis predictions, which can greatly contribute to personalized

treatment approaches.

(3) Expansion of our data collection efforts to include additional quantified and objective parameters, such as descending CMCoh, ascending CMCoh, and functional connectivity (Chapter 3). Investigation of optimization in personalized tsES stimulation parameters and shifted patterns in different lesional locations and impairments level (Chapter 3). These parameters will play a crucial role in deepening our understanding of both immediate effects of tsES and rehabilitation effects of tsES combined with VPT.

(4) Exploration of the rehabilitation effectiveness achieved by incorporating revised sensorimotor relearning strategies into tsES specifically targeted at lesioned side of persons suffering from chronic stroke (Chapter 4). The investigation aims to uncover novel strategies for enhancing rehabilitation outcomes and improving the quality of life for these individuals.

APPENDICES

Appendices A: Clinical Assessments for Upper Extremity

A-1: Mini-mental State Examination (MMSE)

Mini-Mental State Examination (MMSE)

Patient's Name: _____ Date: _____

***Instructions:* Ask the questions in the order listed. Score one point for each correct response within each question or activity.**

Maximum Score	Patient's Score	Questions
5		"What is the year? Season? Date? Day of the week? Month?"
5		"Where are we now: State? County? Town/city? Hospital? Floor?"
3		The examiner names three unrelated objects clearly and slowly, then asks the patient to name all three of them. The patient's response is used for scoring. The examiner repeats them until patient learns all of them, if possible. Number of trials: _____
5		"I would like you to count backward from 100 by sevens." (93, 86, 79, 72, 65, ...) Stop after five answers. Alternative: "Spell WORLD backwards." (D-L-R-O-W)
3		"Earlier I told you the names of three things. Can you tell me what those were?"
2		Show the patient two simple objects, such as a wristwatch and a pencil, and ask the patient to name them.
1		"Repeat the phrase: 'No ifs, ands, or buts.'"
3		"Take the paper in your right hand, fold it in half, and put it on the floor." (The examiner gives the patient a piece of blank paper.)
1		"Please read this and do what it says." (Written instruction is "Close your eyes.")
1		"Make up and write a sentence about anything." (This sentence must contain a noun and a verb.)
1		"Please copy this picture." (The examiner gives the patient a blank piece of paper and asks him/her to draw the symbol below. All 10 angles must be present and two must intersect.) 
30		TOTAL

(Adapted from Rovner & Folstein, 1987)

Instructions for administration and scoring of the MMSE

Orientation (10 points):

- Ask for the date. Then specifically ask for parts omitted (e.g., "Can you also tell me what season it is?"). One point for each correct answer.
- Ask in turn, "Can you tell me the name of this hospital (town, county, etc.)?" One point for each correct answer.

Registration (3 points):

- Say the names of three unrelated objects clearly and slowly, allowing approximately one second for each. After you have said all three, ask the patient to repeat them. The number of objects the patient names correctly upon the first repetition determines the score (0-3). If the patient does not repeat all three objects the first time, continue saying the names until the patient is able to repeat all three items, up to six trials. Record the number of trials it takes for the patient to learn the words. If the patient does not eventually learn all three, recall cannot be meaningfully tested.
- After completing this task, tell the patient, "Try to remember the words, as I will ask for them in a little while."

Attention and Calculation (5 points):

- Ask the patient to begin with 100 and count backward by sevens. Stop after five subtractions (93, 86, 79, 72, 65). Score the total number of correct answers.
- If the patient cannot or will not perform the subtraction task, ask the patient to spell the word "world" backwards. The score is the number of letters in correct order (e.g., dlrow=5, dlorw=3).

Recall (3 points):

- Ask the patient if he or she can recall the three words you previously asked him or her to remember. Score the total number of correct answers (0-3).

Language and Praxis (9 points):

- Naming: Show the patient a wrist watch and ask the patient what it is. Repeat with a pencil. Score one point for each correct naming (0-2).
- Repetition: Ask the patient to repeat the sentence after you ("No ifs, ands, or buts."). Allow only one trial. Score 0 or 1.
- 3-Stage Command: Give the patient a piece of blank paper and say, "Take this paper in your right hand, fold it in half, and put it on the floor." Score one point for each part of the command correctly executed.
- Reading: On a blank piece of paper print the sentence, "Close your eyes," in letters large enough for the patient to see clearly. Ask the patient to read the sentence and do what it says. Score one point only if the patient actually closes his or her eyes. This is not a test of memory, so you may prompt the patient to "do what it says" after the patient reads the sentence.
- Writing: Give the patient a blank piece of paper and ask him or her to write a sentence for you. Do not dictate a sentence; it should be written spontaneously. The sentence must contain a subject and a verb and make sense. Correct grammar and punctuation are not necessary.
- Copying: Show the patient the picture of two intersecting pentagons and ask the patient to copy the figure exactly as it is. All ten angles must be present and two must intersect to score one point. Ignore tremor and rotation.

(Folstein, Folstein & McHugh, 1975)

Interpretation of the MMSE

Method	Score	Interpretation
Single Cutoff	<24	Abnormal
Range	<21	Increased odds of dementia
	>25	Decreased odds of dementia
Education	21	Abnormal for 8th grade education
	<23	Abnormal for high school education
	<24	Abnormal for college education
Severity	24-30	No cognitive impairment
	18-23	Mild cognitive impairment
	0-17	Severe cognitive impairment

Sources:

- Crum RM, Anthony JC, Bassett SS, Folstein MF. Population-based norms for the mini-mental state examination by age and educational level. *JAMA*. 1993;269(18):2386-2391.
- Folstein MF, Folstein SE, McHugh PR. "Mini-mental state": a practical method for grading the cognitive state of patients for the clinician. *J Psychiatr Res*. 1975;12:189-198.
- Rovner BW, Folstein MF. Mini-mental state exam in clinical practice. *Hosp Pract*. 1987;22(1A):99, 103, 106, 110.
- Tombaugh TN, McIntyre NJ. The mini-mental state examination: a comprehensive review. *J Am Geriatr Soc*. 1992;40(9):922-935.

Form adopted from:

http://www.heartinstitutehd.com/Misc/Forms/MMSE.1276128605.pdf

A-2: Modified Ashworth Scale (MAS)

Modified Ashworth Scale Instructions

General Information (derived Bohannon and Smith, 1987):

- Place the patient in a supine position
- If testing a muscle that primarily flexes a joint, place the joint in a maximally flexed position and move to a position of maximal extension over one second (count "one thousand one")
- If testing a muscle that primarily extends a joint, place the joint in a maximally extended position and move to a position of maximal flexion over one second (count "one thousand one")
- Score based on the classification below

Scoring (taken from Bohannon and Smith, 1987):

0	No increase in muscle tone
1	Slight increase in muscle tone, manifested by a catch and release or by minimal resistance at the end of the range of motion when the affected part(s) is moved in flexion or extension
1+	Slight increase in muscle tone, manifested by a catch, followed by minimal resistance throughout the remainder (less than half) of the ROM
2	More marked increase in muscle tone through most of the ROM, but affected part(s) easily moved
3	Considerable increase in muscle tone, passive movement difficult
4	Affected part(s) rigid in flexion or extension

Patient Instructions:

The patient should be instructed to relax.

Modified Ashworth Scale Testing Form

Name:_____ Date:_____

Muscle Tested	Score
_____	____
_____	____
_____	____
_____	____
_____	____
_____	____
_____	____
_____	____
_____	____

Reference for test instructions:

Bohannon, R. and Smith, M. (1987). "Interrater reliability of a modified Ashworth scale of muscle spasticity." Physical Therapy 67(2): 206.

Form adopted from:

https://www.sralab.org/sites/default/files/2017-06/Modified%20Ashworth%20Scale%20Instructions.pdf

A-3: Motor Status Score (MSS)

SEATED ACTIVE RANGE OF MOTION (CHECK WHEELCHAIR POSITIONING)

Shoulder	**Movement**
1. A. Shoulder flexion to 90°, elbow 0°, forearm neutral *Deltoid, Rotator Cuff*	_____
B. If placed, can position be held? *Deltoid, Rotator Cuff*	
2. A. Shoulder abduction to 90°, elbow 0°, forearm pronated *Deltoid, Rotator Cuff*	_____
B. If placed, can position be held? *Deltoid, Rotator Cuff*	_____
3. A. Shoulder flex 90°–150°, elbow 0° *Deltoid, Rotator Cuff*	_____
B. If placed, can position be held? *Deltoid, Rotator Cuff*	_____
4. A. Touch top of head *Deltoid, Rotator Cuff, Biceps Brachii, Triceps Brachii*	_____
B. If placed, can position be held? *Deltoid, Rotator Cuff, Biceps Brachii, Triceps Brachii*	_____
5. A. Touch small of back *Subscapularis, Pectoralis Major, Latissimus Dorsi, Teres Major, Deltoid, Upper Trapezius*	_____
B. If placed, can position be held? *Subscapularis, Pectoralis Major, Latissimus Dorsi, Teres Major*	_____
6. Scapular elevation *Upper Trapezius, Levator Scapulae*	_____
7. Protraction/retraction of the scapula arm supported on table or lap *Serratus Anterior, Rhomboids Major, Minor, Middle Trapezius*	_____
8. A. Shoulder flex 0°–30°, elbow starts at 90° *Deltoid, Supraspinatus*	_____
B. Shoulder to 30° extension with elbow flex, forearm supported on table *Latissimus Dorsi, Teres Major, Posterior Deltoid*	_____
9. A. Shoulder 0°, elbow 90°, shoulder internal rotation to abdomen *Subscapularis, Pectoralis Major, Lattisimus Dorsi, Teres Major*	_____
B. Shoulder 0°, elbow 90°, shoulder external rotation *Infraspinatus, Teres Minor*	_____
10. Touch opposite knee *Pectoralis Major, Triceps Brachii, Pronator Group*	_____
Elbow/Forearm	
1. A. Forearm pronation from midposition shoulder 0°, elbow 90° *Pronator Group*	_____
B. Forearm supination from midposition shoulder 0°, elbow 90° *Biceps Brachii, Supinator*	_____
2. A. Elbow 0°, fully flex *Biceps Brachii, Brachialis, Brachioradialis*	_____
B. If placed, can position be held? *Biceps Brachii, Brachialis, Brachioradialis*	_____
3. Full elbow flexion, extend to 0° (gravity eliminated or against gravity) *Triceps Brachii*	_____
4. Touch opposite shoulder *Deltoid, Rotator Cuff, Pectoralis Major, Biceps*	_____

Wrist	**Movement**
1. Wrist extension with shoulder 0°, elbow 90°, forearm pronated *Extensor Carpi Radialis Longus, Brevis, Extensor Carpi Ulnaris*	_____
2. Wrist flex with shoulder 0°, elbow 90°, forearm supinated *Flexor Carpi Radialis, Flexor Carpi Ulnaris*	_____
3. Wrist circumduction shoulder 0°, elbow 90°, forearm pronated *Extensor Carpi, Radialis, Ulnaris, Flexor Carpi Radialis, Ulnaris*	_____
Hand	
1. Fingers—mass flexion (fingers to palm) *Flexor Digitorum Superficialis, Profundus, Flexor Digiti Minimi*	_____
2. Fingers—mass extension *Extensor Digitorum, Extensor Indicis, Extensor Digiti Minimi*	_____
3. Hook grasp *Flexor Digitorum Superficialis, Profundus*	_____
4. Intrinsic plus position *Interossei Volar, Dorsal*	_____
5. Thumb adduction *Abductor Pollicis Longus, Abductor Pollicis Brevis*	_____
6. Thumb adduction *Adductor Pollicis*	_____
7. Opposition to base of digit *Opponens Pollicis*	_____
8. A. Opposition to digit 2 (tip pinch)	_____
B. Opposition to digit 3 (tip pinch)	_____
C. Opposition to digit 4 (tip pinch) *Opponens Pollicis, Flexor Digitorum Superficialis, Profundus, Flexor Pollicis Longus, Interossei*	_____
D. Opposition to digit 5 (tip pinch) *Opponens Pollicis, Opponens Digiti Minimi, Flexor Pollicis Longus, Flexor Digitorum Superficialis, Profundus, Interossei*	_____
9. A. Opposition to digit 2 (pad pinch)	_____
B. Opposition to digit 3.(pad pinch)	_____
C. Opposition to digit 4 (pad pinch)	_____
D. Opposition to digit 5 (pad pinch) *Opponens Pollicis, Flexor Pollicis Brevis, Abductor Pollicis Brevis, Flexor Digitorum Superficialis, Profundus, Interossei, Opponens Digiti Minimi*	_____
10. Controlled grasp with soda can grasp, place 2–4 inches away, release	_____
11. Pincer grasp with pen (sign name, date, or 3 vertical lines)	_____
12. Lateral pinch with key	_____
Total movement scale	_____

Upper Extremity Motor Status Assessment

Patient name:_____
Scored by: _____
Date:_____

MOVEMENT SCALE—SHOULDER/ELBOW

0 = no volitional movement or no contraction
1– = contraction or patient initiating first few degrees of movement
1 = performs partly/incomplete or uncontrolled motion
1+ = lacking last few degrees of motion
2– = completes full range, decreased control or timing
2 = performs faultlessly (complete, controlled motion)

Place and hold (shoulder: 1B, 2B, 3B, 4B, 5B; elbow: 2B–0 or 1)

MOVEMENT SCALE—WRIST, HAND, AND FINGER

0 = no volitional movement or contraction
1 = performs partial movement
2 = performs complete movement faultlessly

Form adopted from:

https://journals.sagepub.com/doi/abs/10.1177/154596830201600306

A-4: Fugl-Meyer Assessment for Upper Extremity (FMA-UE)

FMA-UE PROTOCOL — Rehabilitation Medicine, University of Gothenburg

FUGL-MEYER ASSESSMENT **ID:**
UPPER EXTREMITY (FMA-UE) **Date:**
Assessment of sensorimotor function **Examiner**:

Fugl-Meyer AR, Jaasko L, Leyman I, Olsson S, Steglind S: The post-stroke hemiplegic patient. A method for evaluation of physical performance. Scand J Rehabil Med 1975, 7:13-31.

A. UPPER EXTREMITY, sitting position					
I. Reflex activity			**none**	**can be elicited**	
Flexors: biceps and finger flexors (at least one) **Extensors**: triceps			0 0	2 2	
Subtotal I (max 4)					
II. Volitional movement within synergies, without gravitational help			**none**	**partial**	**full**
Flexor synergy: Hand from contralateral knee to ipsilateral ear. From extensor synergy (shoulder adduction/ internal rotation, elbow extension, forearm pronation) to flexor synergy (shoulder abduction/ external rotation, elbow flexion, forearm supination). **Extensor synergy:** Hand from ipsilateral ear to the contralateral knee	Shoulder Elbow Forearm	retraction elevation abduction (90°) external rotation flexion supination	0 0 0 0 0 0	1 1 1 1 1 1	2 2 2 2 2 2
	Shoulder Elbow Forearm	adduction/internal rotation extension pronation	0 0 0	1 1 1	2 2 2
Subtotal II (max 18)					
III. Volitional movement mixing synergies, without compensation			**none**	**partial**	**full**
Hand to lumbar spine hand on lap	cannot perform or hand in front of ant-sup iliac spine hand behind ant-sup iliac spine (without compensation) hand to lumbar spine (without compensation)		0	1	2
Shoulder flexion 0°- 90° elbow at 0° pronation-supination 0°	immediate abduction or elbow flexion abduction or elbow flexion during movement flexion 90°, no shoulder abduction or elbow flexion		0	1	2
Pronation-supination elbow at 90° shoulder at 0°	no pronation/supination, starting position impossible limited pronation/supination, maintains starting position full pronation/supination, maintains starting position		0	1	2
Subtotal III (max 6)					
IV. Volitional movement with little or no synergy			**none**	**partial**	**full**
Shoulder abduction 0 - 90° elbow at 0° forearm neutral	immediate supination or elbow flexion supination or elbow flexion during movement abduction 90°, maintains extension and pronation		0	1	2
Shoulder flexion 90° - 180° elbow at 0° pronation-supination 0°	immediate abduction or elbow flexion abduction or elbow flexion during movement flexion 180°, no shoulder abduction or elbow flexion		0	1	2
Pronation/supination elbow at 0° shoulder at 30°- 90° flexion	no pronation/supination, starting position impossible limited pronation/supination, maintains start position full pronation/supination, maintains starting position		0	1	2
Subtotal IV (max 6)					
V. Normal reflex activity assessed only if full score of 6 points is achieved in part IV; compare with the unaffected side			**hyper**	**lively**	**normal**
Biceps, triceps, finger flexors	2 of 3 reflexes markedly hyperactive 1 reflex markedly hyperactive or at least 2 reflexes lively maximum of 1 reflex lively, none hyperactive		0	1	2
Subtotal V (max 2)					
Total A (max 36)					

B. WRIST support may be provided at the elbow to take or hold the starting position, no support at wrist, check the passive range of motion prior testing		**none**	**partial**	**full**
Stability at 15° dorsiflexion elbow at 90°, forearm pronated shoulder at 0°	less than 15° active dorsiflexion dorsiflexion 15°, no resistance tolerated maintains dorsiflexion against resistance	0	1	2
Repeated dorsifexion / volar flexion elbow at 90°, forearm pronated shoulder at 0°, slight finger flexion	cannot perform volitionally limited active range of motion full active range of motion, smoothly	0	1	2
Stability at 15° dorsiflexion elbow at 0°, forearm pronated slight shoulder flexion/abduction	less than 15° active dorsiflexion dorsiflexion 15°, no resistance tolerated maintains dorsiflexion against resistance	0	1	2
Repeated dorsifexion / volar flexion elbow at 0°, forearm pronated slight shoulder flexion/abduction	cannot perform volitionally limited active range of motion full active range of motion, smoothly	0	1	2
Circumduction elbow at 90°, forearm pronated shoulder at 0°	cannot perform volitionally jerky movement or incomplete complete and smooth circumduction	0	1	2
	Total B (max 10)			

C. HAND support may be provided at the elbow to keep 90° flexion, no support at the wrist, compare with unaffected hand, the objects are interposed, active grasp		**none**	**partial**	**full**
Mass flexion from full active or passive extension		0	1	2
Mass extension from full active or passive flexion		0	1	2
GRASP				
a. Hook grasp flexion in PIP and DIP (digits II-V), extension in MCP II-V	cannot be performed can hold position but weak maintains position against resistance	0	1	2
b. Thumb adduction 1-st CMC, MCP, IP at 0°, scrap of paper between thumb and 2-nd MCP joint	cannot be performed can hold paper but not against tug can hold paper against a tug	0	1	2
c. Pincer grasp, opposition pulpa of the thumb against the pulpa of 2-nd finger, pencil, tug upward	cannot be performed can hold pencil but not against tug can hold pencil against a tug	0	1	2
d. Cylinder grasp cylinder shaped object (small can) tug upward, opposition of thumb and fingers	cannot be performed can hold cylinder but not against tug can hold cylinder against a tug	0	1	2
e. Spherical grasp fingers in abduction/flexion, thumb opposed, tennis ball, tug away	cannot be performed can hold ball but not against tug can hold ball against a tug	0	1	2
	Total C (max 14)			

D. COORDINATION/SPEED, sitting, after one trial with both arms, eyes closed, tip of the index finger from knee to nose, 5 times as fast as possible		**marked**	**slight**	**none**
Tremor		0	1	2
Dysmetria	pronounced or unsystematic slight and systematic no dysmetria	0	1	2
		≥ 6s	**2 - 5s**	**< 2s**
Time start and end with the hand on the knee	6 or more seconds slower than unaffected side 2-5 seconds slower than unaffected side less than 2 seconds difference	0	1	2
	Total D (max 6)			

TOTAL A-D (max 66)	

Form adopted from:

https://www.gu.se/en/neuroscience-physiology/fugl-meyer-assessment

A-5: Action Research Arm Test (ARAT)

ACTION RESEARCH ARM TEST

Patient Name: _____

Rater Name: _____

Date: _____

Instructions

There are four subtests: Grasp, Grip, Pinch, Gross Movement. Items in each are ordered so that:

- if the subject passes the first, no more need to be administered and he scores top marks for that subtest;
- if the subject fails the first *and* fails the second, he scores zero, and again no more tests need to be performed in that subtest;
- otherwise he needs to complete all tasks within the subtest

Activity	Score
Grasp	
1. Block, wood, 10 cm cube (If score = 3, total = 18 and to Grip) Pick up a 10 cm block	_____
2. Block, wood, 2.5 cm cube (If score = 0, total = 0 and go to Grip) Pick up 2.5 cm block	_____
3. Block, wood, 5 cm cube	_____
4. Block, wood, 7.5 cm cube	_____
5. Ball (Cricket), 7.5 cm diameter	_____
6. Stone 10 x 2.5 x 1 cm	_____
Coefficient of reproducibility = 0.98	
Coefficient of scalability = 0.94	
Grip	
1. Pour water from glass to glass (If score = 3, total = 12, and go to Pinch)	_____
2. Tube 2.25 cm (If score = 0, total = 0 and go to Pinch)	_____
3. Tube 1 x 16 cm	_____
4. Washer (3.5 cm diameter) over bolt	_____
Coefficient of reproducibility = 0.99	
Coefficient of scalability = 0.98	
Pinch	
1. Ball bearing, 6 mm, 3rd finger and thumb (If score = 3, total = 18 and go to Grossmt)	_____
2. Marble, 1.5 cm, index finger and thumb (If score = 0, total = 0 and go to Grossmt)	_____
3. Ball bearing 2nd finger and thumb	_____
4. Ball bearing 1st finger and thumb	_____
5. Marble 3rd finger and thumb	_____
6. Marble 2nd finger and thumb	_____
Coefficient of reproducibility = 0.99	
Coefficient of scalability = 0.98	

Grossmt (Gross Movement)

1. Place hand behind head (If score = 3, total = 9 and finish) _____
2. (If score = 0, total = 0 and finish _____
3. Place hand on top of head _____
4. Hand to mouth _____

Coefficient of reproducibility = 0.98

Coefficient of scalability = 0.97

References

Carroll D. "A quantitative test of upper extremity function."
J Chronic Diseases. 1965;18:479-491.

Crow JL, Lincoln NNB, Nouri FM, De Weerdt W. "The effectiveness of EMG biofeedback in the treatment of arm function after stroke.
International Disability Studies. 1989;11:155-160.

De Weerdt WJG, Harrison MA. "Measuring recovery of arm-hand function in stroke patients: a comparison of the Brunnstrom-Fugl-Meyer test and the Action Research Arm test.
Physiotherapy Canada. 1985;37:65-70.

Lyle RC. "A performance test for assessment of upper limb function in physical rehabilitation treatment and research."
Int J Rehabil Res. 1981;4:483-492.

Form adopted from:

https://faculty.ksu.edu.sa/sites/default/files/action_research_arm_test.pdf

A-6: Functional Independence Measurement (FIM)

	ADMISSION	DISCHARGE	FOLLOW-UP
Self-Care			
A. Eating			
B. Grooming			
C. Bathing			
D. Dressing - Upper Body			
E. Dressing - Lower Body			
F. Toileting			
Sphincter Control			
G. Bladder Management			
H. Bowel Management			
Transfers			
I. Bed, Chair, Wheelchair			
J. Toilet			
K. Tub, Shower			
Locomotion			
L. Walk/Wheelchair			
M. Stairs			
Motor Subtotal Score			
Communication			
N. Comprehension			
O. Expression			
Social Cognition			
P. Social Interaction			
Q. Problem Solving			
R. Memory			
Cognitive Subtotal Score			
TOTAL FIM Score			

LEVELS		
	Independent 7 Complete Independence (Timely, Safely) 6 Modified Independence (Device)	**NO HELPER**
	Modified Dependence 5 Supervision (Subject = 100%+) 4 Minimal Assist (Subject = 75%+) 3 Moderate Assist (Subject = 50%+) **Complete Dependence** 2 Maximal Assist (Subject = 25%+) 1 Total Assist (Subject = less than 25%)	**HELPER**
Note: Leave no blanks. Enter 1 if patient is not testable due to risk.		

Form adopted from:

https://www.physio-pedia.com/Functional_Independence_Measure_(FIM)

A-7: Wolf Motor Function Test (WMFT)

Type/Purpose of Test: The purpose of this test is to quantify upper extremity UE motor ability through a series of timed and functional tasks.

Population: Used primarily for stroke patients but could be used for people with impaired UE motor ability. *Limited usefulness for patients with chronic stroke and TBI who are lower functioning in motor deficit. Or for acute or sub-acute stroke before spontaneous recovery has completed.

Focus of measurement:
___Organic systems (X)Abilities ___Participation/life habits ___Environmental Factors

Ease of Administration:
General Description of the WMFT
All tasks are performed as quickly as possible and are truncated at
120 seconds. Tasks are as follows:
1. Forearm to table (side): Subject attempts to place forearm on the table by abduction at the shoulder.
2. Forearm to box (side): Subject attempts to place a forearm on the box by abduction at the shoulder.
3. Extend elbow (side): Subject attempts to reach across the table by extending the elbow (to the side).
4. Extend elbow (to the side), with weight: Subject attempts to push the sandbag against outer wrist joint across the table by extending the elbow.
5. Hand to table (front): Subject attempts to place involved hand on the table.
6. Hand to box (front): Subject attempts to place hand on the box.
7. Reach and retrieve (front): Subject attempts to pull 1-lb weight across the table by using elbow flexion and cupped wrist.
8. Lift can (front): Subject attempts to lift can and bring it close to lips with a cylindrical grasp.
9. Lift pencil (front): Subject attempts to pick up pencil by using 3-jaw chuck grasp
10. Pick up paper clip (front): Subject attempts to pick up paper clip by using a pincer grasp.
11. Stack checkers (front): Subject attempts to stack checkers onto the center checker.
12. Flip cards (front): Using the pincer grasp, patient attempts to flip each card over.
13. Turning the key in lock (front): Using pincer grasp, while maintaining contact, patient turns key fully to the left and right.
14. Fold towel (front): Subject grasps towel, folds it lengthwise, and then uses the tested hand to fold the towel in half again.
15. Lift basket (standing): Subject picks up basket by grasping the handles and placing it on bedside table.

Clarity of Directions:
Very clear and easy to follow directions for the administrator of the test and the test taker.

Scoring Procedures:
The speed at which functional tasks can be completed is measured by performance time and the movement quality when completing the tasks is measured by functional ability.
Speed is measured by timing the task with a stopwatch from start to finish.
Movement quality during the task is measured by functional ability using a 6-point ordinal scale, where 0 = does not attempt with the involved arm and 5 = arm does participate/movement appears to be normal.

Examiner Qualification & Training
No qualification or training required.

Standardization: ____ **Norms** ____ **Criterion Referenced** ____ **Other** **None were mentioned in the manual.**

Reliability: The inter-test and inter-rater reliability, and internal consistency and stability of the test is high for both the performance time and Functional Ability rating scale measures, ranging from .88 to .98, with most values ≈ .95

Validity: Construct validity, criterion validity

Manual: ____ **Excellent** **(X) Adequate** ____ **Poor**

What is (are) the setting/s that you would anticipate using this assessment?
I could see this used in any setting where a person with a stroke or UE motor impairment is being treated. Inpatient, outpatient, home health, related research, etc. (acute rehab might be a little premature for this type of test.)

Summary of strengths and weaknesses:

Weakness:
I think that it is very easy for interraters to be consistent with the timing part of the test but I think there could be some difference of opinion for the movement quality assessment. A patient could become very frustrated if they were not able to do well in a timed test environment.

Strength:
There are mostly functional measurements of UE use. It is something that can be used to track progress of a patient. Very easy to learn and administer. Not expensive to simulate in a clinic or wherever you want to use it.

Form adopted from:

https://strokengine.ca/en/assessments/wmft/

Appendices B: Consent Form for Chapter 3 and Chapter 4

THE HONG KONG POLYTECHNIC UNIVERSITY
香港理工大學

CONSENT TO PARTICIPATE IN RESEARCH

Restoring functional capacity of the upper extremity using mass volitional training and trans-spinal electrical stimulation in individuals with chronic Stroke

I _____ hereby consent to participate in the captioned research supervised by Dr. Monzurul Alam, Dr. Xiaoling Hu and Prof. Yong-Ping Zheng.

I understand that information obtained from this research may be used in future research and publication(s). However, my right to privacy will be retained, i.e. my personal details will not be revealed.

The procedure as set out in the attached information sheet has been fully explained. I understand the benefit and potential risks involved. My participation in the project is voluntary.

I acknowledge that I have the right to question any part of the procedure and can withdraw at any time without penalty of any kind.

Name of participant: _____

Signature of participant: _____

Name of researcher: _____

Signature of researcher: _____

Date: _____

Hung Hom Kowloon Hong Kong 香港 九龍 紅磡
Tel 電話 (852) 2766 5111 Fax 傳真 (852) 2784 3374
Email 電郵 polyu@polyu.edu.hk
Website 網址 www.polyu.edu.hk

THE HONG KONG POLYTECHNIC UNIVERSITY
香港理工大學

參與研究同意書

以脊髓電刺激療法及自主活動訓練恢復慢性中風患者的上肢活動能力

本人_____同意參與由 Monzurul Alam 博士，胡曉翎博士及鄭永平教授領導的上述研究。

本人知悉此研究所得的資料可能被用作日後的研究及發表，但本人的私隱權利將得以保留，即本人的個人資料不會被公開。

研究人員已向本人清楚解釋列在所附資料卡上的研究程序，本人明瞭當中涉及的利益及風險；本人自願參與研究項目。

本人知悉本人有權就程序的任何部分提出疑問，並有權隨時退出而不受任何懲處。

參與者姓名: _____

參與者簽署: _____

研究人員姓名: _____

研究人員簽署: _____

日期: _____

Hung Hom Kowloon Hong Kong 香港 九龍 紅磡
Tel 電話 (852) 2766 5111 Fax 傳真 (852) 2784 3374
Email 電郵 polyu@polyu.edu.hk
Website 網址 www.polyu.edu.hk

REFERENCES

1. Triccas, L.T., et al., *A systematic review investigating the relationship of electroencephalography and magnetoencephalography measurements with sensorimotor upper limb impairments after stroke.* Journal of neuroscience methods, 2019. **311**: p. 318-330.
2. Persson, H.C., et al., *Outcome and upper extremity function within 72 hours after first occasion of stroke in an unselected population at a stroke unit. A part of the SALGOT study.* BMC neurology, 2012. **12**: p. 1-6.
3. Canning, C.G., et al., *Loss of strength contributes more to physical disability after stroke than loss of dexterity.* Clinical rehabilitation, 2004. **18**(3): p. 300-308.
4. Raghavan, P., *Upper limb motor impairment after stroke.* Physical Medicine and Rehabilitation Clinics, 2015. **26**(4): p. 599-610.
5. Tyson, S.F., et al., *Sensory loss in hospital-admitted people with stroke: characteristics, associated factors, and relationship with function.* Neurorehabilitation and neural repair, 2008. **22**(2): p. 166-172.
6. Kessner, S.S., U. Bingel, and G. Thomalla, *Somatosensory deficits after stroke: a scoping review.* Topics in stroke rehabilitation, 2016. **23**(2): p. 136-146.
7. Zhang, J., et al., *Evaluation of Post-Stroke Impairment in Fine Tactile Sensation by Electroencephalography (EEG)-Based Machine Learning.* Applied Sciences, 2022. **12**(9): p. 4796.
8. Feigin, V.L., et al., *World Stroke Organization (WSO): global stroke fact sheet 2022.* International Journal of Stroke, 2022. **17**(1): p. 18-29.
9. Feigin, V.L., et al., *Global, regional, and national burden of stroke and its risk factors, 1990–2019: a systematic analysis for the Global Burden of Disease Study 2019.* The Lancet Neurology, 2021. **20**(10): p. 795-820.
10. Kim, J., et al., *Global stroke statistics 2019.* International Journal of Stroke, 2020. **15**(8): p. 819-838.
11. Wang, J., et al., *Trends in age of first-ever stroke following increased incidence and life expectancy in a low-income Chinese population.* Stroke, 2016. **47**(4): p. 929-935.
12. Boot, E., et al., *Ischaemic stroke in young adults: a global perspective.* Journal of Neurology, Neurosurgery & Psychiatry, 2020. **91**(4): p. 411-417.
13. LKS Faculty of Medicine, H. *HKUMed research shows 30% increase in 'young stroke' incidence in Hong Kong and calls for better control of vascular risk factors such as hypertension*. 2022.

14. Johnson, A.J., et al., *Physiological risk profiles and allostatic load: Using latent profile analysis to examine socioeconomic differences in physiological patterns of risk.* European Journal of Environment and Public Health, 2019. **3**(2): p. em0029.

15. Katan, M. and A. Luft. *Global burden of stroke*. in *Seminars in neurology*. 2018. Thieme Medical Publishers.

16. Connell, L.A. and S. Tyson, *Measures of sensation in neurological conditions: a systematic review.* Clinical rehabilitation, 2012. **26**(1): p. 68-80.

17. Winward, C.E., P.W. Halligan, and D.T. Wade, *Current practice and clinical relevance of somatosensory assessment after stroke.* Clinical rehabilitation, 1999. **13**(1): p. 48-55.

18. Pumpa, L.U., L.S. Cahill, and L.M. Carey, *Somatosensory assessment and treatment after stroke: An evidence - practice gap.* Australian occupational therapy journal, 2015. **62**(2): p. 93-104.

19. Cortese, A.M., et al., *Cortical thickness of brain areas beyond stroke lesions and sensory-motor recovery: a systematic review.* Frontiers in neuroscience, 2021. **15**: p. 764671.

20. Kim, B. and C. Winstein, *Can neurological biomarkers of brain impairment be used to predict poststroke motor recovery? A systematic review.* Neurorehabilitation and neural repair, 2017. **31**(1): p. 3-24.

21. Chollet, F., et al., *The functional anatomy of motor recovery after stroke in humans: a study with positron emission tomography.* Annals of neurology, 1991. **29**(1): p. 63-71.

22. Lundgren, J., et al., *Site of brain lesion and functional capacity in rehabilitated hemiplegics.* Scandinavian Journal of Rehabilitation Medicine, 1982. **14**(3): p. 141-143.

23. Giaquinto, S., et al., *EEG recordings in the course of recovery from stroke.* Stroke, 1994. **25**(11): p. 2204-2209.

24. Takeuchi, N. and S.-I. Izumi, *Rehabilitation with poststroke motor recovery: a review with a focus on neural plasticity.* Stroke research and treatment, 2013. **2013**.

25. Olafson, E.R., et al., *Functional connectome reorganization relates to post-stroke motor recovery and structural and functional disconnection.* Neuroimage, 2021. **245**: p. 118642.

26. Ward, N., et al., *Neural correlates of motor recovery after stroke: a longitudinal fMRI study.* Brain, 2003. **126**(11): p. 2476-2496.

27. Hou, Y., et al., *Research Applications of Positron Emission*

Tomography/Magnetic Resonance (PET/MR) Imaging in Cerebrovascular Diseases. PET/MR: Functional and Molecular Imaging of Neurological Diseases and Neurosciences, 2023: p. 265-296.

28. Milani, G., et al., *Relation Between EEG Measures and Upper Limb Motor Recovery in Stroke Patients: A Scoping Review.* Brain Topography, 2022. **35**(5-6): p. 651-666.

29. Jiang, R., et al., *Interpreting Brain Biomarkers: Challenges and solutions in interpreting machine learning-based predictive neuroimaging.* IEEE Signal Processing Magazine, 2022. **39**(4): p. 107-118.

30. Sirsat, M.S., E. Fermé, and J. Camara, *Machine learning for brain stroke: a review.* Journal of Stroke and Cerebrovascular Diseases, 2020. **29**(10): p. 105162.

31. Kotsiantis, S.B., I. Zaharakis, and P. Pintelas, *Supervised machine learning: A review of classification techniques.* Emerging artificial intelligence applications in computer engineering, 2007. **160**(1): p. 3-24.

32. Bentley, P., et al., *Prediction of stroke thrombolysis outcome using CT brain machine learning.* NeuroImage: Clinical, 2014. **4**: p. 635-640.

33. Fernández-Delgado, M., et al., *Do we need hundreds of classifiers to solve real world classification problems?* The journal of machine learning research, 2014. **15**(1): p. 3133-3181.

34. Pierella, C., et al., *A multimodal approach to capture post-stroke temporal dynamics of recovery.* Journal of neural engineering, 2020. **17**(4): p. 045002.

35. Mateos-Pérez, J.M., et al., *Structural neuroimaging as clinical predictor: A review of machine learning applications.* NeuroImage: Clinical, 2018. **20**: p. 506-522.

36. Calik, N., et al., *Deep-learning-based precise characterization of microwave transistors using fully-automated regression surrogates.* Scientific Reports, 2023. **13**(1): p. 1445.

37. Soman, K., R. Loganathan, and V. Ajay, *Machine learning with SVM and other kernel methods*. 2009: PHI Learning Pvt. Ltd.

38. Van Peppen, R.P., et al., *The impact of physical therapy on functional outcomes after stroke: what's the evidence?* Clinical rehabilitation, 2004. **18**(8): p. 833-862.

39. Bobath, B., *Adult hemiplegia: evaluation and treatment.* (No Title), 1990.

40. Voss, D.E., *Proprioceptive neuromuscular facilitation.* American Journal of Physical Medicine & Rehabilitation, 1967. **46**(1): p. 838-898.

41. Chan, D.Y., C.C. Chan, and D.K. Au, *Motor relearning programme for stroke patients: a randomized controlled trial.* Clinical rehabilitation, 2006. **20**(3): p. 191-200.

42. Jones, M.L., et al., *Activity-based therapy for recovery of walking in individuals with chronic spinal cord injury: results from a randomized clinical trial.* Archives of physical medicine and rehabilitation, 2014. **95**(12): p. 2239-2246. e2.

43. Woldag, H. and H. Hummelsheim, *Evidence-based physiotherapeutic concepts for improving arm and hand function in stroke patients: a review.* Journal of neurology, 2002. **249**: p. 518-528.

44. Basmajian, J., et al., *Stroke treatment: comparison of integrated behavioral-physical therapy vs traditional physical therapy programs.* Archives of Physical Medicine and Rehabilitation, 1987. **68**(5 Pt 1): p. 267-272.

45. Langhammer, B. and J.K. Stanghelle, *Bobath or motor relearning programme? A comparison of two different approaches of physiotherapy in stroke rehabilitation: a randomized controlled study.* Clinical rehabilitation, 2000. **14**(4): p. 361-369.

46. Van Vliet, P., N. Lincoln, and A. Foxall, *Comparison of Bobath based and movement science based treatment for stroke: a randomised controlled trial.* Journal of Neurology, Neurosurgery & Psychiatry, 2005. **76**(4): p. 503-508.

47. Chen, J.-C. and F.-Z. Shaw, *Progress in sensorimotor rehabilitative physical therapy programs for stroke patients.* World Journal of Clinical Cases: WJCC, 2014. **2**(8): p. 316.

48. Harkema, S., A. Behrman, and H. Barbeau, *Evidence-based therapy for recovery of function after spinal cord injury.* Handbook of clinical neurology, 2012. **109**: p. 259-274.

49. Martin, R., *Utility and Feasibility of Transcutaneous Spinal Cord Stimulation for Patients with Incomplete SCI in Therapeutic Settings: A Review of Topic.* Frontiers in Rehabilitation Sciences, 2021. **2**: p. 724003.

50. Lang, C.E., et al., *Observation of amounts of movement practice provided during stroke rehabilitation.* Archives of physical medicine and rehabilitation, 2009. **90**(10): p. 1692-1698.

51. Zorowitz, R. and M. Brainin, *Advances in brain recovery and rehabilitation 2010.* Stroke, 2011. **42**(2): p. 294-297.

52. Pollock, A., et al., *Physiotherapy treatment approaches for the recovery of postural control and lower limb function following stroke: a systematic review.* Clinical rehabilitation, 2007. **21**(5): p. 395-410.

53. Paro, M.R., et al., *Deep brain stimulation for movement disorders after stroke: a systematic review of the literature.* Journal of Neurosurgery, 2022. **138**(6): p. 1688-1701.

54. Levy, R.M., et al., *Epidural electrical stimulation for stroke rehabilitation: results of the prospective, multicenter, randomized, single-blinded everest trial.* Neurorehabilitation and neural repair, 2016. **30**(2): p. 107-119.

55. Angeli, C.A., et al., *Recovery of over-ground walking after chronic motor complete spinal cord injury.* New England Journal of Medicine, 2018. **379**(13): p. 1244-1250.

56. Peña Pino, I., et al., *Long-term spinal cord stimulation after chronic complete spinal cord injury enables volitional movement in the absence of stimulation.* Frontiers in systems neuroscience, 2020. **14**: p. 35.

57. Bonizzato, M., et al., *Multi-pronged neuromodulation intervention engages the residual motor circuitry to facilitate walking in a rat model of spinal cord injury.* Nature Communications, 2021. **12**(1): p. 1925.

58. Tharu, N.S., *Trans-spinal electrical stimulation for improving trunk and sitting function in tetraplegics with cervical cord injury.* 2023.

59. Barss, T.S., et al., *Neural substrates of transcutaneous spinal cord stimulation: neuromodulation across multiple segments of the spinal cord.* Journal of Clinical Medicine, 2022. **11**(3): p. 639.

60. Sayenko, D.G., et al., *Self-assisted standing enabled by non-invasive spinal stimulation after spinal cord injury.* Journal of neurotrauma, 2019. **36**(9): p. 1435-1450.

61. Powell, M.P., et al., *Epidural stimulation of the cervical spinal cord for post-stroke upper-limb paresis.* Nature medicine, 2023. **29**(3): p. 689-699.

62. Paget-Blanc, A., et al., *Non-invasive treatment of patients with upper extremity spasticity following stroke using paired trans-spinal and peripheral direct current stimulation.* Bioelectronic medicine, 2019. **5**(1): p. 1-10.

63. Grecco, L.H., et al., *Transcutaneous spinal stimulation as a therapeutic strategy for spinal cord injury: state of the art.* Journal of Neurorestoratology, 2015. **3**(1): p. 73-82.

64. Gerasimenko, Y.P., et al., *Noninvasive reactivation of motor descending control after paralysis.* Journal of neurotrauma, 2015. **32**(24): p. 1968-1980.

65. Zhang, H., et al., *Restoring sensorimotor function through neuromodulation after spinal cord injury: progress and remaining challenges.* Frontiers in Neuroscience, 2021. **15**: p. 749465.

66. Doyle, S.D., S. Bennett, and B. Dudgeon, *Upper limb post-stroke sensory*

impairments: the survivor's experience. Disability and rehabilitation, 2014. **36**(12): p. 993-1000.

67. Pandyan, A.D., et al., *A review of the properties and limitations of the Ashworth and modified Ashworth Scales as measures of spasticity.* Clinical rehabilitation, 1999. **13**(5): p. 373-383.

68. Fugl-Meyer, A.R., et al., *The post-stroke hemiplegic patient. 1. a method for evaluation of physical performance.* Scandinavian journal of rehabilitation medicine, 1975. **7**(1): p. 13-31.

69. Winward, C.E., P.W. Halligan, and D.T. Wade, *The Rivermead Assessment of Somatosensory Performance (RASP): standardization and reliability data.* Clinical rehabilitation, 2002. **16**(5): p. 523-533.

70. Pan, N., *Quantification and evaluation of human tactile sense towards fabrics.* International Journal of Design & Nature and Ecodynamics, 2006. **1**(1): p. 48-60.

71. Auriat, A.M., et al., *A Review of Transcranial Magnetic Stimulation and Multimodal Neuroimaging to Characterize Post-Stroke Neuroplasticity.* Frontiers in Neurology, 2015. **6**: p. 226.

72. Lundgren, J., et al., *Site of brain lesion and functional capacity in rehabilitated hemiplegics.* Scandinavian journal of rehabilitation medicine, 1982. **14**(3): p. 141-143.

73. Chollet, F., et al., *The functional anatomy of motor recovery after stroke in humans: a study with positron emission tomography.* Annals of neurology, 1991. **29**(1): p. 63-71.

74. Broderick, P.A. and E.H. Kolodny, *Biosensors for brain trauma and dual laser doppler flowmetry: Enoxaparin simultaneously reduces stroke-induced dopamine and blood flow while enhancing serotonin and blood flow in motor neurons of brain, in vivo.* Sensors, 2010. **11**(1): p. 138-161.

75. Radaelli, A., et al., *New Concepts in Stroke Diagnosis and Therapy*. Vol. 1. 2017: Bentham Science Publishers.

76. Chen, Q., et al., *Radiomics in stroke neuroimaging: techniques, applications, and challenges.* Aging and disease, 2021. **12**(1): p. 143.

77. Militello, C., et al., *3D DCE-MRI Radiomic Analysis for Malignant Lesion Prediction in Breast Cancer Patients.* Academic Radiology, 2021.

78. Sharaev, M., et al. *Pattern recognition pipeline for neuroimaging data*. Springer.

79. Caliandro, P., et al., *Small-world characteristics of cortical connectivity changes in acute stroke.* Neurorehabilitation and neural repair, 2017. **31**(1): p. 81-94.

80. Bentes, C., et al., *Quantitative EEG and functional outcome following acute ischemic stroke.* Clinical Neurophysiology, 2018. **129**(8): p. 1680-1687.

81. Ahn, S.-N., J.-W. Lee, and S. Hwang, *Tactile Perception for Stroke Induce Changes in Electroencephalography.* Hong Kong Journal of Occupational Therapy, 2016. **28**: p. 1-6.

82. Huang, Y., et al., *Measurement of sensory deficiency in fine touch after stroke during textile fabric stimulation by electroencephalography (EEG).* 2020. **17**(4): p. 045007.

83. Roy, S., I. Kiral-Kornek, and S. Harrer. *ChronoNet: a deep recurrent neural network for abnormal EEG identification*. in *Conference on Artificial Intelligence in Medicine in Europe*. 2019. Springer.

84. Golmohammadi, M., et al., *Deep architectures for automated seizure detection in scalp EEGs.* arXiv preprint arXiv:1712.09776, 2017.

85. Hosseini, M.-P., et al., *Review of Machine Learning Algorithms for Brain Stroke Diagnosis and Prognosis by EEG Analysis.* 2020.

86. Jochumsen, M., et al., *Classification of Hand Grasp Kinetics and Types Using Movement-Related Cortical Potentials and EEG Rhythms.* Computational Intelligence and Neuroscience, 2017. **2017**: p. 7470864.

87. Usama, N., et al., *Detection of Error-Related Potentials in Stroke Patients from EEG Using an Artificial Neural Network.* Sensors, 2021. **21**(18): p. 6274.

88. Iáñez, E., et al. *LDA-based classifiers for a mental tasks-based brain-computer interface*. 2010. IEEE.

89. Garrett, D., et al., *Comparison of linear, nonlinear, and feature selection methods for EEG signal classification.* IEEE Transactions on neural systems and rehabilitation engineering, 2003. **11**(2): p. 141-144.

90. Cao, J., et al., *An accurate traffic classification model based on support vector machines.* International Journal of Network Management, 2017. **27**(1): p. e1962.

91. Vapnik, V., *The nature of statistical learning theory*. 2013: Springer science & business media.

92. Liu, Y., et al., *A boosting-based spatial-spectral model for stroke patients' EEG analysis in rehabilitation training.* IEEE Transactions on Neural Systems and Rehabilitation Engineering, 2015. **24**(1): p. 169-179.

93. Ghumman, M.K., et al., *Optimization of parameters for improving the performance of EEG-based BCI system.* Journal of Reliable Intelligent Environments, 2021. **7**(2): p. 145-156.

94. Bousseta, R., et al. *EEG efficient classification of imagined hand movement*

using RBF kernel SVM. IEEE.

95. Hsu, C.-W., C.-C. Chang, and C.-J. Lin, *A practical guide to support vector classification*. 2003, Taipei, Taiwan.

96. Farid, N., et al., *A comparative analysis for support vector machines for stroke patients.* Recent Adv Inf Sci, 2013: p. 71-76.

97. Kim, M.-K., J.-H. Cho, and J.-H. Jeong. *Classification of Tactile Perception and Attention on Natural Textures from EEG Signals*. in *2021 9th International Winter Conference on Brain-Computer Interface (BCI)*. 2021. IEEE.

98. Lilliefors, H.W., *On the Kolmogorov-Smirnov test for the exponential distribution with mean unknown.* Journal of the American Statistical Association, 1969. **64**(325): p. 387-389.

99. Homan, R.W., J. Herman, and P. Purdy, *Cerebral location of international 10–20 system electrode placement.* Electroencephalography and clinical neurophysiology, 1987. **66**(4): p. 376-382.

100. Welch, P., *The use of fast Fourier transform for the estimation of power spectra: a method based on time averaging over short, modified periodograms.* IEEE Transactions on audio and electroacoustics, 1967. **15**(2): p. 70-73.

101. Teplan, M., *Fundamentals of EEG measurement.* Measurement science review, 2002. **2**(2): p. 1-11.

102. Bronzino, J.D., *Biomedical Engineering Handbook 2*. Vol. 2. 2000: Springer Science & Business Media.

103. Patro, S. and K.K. Sahu, *Normalization: A preprocessing stage.* arXiv preprint arXiv:1503.06462, 2015.

104. Liao, X., et al., *Psychophysical Relations between Interacted Fabric Thermal-Tactile Properties and Psychological Touch Perceptions.* Journal of Sensory Studies, 2016. **31**(3): p. 181-192.

105. Hu, J.Y., et al., *Fabric Touch Tester: Integrated evaluation of thermal–mechanical sensory properties of polymeric materials.* Polymer testing, 2006. **25**(8): p. 1081-1090.

106. Bishop, C.M., *Pattern recognition and machine learning*. 2006: springer.

107. Syarif, I., A. Prugel-Bennett, and G. Wills, *SVM parameter optimization using grid search and genetic algorithm to improve classification performance.* Telkomnika, 2016. **14**(4): p. 1502.

108. Zhang, Y., et al., *Combined feature extraction method for classification of EEG signals.* Neural Computing and Applications, 2017. **28**(11): p. 3153-3161.

109. Guler, I. and E.D. Ubeyli, *Multiclass support vector machines for EEG-signals*

classification. IEEE transactions on information technology in biomedicine, 2007. **11**(2): p. 117-126.

110. Avelino, J., et al. *Human-aware natural handshaking using tactile sensors for Vizzy, a social robot*.

111. Pedregosa, F., et al., *Scikit-learn: Machine learning in Python.* the Journal of machine Learning research, 2011. **12**: p. 2825-2830.

112. Kattenstroth, J.-C., et al., *Long-term sensory stimulation therapy improves hand function and restores cortical responsiveness in patients with chronic cerebral lesions. Three single case studies.* Frontiers in Human Neuroscience, 2012. **6**: p. 244.

113. Pfurtscheller, G. and C. Neuper, *Motor imagery activates primary sensorimotor area in humans.* Neuroscience letters, 1997. **239**(2-3): p. 65-68.

114. James, G., et al., *An introduction to statistical learning*. Vol. 112. 2013: Springer.

115. Breiman, L., *Heuristics of instability and stabilization in model selection.* The annals of statistics, 1996. **24**(6): p. 2350-2383.

116. Witten, I.H. and E. Frank, *Data mining: practical machine learning tools and techniques with Java implementations.* Acm Sigmod Record, 2002. **31**(1): p. 76-77.

117. Bouckaert, R.R. *Choosing between two learning algorithms based on calibrated tests*.

118. Kuhn, M. and K. Johnson, *Applied predictive modeling*. Vol. 26. 2013: Springer.

119. Chang, M.-W. and C.-J. Lin, *Leave-one-out bounds for support vector regression model selection.* Neural Computation, 2005. **17**(5): p. 1188-1222.

120. Burges, C.J.C., *A tutorial on support vector machines for pattern recognition.* Data mining and knowledge discovery, 1998. **2**(2): p. 121-167.

121. Vivaldi, N., et al., *Evaluating performance of eeg data-driven machine learning for traumatic brain injury classification.* IEEE Transactions on Biomedical Engineering, 2021. **68**(11): p. 3205-3216.

122. Gao, L., et al., *EEG classification for motor imagery and resting state in BCI applications using multi-class Adaboost extreme learning machine.* Review of scientific instruments, 2016. **87**(8): p. 085110.

123. Kira, K. and L.A. Rendell, *A practical approach to feature selection*, in *Machine learning proceedings 1992*. 1992, Elsevier. p. 249-256.

124. Kitada, R., et al., *Tactile estimation of the roughness of gratings yields a graded response in the human brain: an fMRI study.* Neuroimage, 2005. **25**(1): p. 90-100.

125. Wu, J., et al., *Utility of EEG measures of brain function in patients with acute stroke.* Journal of neurophysiology, 2016. **115**(5): p. 2399-2405.

126. Singh, H., et al., *The brain's response to pleasant touch: An EEG investigation of tactile caressing.* Frontiers in human neuroscience, 2014. **8**: p. 893.

127. Merabet, L.B. and A. Pascual-Leone, *Neural reorganization following sensory loss: the opportunity of change.* Nature reviews. Neuroscience, 2010. **11**(1): p. 44-52.

128. Ackerley, R., et al., *Touch perceptions across skin sites: differences between sensitivity, direction discrimination and pleasantness.* Frontiers in behavioral neuroscience, 2014. **8**: p. 54.

129. Hoefer, D., et al., *Electroencephalographic study showing that tactile stimulation by fabrics of different qualities elicit graded event - related potentials.* Skin Research and Technology, 2016. **22**(4): p. 470-478.

130. Simões, C., et al., *Phase locking between human primary and secondary somatosensory cortices.* Proceedings of the National Academy of Sciences, 2003. **100**(5): p. 2691-2694.

131. Brovelli, A., et al., *Beta oscillations in a large-scale sensorimotor cortical network: directional influences revealed by Granger causality.* Proceedings of the National Academy of Sciences, 2004. **101**(26): p. 9849-9854.

132. Greco, A., et al., *Brain dynamics induced by pleasant/unpleasant tactile stimuli conveyed by different fabrics.* IEEE journal of biomedical and health informatics, 2019. **23**(6): p. 2417-2427.

133. Hasenstaub, A., et al., *Inhibitory postsynaptic potentials carry synchronized frequency information in active cortical networks.* Neuron, 2005. **47**(3): p. 423-35.

134. Engel, A.K. and W. Singer, *Temporal binding and the neural correlates of sensory awareness.* Trends Cogn Sci, 2001. **5**(1): p. 16-25.

135. Ihara, A., et al., *Neuromagnetic gamma-band activity in the primary and secondary somatosensory areas.* NeuroReport, 2003. **14**(2).

136. Bauer, M., et al., *Tactile spatial attention enhances gamma-band activity in somatosensory cortex and reduces low-frequency activity in parieto-occipital areas.* Journal of Neuroscience, 2006. **26**(2): p. 490-501.

137. Xiong, Z., et al., *Evaluating explorative prediction power of machine learning algorithms for materials discovery using k-fold forward cross-validation.* Computational Materials Science, 2020. **171**: p. 109203.

138. Refaeilzadeh, P., L. Tang, and H. Liu, *Cross-validation.* Encyclopedia of database systems, 2009. **5**: p. 532-538.

139. Jung, Y., *Multiple predicting K-fold cross-validation for model selection.* Journal of Nonparametric Statistics, 2018. **30**(1): p. 197-215.

140. Chen, A., et al., *Behavioral oscillations in visual attention modulated by task difficulty.* Frontiers in psychology, 2017. **8**: p. 1630.

141. Jiao, J., et al., *Neuro-perceptive discrimination on fabric tactile stimulation by Electroencephalographic (EEG) spectra.* 2020. **15**(10): p. e0241378.

142. Snyder, D.B., et al., *Electroencephalography resting-state networks in people with Stroke.* Brain and behavior, 2021. **11**(5): p. e02097-e02097.

143. Dąbrowski, J., et al., *Brain functional reserve in the context of neuroplasticity after stroke.* Neural Plasticity, 2019.

144. Voss, P., et al., *Dynamic brains and the changing rules of neuroplasticity: implications for learning and recovery.* Frontiers in psychology, 2017. **8**: p. 1657.

145. Lin, M.P. and D.S. Liebeskind, *Imaging of ischemic stroke.* Continuum: Lifelong Learning in Neurology, 2016. **22**(5): p. 1399.

146. Sun, S. and C. Zhang, *Adaptive feature extraction for EEG signal classification.* Medical and Biological Engineering and Computing, 2006. **44**(10): p. 931-935.

147. Al-Qazzaz, N.K., et al., *Discrimination of stroke-related mild cognitive impairment and vascular dementia using EEG signal analysis.* Medical & biological engineering & computing, 2018. **56**(1): p. 137-157.

148. Olsen, T.S.j., *Arm and leg paresis as outcome predictors in stroke rehabilitation.* Stroke, 1990. **21**(2): p. 247-251.

149. Krakauer, J.W. and S.T. Carmichael, *Broken movement: the neurobiology of motor recovery after stroke*. 2022: MIT Press.

150. Nielsen, J.B., C. Crone, and H. Hultborn, *The spinal pathophysiology of spasticity–from a basic science point of view.* Acta physiologica, 2007. **189**(2): p. 171-180.

151. Kuo, C.-L. and G.-C. Hu, *Post-stroke spasticity: a review of epidemiology, pathophysiology, and treatments.* International Journal of Gerontology, 2018. **12**(4): p. 280-284.

152. Wissel, J., et al., *Early development of spasticity following stroke: a prospective, observational trial.* Journal of neurology, 2010. **257**: p. 1067-1072.

153. Kitago, T., et al., *Improvement after constraint-induced movement therapy: recovery of normal motor control or task-specific compensation?* Neurorehabilitation and neural repair, 2013. **27**(2): p. 99-109.

154. Hu, X., et al., *Joint-angle–dependent neuromuscular dysfunctions at the wrist*

in persons after stroke. Archives of physical medicine and rehabilitation, 2006. **87**(5): p. 671-679.

155. Ward, N., *Assessment of cortical reorganisation for hand function after stroke.* The Journal of physiology, 2011. **589**(23): p. 5625-5632.

156. Guo, Z., et al., *Corticomuscular integrated representation of voluntary motor effort in robotic control for wrist-hand rehabilitation after stroke.* Journal of Neural Engineering, 2022. **19**(2): p. 026004.

157. Pandian, S. and K.N. Arya, *Motor impairment of the ipsilesional body side in poststroke subjects.* Journal of bodywork and movement therapies, 2013. **17**(4): p. 495-503.

158. Darling, W.G., S.L. Wolf, and A.J. Butler, *Variability of motor potentials evoked by transcranial magnetic stimulation depends on muscle activation.* Experimental brain research, 2006. **174**: p. 376-385.

159. Lai, M.-I., et al., *Investigating the effects of peripheral electrical stimulation on corticomuscular functional connectivity stroke survivors.* Topics in Stroke Rehabilitation, 2016. **23**(3): p. 154-162.

160. Liu, J., Y. Sheng, and H. Liu, *Corticomuscular coherence and its applications: a review.* Frontiers in human neuroscience, 2019. **13**: p. 100.

161. Classen, J., et al., *The motor syndrome associated with exaggerated inhibition within the primary motor cortex of patients with hemiparetic.* Brain: a journal of neurology, 1997. **120**(4): p. 605-619.

162. Gharabaghi, A., et al., *Coupling brain-machine interfaces with cortical stimulation for brain-state dependent stimulation: enhancing motor cortex excitability for neurorehabilitation.* Frontiers in Human Neuroscience, 2014. **8**: p. 122.

163. Huang, Y., et al., *Translation of robot-assisted rehabilitation to clinical service: a comparison of the rehabilitation effectiveness of EMG-driven robot hand assisted upper limb training in practical clinical service and in clinical trial with laboratory configuration for chronic stroke.* Biomedical engineering online, 2018. **17**: p. 1-17.

164. Pirondini, E., et al., *Poststroke arm and hand paresis: should we target the cervical spinal cord?* Trends in neurosciences, 2022.

165. Gerasimenko, Y., et al., *Transcutaneous electrical spinal-cord stimulation in humans.* Annals of physical and rehabilitation medicine, 2015. **58**(4): p. 225-231.

166. Inanici, F., et al., *Transcutaneous spinal cord stimulation restores hand and arm function after spinal cord injury.* 2021. **29**: p. 310-319.

167. Chandrasekaran, S., et al., *Targeted transcutaneous spinal cord stimulation promotes persistent recovery of upper limb strength and tactile sensation in spinal cord injury: a pilot study.* Frontiers in Neuroscience, 2023. **17**: p. 1210328.

168. Inanici, F., et al., *Transcutaneous electrical spinal stimulation promotes long-term recovery of upper extremity function in chronic tetraplegia.* 2018. **26**(6): p. 1272-1278.

169. Hofstoetter, U.S., et al., *Probing the human spinal locomotor circuits by phasic step-induced feedback and by tonic electrical and pharmacological neuromodulation.* Curr Pharm Des, 2017. **23**(12): p. 1805-20.

170. Minassian, K., et al., *Targeting lumbar spinal neural circuitry by epidural stimulation to restore motor function after spinal cord injury.* Neurotherapeutics, 2016. **13**: p. 284-294.

171. Freyvert, Y., et al., *Engaging cervical spinal circuitry with non-invasive spinal stimulation and buspirone to restore hand function in chronic motor complete patients.* Scientific reports, 2018. **8**(1): p. 15546.

172. Hofstoetter, U.S., et al., *Modification of spasticity by transcutaneous spinal cord stimulation in individuals with incomplete spinal cord injury.* The journal of spinal cord medicine, 2014. **37**(2): p. 202-211.

173. Taccola, G., et al., *Complications of epidural spinal stimulation: lessons from the past and alternatives for the future.* Spinal Cord, 2020. **58**(10): p. 1049-1059.

174. Johanson, M.E., et al., *Phasic relationships of the extrinsic muscles of the normal hand.* The Journal of hand surgery, 1990. **15**(4): p. 587-594.

175. Wecht, J.R., et al., *Posteroanterior cervical transcutaneous spinal cord stimulation: interactions with cortical and peripheral nerve stimulation.* Journal of Clinical Medicine, 2021. **10**(22): p. 5304.

176. McGeady, C., et al., *Brain-computer interface priming for cervical transcutaneous spinal cord stimulation therapy: an exploratory case study.* Frontiers in Rehabilitation Sciences, 2022.

177. Harnack, D., et al., *The effects of electrode material, charge density and stimulation duration on the safety of high-frequency stimulation of the subthalamic nucleus in rats.* Journal of neuroscience methods, 2004. **138**(1-2): p. 207-216.

178. Hofmann, L., et al., *Modified pulse shapes for effective neural stimulation.* Frontiers in neuroengineering, 2011. **4**: p. 9.

179. Militskova, A., et al., *Supraspinal and afferent signaling facilitate spinal sensorimotor network excitability after discomplete spinal cord injury: a case*

report. Frontiers in neuroscience, 2020: p. 552.

180. Zhang, F., et al., *Cervical Spinal Cord Transcutaneous Stimulation Improves Upper Extremity and Hand Function in People With Complete Tetraplegia: A Case Study.* 2020. **28**(12): p. 3167-3174.

181. Zandvoort, C.S., et al., *The human sensorimotor cortex fosters muscle synergies through cortico-synergy coherence.* Neuroimage, 2019. **199**: p. 30-37.

182. Meng, F., et al., *Cerebral plasticity after subcortical stroke as revealed by cortico-muscular coherence.* IEEE Transactions on Neural Systems and Rehabilitation Engineering, 2008. **17**(3): p. 234-243.

183. Guo, Z., et al., *Altered Corticomuscular Coherence (CMCoh) Pattern in the Upper Limb During Finger Movements After Stroke.* Frontiers in Neurology, 2020. **11**(410).

184. Tecchio, F., et al., *Cortical short-term fatigue effects assessed via rhythmic brain–muscle coherence.* Experimental brain research, 2006. **174**: p. 144-151.

185. Yamada, E., et al., *Relationship between muscle oxygenation and electromyography activity during sustained isometric contraction.* Clinical physiology and functional imaging, 2008. **28**(4): p. 216-221.

186. McGeady, C., et al., *EEG monitoring is feasible and reliable during simultaneous transcutaneous electrical spinal cord stimulation.* Sensors, 2021. **21**(19): p. 6593.

187. Kilner, J.M., et al., *Human cortical muscle coherence is directly related to specific motor parameters.* Journal of Neuroscience, 2000. **20**(23): p. 8838-8845.

188. Conway, B.A., et al., *Synchronization between motor cortex and spinal motoneuronal pool during the performance of a maintained motor task in man.* The Journal of physiology, 1995. **489**(3): p. 917-924.

189. Omlor, W., et al., *Gamma-range corticomuscular coherence during dynamic force output.* Neuroimage, 2007. **34**(3): p. 1191-1198.

190. Park, C.-h., et al., *Longitudinal changes of resting-state functional connectivity during motor recovery after stroke.* Stroke, 2011. **42**(5): p. 1357-1362.

191. Chalard, A., et al., *Impact of the EMG normalization method on muscle activation and the antagonist-agonist co-contraction index during active elbow extension: Practical implications for post-stroke subjects.* Journal of Electromyography and Kinesiology, 2020. **51**: p. 102403.

192. Angeli, C.A., et al., *Altering spinal cord excitability enables voluntary movements after chronic complete paralysis in humans.* Brain, 2014. **137**(5): p. 1394-1409.

193. de Freitas, R.M., et al., *Preferential activation of proprioceptive and cutaneous sensory fibers compared to motor fibers during cervical transcutaneous spinal cord stimulation: A computational study.* Journal of Neural Engineering, 2022. **19**(3): p. 036012.

194. Milosevic, M., et al., *On the reflex mechanisms of cervical transcutaneous spinal cord stimulation in human subjects.* Journal of neurophysiology, 2019. **121**(5): p. 1672-1679.

195. Willis Jr, W.D. and R.E. Coggeshall, *Sensory mechanisms of the spinal cord: Volume 1 primary afferent neurons and the spinal dorsal horn*. 2012: Springer Science & Business Media.

196. Rattay, F., *The basic mechanism for the electrical stimulation of the nervous system.* Neuroscience, 1999. **89**(2): p. 335-346.

197. Koch, S.C., D. Acton, and M. Goulding, *Spinal circuits for touch, pain, and itch.* Annual review of physiology, 2018. **80**: p. 189-217.

198. Hofstoetter, U.S., et al., *Common neural structures activated by epidural and transcutaneous lumbar spinal cord stimulation: Elicitation of posterior root-muscle reflexes.* PloS one, 2018. **13**(1): p. e0192013.

199. Minassian, K., et al., *Human lumbar cord circuitries can be activated by extrinsic tonic input to generate locomotor-like activity.* Human movement science, 2007. **26**(2): p. 275-295.

200. Tanaka, R., *Reciprocal Ia inhibition during voluntary movements in man.* Experimental Brain Research, 1974. **21**: p. 529-540.

201. Crone, C., L. Johnsen, and J. Nielsen, *Reciprocal inhibition in hemiplegic patients–a longitudinal study*, in *Supplements to Clinical neurophysiology*. 2000, Elsevier. p. 187-191.

202. Crone, C., et al., *Appearance of reciprocal facilitation of ankle extensors from ankle flexors in patients with stroke or spinal cord injury.* Brain, 2003. **126**(2): p. 495-507.

203. Jankowska, E., *Interneuronal relay in spinal pathways from proprioceptors.* Progress in neurobiology, 1992. **38**(4): p. 335-378.

204. Hofstötter, U., *Model of spinal cord reflex circuits in humans: Stimulation frequency-dependence of segmental activities and their interactions*. 2009.

205. Hofstoetter, U., et al., *Effects of transcutaneous spinal cord stimulation on voluntary locomotor activity in an incomplete spinal cord injured individual.* Biomedical Engineering/Biomedizinische Technik, 2013. **58**(SI-1-Track-A): p. 000010151520134014.

206. Harkema, S., et al., *Effect of epidural stimulation of the lumbosacral spinal cord*

on voluntary movement, standing, and assisted stepping after motor complete paraplegia: a case study. The Lancet, 2011. **377**(9781): p. 1938-1947.

207. Jones, T.A., *Motor compensation and its effects on neural reorganization after stroke.* Nature Reviews Neuroscience, 2017. **18**(5): p. 267-280.

208. Zaaimi, B., et al., *Changes in descending motor pathway connectivity after corticospinal tract lesion in macaque monkey.* Brain, 2012. **135**(7): p. 2277-2289.

209. Azzollini, V., S. Dalise, and C. Chisari, *How does stroke affect skeletal muscle? State of the art and rehabilitation perspective.* Frontiers in Neurology, 2021. **12**: p. 797559.

210. Lu, D.C., et al., *Engaging cervical spinal cord networks to reenable volitional control of hand function in tetraplegic patients.* Neurorehabilitation and neural repair, 2016. **30**(10): p. 951-962.

211. D'amico, J.M., et al., *Recovery of neuronal and network excitability after spinal cord injury and implications for spasticity.* Frontiers in integrative neuroscience, 2014. **8**: p. 36.

212. Gad, P., et al., *Non-invasive activation of cervical spinal networks after severe paralysis.* Journal of neurotrauma, 2018. **35**(18): p. 2145-2158.

213. Hamid, S. and R. Hayek, *Role of electrical stimulation for rehabilitation and regeneration after spinal cord injury: an overview.* European Spine Journal, 2008. **17**: p. 1256-1269.

214. Rushton, D.N., *Functional electrical stimulation and rehabilitation—an hypothesis.* Medical engineering & physics, 2003. **25**(1): p. 75-78.

215. Lawrence, E.S., et al., *Estimates of the prevalence of acute stroke impairments and disability in a multiethnic population.* Stroke, 2001. **32**(6): p. 1279-1284.

216. Hatem, S.M., et al., *Rehabilitation of motor function after stroke: a multiple systematic review focused on techniques to stimulate upper extremity recovery.* Frontiers in human neuroscience, 2016. **10**: p. 442.

217. Wolf, S.L., et al., *Effect of constraint-induced movement therapy on upper extremity function 3 to 9 months after stroke: the EXCITE randomized clinical trial.* Jama, 2006. **296**(17): p. 2095-2104.

218. Rodgers, H. and C. Price, *Stroke unit care, inpatient rehabilitation and early supported discharge.* Clinical Medicine, 2017. **17**(2): p. 173.

219. Krucoff, M.O., et al., *Enhancing nervous system recovery through neurobiologics, neural interface training, and neurorehabilitation.* Frontiers in neuroscience, 2016. **10**: p. 584.

220. Elias, G.J., A.A. Namasivayam, and A.M. Lozano, *Deep brain stimulation for stroke: Current uses and future directions.* Brain stimulation, 2018. **11**(1): p. 3-28.

221. Powell, M.P., et al., *Epidural stimulation of the cervical spinal cord improves voluntary motor control in post-stroke upper limb paresis.* medRxiv, 2022: p. 2022.04. 11.22273635.

222. Evancho, A., W.J. Tyler, and K. McGregor, *A review of combined neuromodulation and physical therapy interventions for enhanced neurorehabilitation.* Frontiers in Human Neuroscience, 2023. **17**.

223. Pape, T.L.B., et al., *Neuromodulatory interventions for traumatic brain injury.* The Journal of Head Trauma Rehabilitation, 2020. **35**(6): p. 365-370.

224. James, N.D., et al., *Neuromodulation in the restoration of function after spinal cord injury.* The Lancet Neurology, 2018. **17**(10): p. 905-917.

225. Boddington, L. and J. Reynolds, *Targeting interhemispheric inhibition with neuromodulation to enhance stroke rehabilitation.* Brain stimulation, 2017. **10**(2): p. 214-222.

226. Wilson, R.D., et al., *Neuromodulation for functional electrical stimulation.* Physical Medicine and Rehabilitation Clinics, 2019. **30**(2): p. 301-318.

227. Ganguly, J., et al., *Non-invasive transcranial electrical stimulation in movement disorders.* Frontiers in neuroscience, 2020. **14**: p. 522.

228. Hofstoetter, U.S., et al., *Transcutaneous spinal cord stimulation induces temporary attenuation of spasticity in individuals with spinal cord injury.* Journal of neurotrauma, 2020. **37**(3): p. 481-493.

229. Spagnolo, P.A. and D. Goldman, *Neuromodulation interventions for addictive disorders: challenges, promise, and roadmap for future research.* Brain, 2017. **140**(5): p. 1183-1203.

230. Fishman, S.M., *Spinal cord stimulation: percutaneous implantation techniques*. 2023: Oxford University Press.

231. Larsen, L.H., et al., *Corticomuscular coherence in the acute and subacute phase after stroke.* Clinical Neurophysiology, 2017. **128**(11): p. 2217-2226.

232. Aikio, R., et al., *CMC is more than a measure of corticospinal tract integrity in acute stroke patients.* NeuroImage: Clinical, 2021. **32**: p. 102818.

233. Pichiorri, F., et al., *Exploring high-density corticomuscular networks after stroke to enable a hybrid Brain-Computer Interface for hand motor rehabilitation.* Journal of NeuroEngineering and Rehabilitation, 2023. **20**(1): p. 5.

234. Ward, A.R. and V.J. Robertson, *Sensory, motor, and pain thresholds for stimulation with medium frequency alternating current.* Archives of physical medicine and rehabilitation, 1998. **79**(3): p. 273-278.

235. Hofmann, G.E., et al., *High-frequency dynamics of ocean pH: a multi-ecosystem comparison.* PloS one, 2011. **6**(12): p. e28983.

236. McGeady, C., et al., *Brain-computer interface priming for cervical transcutaneous spinal cord stimulation therapy: an exploratory case study.* Frontiers in Rehabilitation Sciences, 2022. **3**: p. 896766.

237. Zhang, F., et al., *Cervical spinal cord transcutaneous stimulation improves upper extremity and hand function in people with complete tetraplegia: a case study.* IEEE Transactions on Neural Systems and Rehabilitation Engineering, 2020. **28**(12): p. 3167-3174.

238. Huang, Y., et al., *A comparison of the rehabilitation effectiveness of neuromuscular electrical stimulation robotic hand training and pure robotic hand training after stroke: A randomized controlled trial.* Biomedical Signal Processing and Control, 2020. **56**: p. 101723.

239. Taylor, C., et al., *Transcutaneous spinal cord stimulation and motor responses in individuals with spinal cord injury: A methodological review.* PloS one, 2021. **16**(11): p. e0260166.

240. Sullivan, K.J., et al., *Fugl-Meyer assessment of sensorimotor function after stroke: standardized training procedure for clinical practice and clinical trials.* Stroke, 2011. **42**(2): p. 427-432.

241. Brunnstrom, S., *Movement therapy in hemiplegia.* A neurophysiological approach, 1970.

242. Wolf, S.L., et al., *Assessing Wolf motor function test as outcome measure for research in patients after stroke.* Stroke, 2001. **32**(7): p. 1635-1639.

243. Nijland, R.H., et al., *A comparison of two validated tests for upper limb function after stroke: The Wolf Motor Function Test and the Action Research Arm Test.* Journal of rehabilitation medicine, 2010. **42**(7): p. 694-696.

244. Morris, D.M., et al., *The reliability of the wolf motor function test for assessing upper extremity function after stroke.* Archives of physical medicine and rehabilitation, 2001. **82**(6): p. 750-755.

245. Carroll, D., *A quantitative test of upper extremity function.* Journal of chronic diseases, 1965. **18**(5): p. 479-491.

246. Rabadi, M.H. and F.M. Rabadi, *Comparison of the action research arm test and the Fugl-Meyer assessment as measures of upper-extremity motor weakness after stroke.* Archives of physical medicine and rehabilitation, 2006. **87**(7): p.

962-966.

247. Bohannon, R.W. and M.B. Smith, *Interrater reliability of a modified Ashworth scale of muscle spasticity.* Physical therapy, 1987. **67**(2): p. 206-207.

248. Pandyan, A., et al., *Biomechanical examination of a commonly used measure of spasticity.* Clinical biomechanics, 2001. **16**(10): p. 859-865.

249. O'Dell, M.W., C.-C.D. Lin, and V. Harrison, *Stroke rehabilitation: strategies to enhance motor recovery.* Annual review of medicine, 2009. **60**: p. 55-68.

250. Lee, R.G. and P. van Donkelaar, *Mechanisms underlying functional recovery following stroke.* Canadian Journal of neurological sciences, 1995. **22**(4): p. 257-263.

251. Rouiller, E.M. and E. Olivier, *Functional recovery after lesions of the primary motor cortex.* Progress in brain research, 2004. **143**: p. 467-475.

252. Gerasimenko, Y., R.R. Roy, and V.R. Edgerton, *Epidural stimulation: comparison of the spinal circuits that generate and control locomotion in rats, cats and humans.* Experimental neurology, 2008. **209**(2): p. 417-425.

253. Parazzini, M., et al., *Modeling the current density generated by transcutaneous spinal direct current stimulation (tsDCS).* Clinical Neurophysiology, 2014. **125**(11): p. 2260-2270.

254. Fiocchi, S., et al., *Cerebellar and spinal direct current stimulation in children: computational modeling of the induced electric field.* Frontiers in human neuroscience, 2016. **10**: p. 522.

255. Hofstoetter, U.S., et al., *Augmentation of voluntary locomotor activity by transcutaneous spinal cord stimulation in motor-incomplete spinal cord-injured individuals.* Artificial organs, 2015. **39**(10): p. E176-E186.

256. Einhorn, J., et al., *Cervicothoracic multisegmental transpinal evoked potentials in humans.* PLoS One, 2013. **8**(10): p. e76940.

257. Taylor, J.L., et al., *Neural contributions to muscle fatigue: from the brain to the muscle and back again.* Medicine and science in sports and exercise, 2016. **48**(11): p. 2294.

258. Trompetto, C., et al., *Pathophysiology of spasticity: implications for neurorehabilitation.* BioMed research international, 2014. **2014**.

259. Bourbonnais, D. and S.V. Noven, *Weakness in patients with hemiparesis.* The American journal of occupational therapy, 1989. **43**(5): p. 313-319.

260. Hughes, B.W., L.L. Kusner, and H.J. Kaminski, *Molecular architecture of the neuromuscular junction.* Muscle & Nerve: Official Journal of the American Association of Electrodiagnostic Medicine, 2006. **33**(4): p. 445-461.

261. Bradnam, L.V., et al., *Contralesional hemisphere control of the proximal paretic upper limb following stroke.* Cerebral Cortex, 2012. **22**(11): p. 2662-2671.

262. Jones, T.A. and D.L. Adkins, *Motor system reorganization after stroke: stimulating and training toward perfection.* Physiology, 2015. **30**(5): p. 358-370.

263. Haavik, H., et al., *Impact of spinal manipulation on cortical drive to upper and lower limb muscles.* Brain sciences, 2016. **7**(1): p. 2.